ERDC/GSL TR-12-24

Geotechnical and Structures Laboratory

US Army Corps
of Engineers®
Engineer Research and
Development Center

Brick Paving Systems in Expeditionary Environments: Field Testing

Haley P. Bell and Quint Mason

July 2012

ERDC/GSL TR-12-24
July 2012

Brick Paving Systems in Expeditionary Environments: Field Testing

Haley P. Bell and Quint Mason

Geotechnical and Structures Laboratory
U.S. Army Engineer Research and Development Center
3909 Halls Ferry Road
Vicksburg, MS 39180-6199

Final report

Prepared for Headquarters, Air Force Civil Engineer Support Agency
139 Barnes Avenue, Suite 1
Tyndall AFB, FL 32403-5319

Abstract

Personnel of the U.S. Army Engineer Research and Development Center were tasked by Headquarters, Air Force Civil Engineer Support Agency, to determine the feasibility of using face bricks as an alternative to concrete or asphalt paving for low-volume roads and military aircraft parking aprons in expeditionary environments. Because paving materials and equipment can be scarce in these areas, the use of recycled bricks from existing infrastructure might provide a local resource for constructing pavements suitable for meeting the military's mission requirements. The field testing documented in this report follows a laboratory study in which a series of tests, including compressive strength, absorption, Los Angeles abrasion, and specific gravity, were conducted on selected face bricks. The success of the laboratory testing led to the full-scale field testing and evaluation of the face bricks under a commercial dump truck load of approximately 54,000 lb and then under a 45,000-lb single-wheel C-17 aircraft load cart. The field testing indicated that brick-paved roads constructed with a moderately high strength base are capable of sustaining more than 10,000 passes of truck traffic without failure. The same brick-paved roads were not capable of withstanding C-17 aircraft traffic. Further results from the evaluation are presented, including material characterization test data, rut depth measurements, wheel path and cross-section profile measurements, instrumentation response data, and forensic assessments. Recommendations for continuing the study through the use of additional full-scale test sections also are provided.

Permission to publish this information was granted by the Director, Geotechnical and Structures Laboratory.

Contents

Abstract ii

Figures and Tables v

Preface ix

Unit Conversion Factors x

1 Introduction 1

Background 1

Objective and scope 1

2 Materials Characterization 3

Subgrade 3

Base 3

Geotextile 6

Sand 6

Brick 8

3 Test Section Construction 14

Test section description 14

Construction procedures 15

Subgrade 15

Base 18

Concrete edge restraint 20

Geotextile and bedding sand 20

Brick surface 22

Instrumentation 22

4 Traffic and Evaluation Procedures 27

Traffic 27

Data collection 28

Rut depth 29

Center-line and cross-section profiles 29

Instrumentation response 30

Forensic investigation 32

5 Brick Pavement Performance Results 33

Performance analysis 33

Truck evaluation 33

Item 1 33

Item 2 36

Item 3 41

Item 4 ..... *45*
Item 5 ..... *50*
Item 6 ..... *55*
C-17 evaluation 60
Item 1 ..... *60*
Item 2 ..... *62*
Item 3 ..... *65*
Item 4 ..... *70*
Item 5 ..... *72*
Item 6 ..... *75*
Forensic assessment 78
Summary 84

6 Conclusions and Recommendations 87
Conclusions 87
Recommendations 88

References 89

Report Documentation Page

Figures and Tables

Figures

Figure 1. Gradation curve for CH material. 4
Figure 2. CBR versus moisture content for CH material. 4
Figure 3. Dry density versus moisture content for CH material. 5
Figure 4. Blended GM base course gradation. 6
Figure 5. Dry density versus moisture content for blended GM base course. 7
Figure 6. Geotextile material used for supporting bedding sand. 7
Figure 7. Queen brick. 9
Figure 8. Utility brick. 9
Figure 9. Reclaimed brick. 10
Figure 10. Standard modular brick. 11
Figure 11. Brick paver. 12
Figure 12. Test section plan view. 14
Figure 13. Test pit lined with polyethylene tarp for retaining moisture. 16
Figure 14. Processing CH material for subgrade. 16
Figure 15. Motor grader being used to level subgrade. 17
Figure 16. GM base course material drying to optimum moisture content. 18
Figure 17. Rubber tire roller compacting GM base course material. 19
Figure 18. Installing concrete curbing between test section items. 21
Figure 19. Installing concrete curbing. 21
Figure 20. Installing queen bricks and measuring and spreading bedding sand. 22
Figure 21. Partial brick test section before jointing sand. 23
Figure 22. Measuring brick for installation at edges. 23
Figure 23. Sawing brick for installation at edges. 24
Figure 24. Using plate compactor to vibrate sand into joints. 24
Figure 25. Completed test section. 25
Figure 26. Example profile view showing instrumentation in each test item. 25
Figure 27. Plan view showing instrumentation locations of each test item. 26
Figure 28. Loaded commercial dump truck. 27
Figure 29. Single-wheel C-17 load cart. 28
Figure 30. Single-wheel C-17 load cart on test section. 29
Figure 31. Rut depth measurements on Item 1. 30
Figure 32. Longitudinal rod and level profile readings on Item 1. 31
Figure 33. Collecting instrumentation measurements during truck traffic. 31
Figure 34. Subgrade CBR testing in trenched test item. 32
Figure 35. Item 1 truck traffic at approximately 200 passes. 34

Figure 36. Item 1 at completion of 10,010 passes of truck traffic. 34
Figure 37. Item 1 rut depth measurements in left wheel path of truck traffic (west)..... 35
Figure 38. Item 1 longitudinal profiles in left wheel path of truck traffic. 36
Figure 39. Item 1 cross-section profiles at Station 30 with truck traffic. 37
Figure 40. Item 1 average peak pressure measurements at various traffic intervals. 37
Figure 41. Reclaimed bricks before truck traffic. 38
Figure 42. Reclaimed bricks at 5,000 passes of truck traffic. 39
Figure 43. Item 2 at completion of 10,010 passes of truck traffic. 39
Figure 44. Item 2 rut depth measurements in right wheel path of truck traffic. 40
Figure 45. Item 2 longitudinal profiles in left wheel path of truck traffic. 40
Figure 46. Item 2 cross-section profiles at Station 30 with truck traffic. 41
Figure 47. Item 2 average peak pressure measurements at various traffic intervals. 42
Figure 48. Item 3 wheel path before truck traffic. 43
Figure 49. Item 3 wheel path at 10,010 passes of truck traffic. 43
Figure 50. Item 3 rut depth measurements in left wheel path of truck traffic. 44
Figure 51. Item 3 longitudinal profiles in left wheel path of truck traffic. 44
Figure 52. Item 3 cross-section profiles at Station 10 with truck traffic. 45
Figure 53. Item 3 average peak pressure measurements at various traffic intervals. 46
Figure 54. Item 4 utility bricks before truck traffic. 46
Figure 55. Item 4 overall view at 1,200 passes of truck traffic. 47
Figure 56. Chipped and broken edges of utility bricks in Item 4 at 1,200 passes of truck traffic. 47
Figure 57. Item 4 at 10,010 passes of truck traffic. 48
Figure 58. Item 4 rut depth measurements in right wheel path of truck traffic. 49
Figure 59. Item 4 longitudinal profiles in left wheel path of truck traffic. 49
Figure 60. Item 4 cross-section profiles at Station 20 with truck traffic. 50
Figure 61. Item 4 average peak pressure measurements at various traffic intervals. 51
Figure 62. Item 5 brick pavers before truck traffic. 51
Figure 63. Item 5 overall view at 10,010 passes of truck traffic. 52
Figure 64. Item 5 rut depth measurements in right wheel path of truck traffic. 53
Figure 65. Item 5 longitudinal profiles in left wheel path of truck traffic. 54
Figure 66. Item 5 cross-section profiles at Station 20 with truck traffic. 54
Figure 67. Item 5 average peak pressure measurements at various traffic intervals. 55
Figure 68. Item 6 before truck traffic. 56
Figure 69. Overall view of Item 6 at approximately 5,000 passes of truck traffic. 56
Figure 70. Item 6 at approximately 5,000 passes of truck traffic. 57
Figure 71. Item 6 wheel path at 10,010 passes of truck traffic. 57
Figure 72. Item 6 rut depth measurements in right wheel path of truck traffic. 58
Figure 73. Item 6 longitudinal profiles in left wheel path of truck traffic. 59
Figure 74. Item 6 cross-section profiles at Station 30 with truck traffic. 59
Figure 75. Item 6 average peak pressure measurements at various traffic intervals. 60

Figure 76. Item 1 during first pass of single-wheel C-17 traffic. 61
Figure 77. Item 1 wheel path at 88 passes of C-17 traffic. 61
Figure 78. Item 1 rut depth measurements with C-17 traffic. 62
Figure 79. Item 1 center-line profile measurements with C-17 traffic. 63
Figure 80. Item 1 cross-section profiles at Station 10 with C-17 traffic. 63
Figure 81. Item 2 at 16 passes of single-wheel C-17 traffic. 64
Figure 82. Center of wheel path of Item 2 at 44 passes of C-17 traffic. 64
Figure 83. Item 2 rut depth measurements with C-17 traffic. 65
Figure 84. Item 2 center-line profiles measurements with C-17 traffic. 66
Figure 85. Item 2 cross-section profiles measurements at Station 10 with C-17 traffic. 66
Figure 86. Overall view of Item 3 at 74 passes of C-17 traffic. 67
Figure 87. Item 3 rut depth measurement at Station 30 at 74 passes of C-17 traffic. 67
Figure 88. Item 3 rut depth measurements with C-17 traffic. 68
Figure 89. Item 3 center-line profile measurements with C-17 traffic. 69
Figure 90. Item 3 cross-section profile measurements at Station 30 with C-17 traffic. 69
Figure 91. C-17 load cart trafficking near Station 30 at approximately 75 passes on Item 4. 70
Figure 92. Item 4 rut depth measurements with C-17 traffic. 71
Figure 93. Item 4 center-line profile measurements with C-17 traffic. 71
Figure 94. Item 4 cross-section profile measurements at Station 20 with C-17 traffic. 72
Figure 95. Item 5 wheel path at 150 passes of C-17 traffic. 73
Figure 96. Item 5 rut depth measurements with C-17 traffic. 73
Figure 97. Item 5 center-line profile measurements with C-17 traffic. 74
Figure 98. Item 5 cross-section profile measurements at Station 20 with C-17 traffic. 74
Figure 99. Item 6 overall view at 104 passes of C-17 traffic. 75
Figure 100. Item 6 overall view at 300 passes of single-wheel C-17 traffic 76
Figure 101. Item 6 rut depth measurements with C-17 traffic. 77
Figure 102. Item 6 center-line profile measurements with C-17 traffic. 77
Figure 103. Item 6 cross-section profile measurements at Station 20 with C-17 traffic. 78
Figure 104. Test section after truck traffic. 79
Figure 105. Test section after single-wheel C-17 traffic. 79
Figure 106. CBR post-testing on Item 2 base course after trafficking. 80
Figure 107. Item 1 cross-section profile measurements after C-17 traffic. 81
Figure 108. Item 2 cross-section profile measurements after C-17 traffic. 82
Figure 109. Item 3 cross-section profile measurements after C-17 traffic. 82
Figure 110. Item 4 cross-section profile measurements after C-17 traffic. 83
Figure 111. Item 5 cross-section profile measurements after C-17 traffic. 83
Figure 112. Item 6 cross-section profile measurements after C-17 traffic. 84

Tables

Table 1. Individual material gradations for base course blend. 5

Table 2. Brick dimensions and weights. 8
Table 3. LAA test results. 12
Table 4. Specific gravity and 24-hr water absorption test results. 12
Table 5. Boiling water absorption test results. 13
Table 6. Compressive strength test results (brick face up). 13
Table 7. Compressive strength test results (brick on sides). 13
Table 8. Test section matrix. 15
Table 9. In situ subgrade test results. 17
Table 10. In situ base test results. 19
Table 11. C-17 traffic post-test base measurements. 81
Table 12. C-17 traffic post-test subgrade measurements. 81
Table 13. Laboratory and field performance summary of bricks. 86

Preface

Headquarters, Air Force Civil Engineer Support Agency, located at Tyndall Air Force Base, Florida, sponsored the research project described in this report.

Personnel of the U.S. Army Engineer Research and Development Center (ERDC), Geotechnical and Structures Laboratory (GSL), Vicksburg, Mississippi, prepared this publication. The findings and recommendations presented in this report are based upon a comprehensive literature review, a series of laboratory tests conducted on selected face bricks (e.g., house or building bricks) manufactured in the United States, and full-scale field testing on the face bricks for use as road paving or military aircraft parking in expeditionary environments. The field construction and testing documented in this report were conducted during November 2010 through July 2011. The ERDC research team for the field testing consisted of Haley P. Bell, Quint Mason, Jamie Davis, John L. Newton, Chase T. Bradley, and Matthew R. Hall, Airfields and Pavements Branch (APB), GSL; Alfred B. Crawley, Materials Testing Center, GSL; Harold T. Carr and Tony N. Brogdon, ERDC Information Technology Laboratory (ITL); and Leroy Hardin, Stacy L. Washington, and Daniel A. Butler, ERDC Department of Public Works. Bell and Mason prepared this publication under the supervision of Dr. Gary L. Anderton, Chief, APB; Dr. Larry N. Lynch, Chief, Engineering Systems and Materials Division; Dr. William P. Grogan, Deputy Director, GSL; and Dr. David W. Pittman, Director, GSL.

At the time of publication, COL Kevin J. Wilson was Commander of ERDC. Dr. Jeffery P. Holland was Director.

Recommendations for improving the content and/or format of this publication should be submitted on DA Form 2028 (Recommended Changes to Publications and Blank Forms) and forwarded to Headquarters, U.S. Army Corps of Engineers, ATTN: CECW-EW, 441 G Street NW, Washington, DC 20314-1000.

Unit Conversion Factors

Multiply	By	To Obtain
degrees Fahrenheit	(F-32)/1.8	degrees Celsius
feet	0.3048	meters
inches	0.0254	meters
ounces (mass) per square yard	0.03390575	kilograms per square meter
pounds (force) per square inch	0.006894757	megapascals
pounds (mass)	0.45359237	kilograms
pounds (mass) per cubic foot	16.01846	kilograms per cubic meter

1 Introduction

Background

Resources for construction of infrastructure, particularly roads and airfields, are limited in the Middle East. Contractors are continuously seeking readily available materials for construction of pavements. In locations where paving materials and equipment are scarce, recycled or recently manufactured face bricks (e.g., house or building bricks) might provide a local resource for constructing pavements suitable for meeting the military's mission requirements. Face bricks are among the most commonly reclaimed building materials; however, they generally are not used for road paving. Face bricks might provide a low-maintenance and aesthetically pleasing pavement surface with comparable structural characteristics to typical hot-mix asphalt (HMA) or portland cement concrete (PCC) pavements. Brick-paved roads are classified as flexible pavement.

During 2010, an extensive literature review was conducted to identify various types of bricks, composition, manufacturing processes, strength characteristics, previous uses of bricks for roads and floors, specifications, and common laboratory testing suitable for brick specimens. Following the literature review, a laboratory study was completed on five selected face brick types to evaluate their strength and durability. A brick paver also was included to use as a control for the study. The procedures, results, and analysis of the laboratory testing were well documented and can be found in Bell (2011). The results from the 2010 laboratory testing supported the need to evaluate, through full-scale field testing, the use of face bricks as a surface for low-volume roads and military aircraft parking ramps.

Objective and scope

The purpose of the research described in this report was to evaluate the use of face bricks for paving surfaces on low-volume roads (< 40 mph), parking lots, and cargo areas by full-scale field testing and evaluation. Four types of face bricks and a brick paver were selected, based on the results of the laboratory testing, to be included in the field testing.

The full-scale field testing included six test items with the same subgrade and base course. Each item had a different brick surface and was instru-

mented with multiple earth pressure cells in the base and subgrade. Channelized traffic was applied with a loaded commercial dump truck of approximately 54,000 lb with 109-psi tire pressure.[1] At selected traffic intervals, the brick surface was inspected for distress, and permanent deformation was measured. Ruts occurred near the edges of the test items. Traffic continued on each item until surface rutting reached an average depth of 3 in. (failure) or 10,000 passes.

Channelized traffic with a single-wheel C-17 load cart of approximately 45,000 lb and 142-psi tire pressure then was applied to the center of each item. At selected traffic intervals, the brick surface was inspected for distress, and permanent deformation was measured. Traffic continued on each item until surface rutting reached an average depth of 3 in. or more (well beyond the approximately 1-in. rut depth considered as failure for aircraft traffic) or 1,000 passes were achieved.

This report presents brief results from the laboratory testing of the face bricks and brick paver and a description of the procedures, results, and analysis of the field testing of the selected bricks. Recommendations for further testing of brick paving systems through additional full-scale field testing also are provided.

[1] A table of factors for converting non-SI units of measure to SI units is found on page x.

2 Materials Characterization

The test section consisted of a brick surface constructed over a bedding sand layer, geotextile material, base course, and subgrade. Each layer of the pavement structure was characterized through laboratory tests or visual inspection before construction of the full-scale test section. This was done to ensure that each material displayed the desired in-place properties. The following paragraphs describe the laboratory results and/or characteristics of the materials used in the test section.

Subgrade

High-plasticity clay material, classified by the Unified Soil Classification System (USCS) (American Society for Testing and Materials (ASTM) D 2487-06 (ASTM 2006)) as CH, was used for the subgrade. The CH material has been used as a subgrade material for numerous test sections at the U.S. Army Engineer Research and Development Center (ERDC) over previous years. This material often is used because of the uniform conditions the clay provides over time and because of its ability to control strength by controlling moisture. Because the CH material has been characterized in ERDC's Geotechnical and Structures Laboratory several times, the specific subgrade material for this project was not characterized as a part of this study. The results of previous laboratory tests were used for this project, as summarized in Figures 1 through 3.

The data shown in Figures 2 and 3 were used to determine the target moisture content and dry density needed to obtain the desired California Bearing Ratio (CBR) of 6 for the in situ soil. The CBR is an index of strength measured by comparing the resistance to penetration by a standard diameter device of the test specimen to the resistance measured by the same device for a standard crushed stone, expressed as a percentage. According to the laboratory results, the subgrade soil should have a moisture content of about 34 percent (Figure 2) and a dry density of approximately 85 pcf (Figure 3) to obtain the desired CBR of 6.

Base

ERDC's Materials Testing Center (MTC) conducted the laboratory testing of four soils blended to obtain a silty gravel base course material, classified

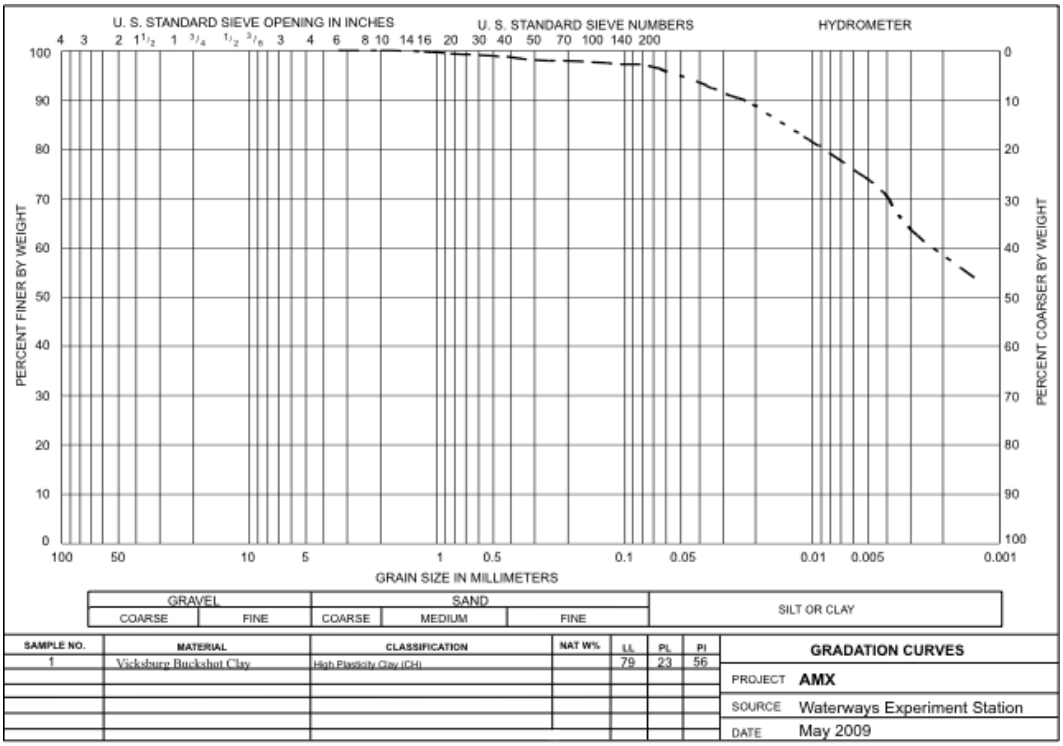

Figure 1. Gradation curve for CH material.

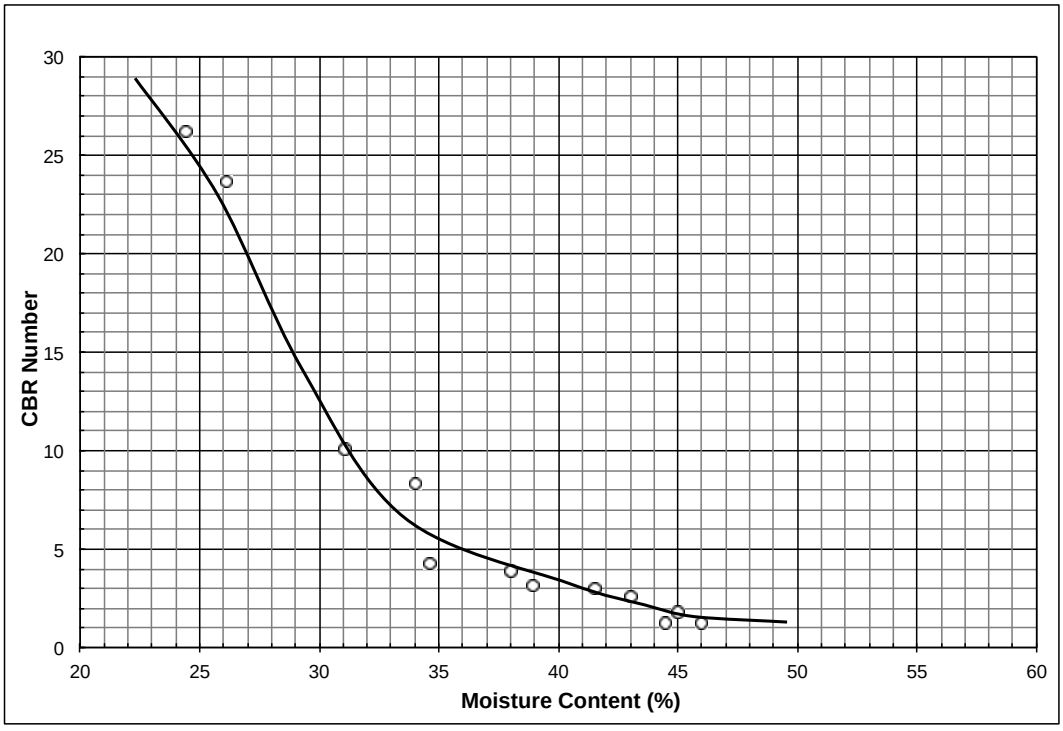

Figure 2. CBR versus moisture content for CH material.

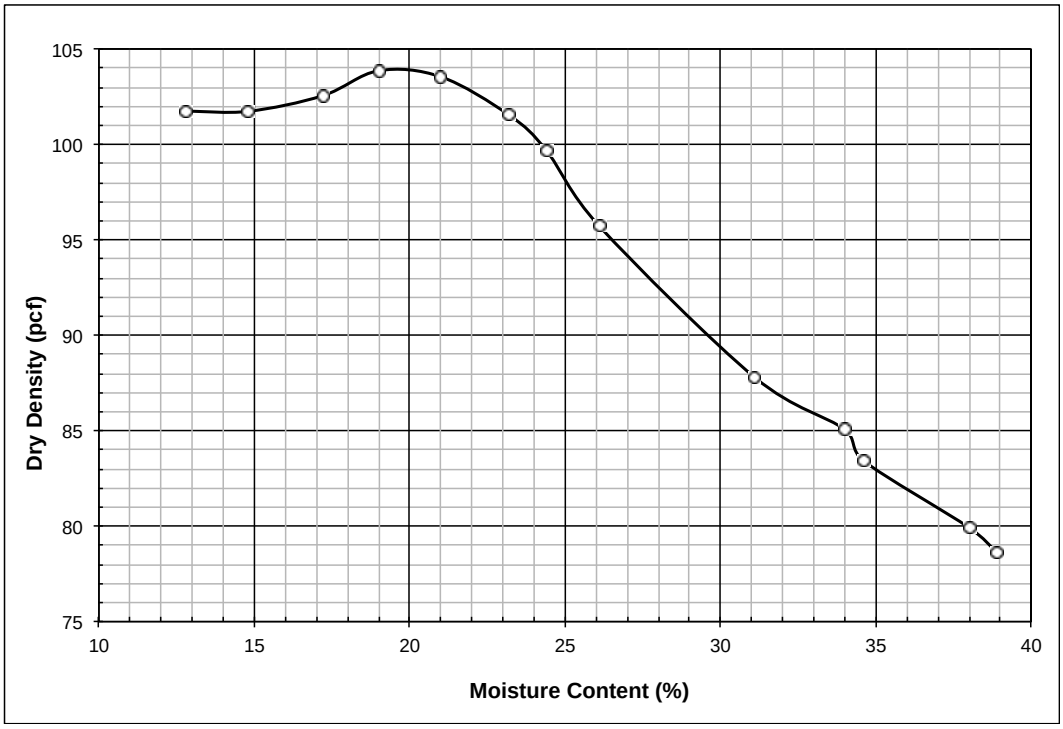

Figure 3. Dry density versus moisture content for CH material.

by the USCS as GM, with a target in-place CBR of approximately 50. The MTC developed a blend using two types of crushed gravels (30 percent each), sand (35 percent), and silt (5 percent). Table 1 shows the gradations of each soil used for the blend, and Figure 4 shows the gradations of the GM blend used for the base course.

Table 1. Individual material gradations for base course blend.

	-1" + 0.75" Crushed Gravel	-0.75" + 0.5" Crushed Gravel	Concrete Sand	Silt
Sieve Size	Percent Finer			
1.5 in.	100	100	100	100
1.0 in.	100	100	100	100
3/4 in.	99.0	100	100	100
1/2 in.	53.6	53.9	100	100
3/8 in.	9.0	3.9	99.9	100
No. 4	1.5	0.9	94.0	97.8
No. 8	1.4	0.8	80.6	93.0
No. 16	1.1	0.4	72.8	88.0
No. 30	1.1	0.4	57.7	75.0
No. 50	1.1	0.4	4.8	22.2
No. 100	1.1	0.4	2.1	16.3
No. 200	1.1	0.4	1.4	15.6

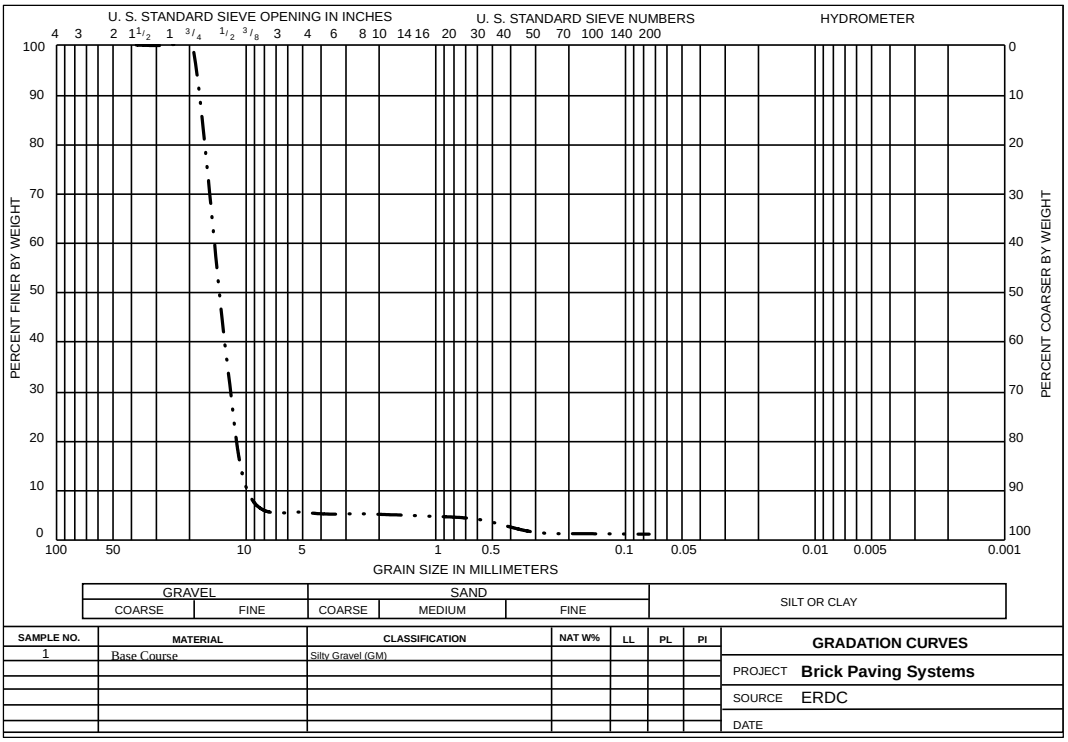

Figure 4. Blended GM base course gradation.

Laboratory results indicate that the GM blend has an estimated specific gravity of 2.7, optimum moisture content of 2.6 percent, and a maximum dry density of 114.2 pcf. Figure 5 shows the Proctor curve developed by the MTC for the GM blend. The MTC followed ASTM D 698-07 Method C (ASTM 2007b) and ASTM D 1883-07 specifications for the testing (ASTM 2007a).

Geotextile

A nonwoven needle-punched geotextile composed of polypropylene fibers was used on top of the base course to support the bedding sand layer needed for the brick surface. The geotextile material used in the test section weighed approximately 4 oz./yd^2 and was about 0.04 in. thick. Each roll was approximately 12.5 ft wide and 360 ft long. The geotextile material is capable of containing the bedding sand layer while still allowing water to penetrate through the pavement structure. Figure 6 shows the geotextile material used in the test section.

Sand

Bedding sand was used on top of the geotextile material and underneath the brick surface for stability. Jointing sand was used between the bricks

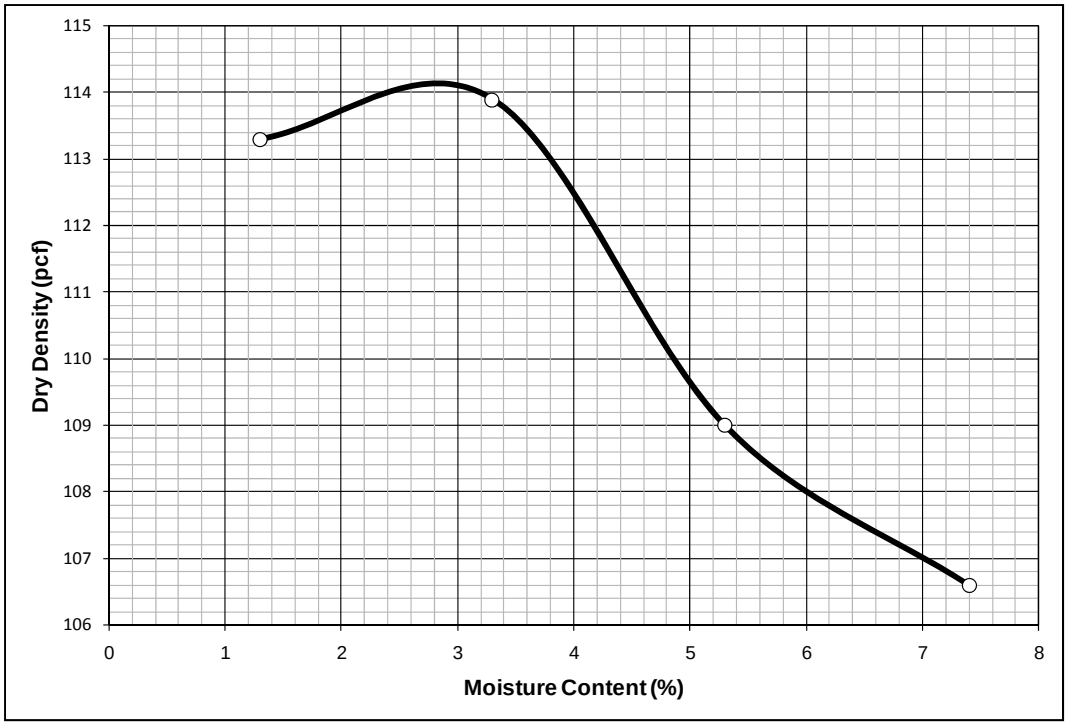

Figure 5. Dry density versus moisture content for blended GM base course.

Figure 6. Geotextile material used for supporting bedding sand.

for adhesion. Table 1 gives the gradation of the concrete sand that was used for adhesion between the bricks and as a bedding layer underneath the bricks.

Brick

Based on the results of laboratory testing, four types of bricks were selected for the field study. The bricks were obtained from a local manufacturer/distributor and included queen, standard modular, reclaimed, and utility types. A brick paver also was selected as a control. Note that the names of bricks might differ depending on the region. The exact compositions of the bricks are unknown; however, the brick manufacturer/distributor noted that they are made mostly of clay and shale. Table 2 presents the approximate dimensions and weights of each brick type, and the following paragraphs give detailed information about the bricks.

Table 2. Brick dimensions and weights.

Brick Name/Type	Length (in.)	Width (in.)	Height (in.)	Weight (lb)
Queen	7.5000	2.7500	2.7500	3.09
Utility	11.6250	3.6250	3.5000	7.72
Reclaimed	8.2500	3.7500	2.3750	4.41
Standard Modular	7.6250	3.5000	2.2500	3.31
Paver	7.6250	3.5625	2.5000	4.63

The brick distributor noted that the queen bricks are most likely what is used in areas such as Afghanistan. This was confirmed with employees of the U.S. Army Corps of Engineers, Afghanistan Engineer District (Reed Freeman, e-mail and telephone interviews, November 5, 2010; Gregory Hales, e-mail interview, November 9 and 10, 2010; John P. Heard, e-mail interview, November 8, 2010). These particular bricks were cast in a wood mold and fired in a kiln. This type of process and brick appearance likely are indicative of the type of bricks used in more primitive parts of the world. Figure 7 shows the queen brick used in the test section.

The utility brick types are commonly used for commercial buildings because their larger size allows for a more efficient laying practice (Figure 8). The reclaimed bricks were gathered from an old burned building in Chicago (Figure 9). Reclaimed bricks are not as durable as other face bricks because of their worn edges and irregular shapes.

Figure 7. Queen brick.

Figure 8. Utility brick.

Figure 9. Reclaimed brick.

Standard modular bricks are the most commonly used in the United States because their smaller size makes handling and construction easier (Brick Industry Association 2009). Figure 10 shows the standard modular brick. Figure 11 shows the brick paver used in the test section as the control.

The strength properties of the five brick types were tested in the laboratory. Laboratory tests, including Los Angeles abrasion (LAA), water absorption, specific gravity, and compressive strength were conducted on the bricks during the initial brick study in 2010 (Bell 2011). Tables 3 through 7 present the laboratory results.

The laboratory test results revealed that some of the selected face bricks had characteristics that were similar to or better than the brick pavers. The LAA test results on the bricks were within the typical ranges for traditional aggregate material, indicating a strong possibility that bricks could prove satisfactory for use as a paved surface. Also, literature stated that concrete pavers with compressive strengths of 8,000 psi have proved to be adequate for military road applications (Anderton 1991). The compressive strengths of all brick types tested, with the exception of the queen and reclaimed brick types, exceeded 8,000 psi. However, the measured specific gravities and

water absorptions of the face bricks indicated there could be a problem with durability during freezing and thawing periods. The specific gravities of the bricks were lower than the standard values of natural aggregates. Full details from the laboratory testing and results are documented in Bell (2011).

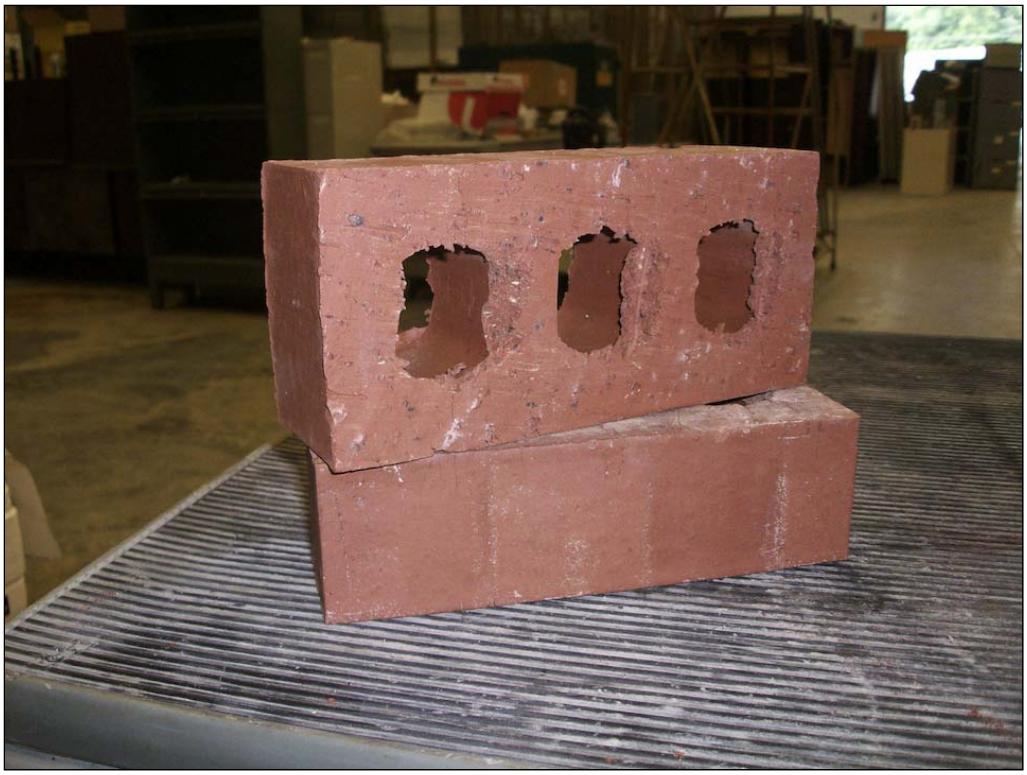

Figure 10. Standard modular brick.

Figure 11. Brick paver.

Table 3. LAA test results.

Brick	Sample Mass (g)	Retained Mass (g)	Mass Loss (g)	% Loss
Queen	10,058.4	4,442.2	5,616.2	55.84
Utility	10,049.1	5,864.1	4,185.0	41.65
Reclaimed	10,020.2	5,608.4	4,411.8	44.03
Standard Modular	10,040.1	7,383.3	2,656.8	26.46
Paver	9,946.0	7,679.8	2,266.2	22.79

Table 4. Specific gravity and 24-hr water absorption test results.

Brick	Specific Gravity	Absorption (%)
Queen	2.02	11.1
Utility	2.22	5.3
Reclaimed	2.02	23.4
Standard Modular	2.24	4.9
Paver	2.32	4.8

Table 5. Boiling water absorption test results.

Brick	Absorption (%)				Saturation Coefficient
	5-hr Cold	1-hr Boil	2-hr Boil	5-hr Boil	
Queen	9.5	16.1	16.7	16.9	0.66
Utility	4.8	7.9	8.3	8.6	0.62
Reclaimed	11.6	16.0	16.8	17.2	1.36
Standard Modular	4.9	7.7	7.9	8.1	0.60
Paver	4.5	6.7	6.9	7.1	0.68

Table 6. Compressive strength test results (brick face up).

Brick	Compressive Strength (psi)			Average (psi)
	Rep. A	Rep. B	Rep. C	
Queen	5,134	4,794	4,414	4,781
Utility	9,895	11,190	10,705	10,597
Reclaimed	2,396	4,138	4,188	3,574
Standard Modular	16,999	20,481	21,233	19,571
Paver	17,227	19,000	15,590	17,272

Table 7. Compressive strength test results (brick on sides).

Brick	Compressive Strength (psi)			Average (psi)
	Rep. A	Rep. B	Rep. C	
Utility	2,945	2,254	2,912	2,704
Standard Modular	7,763	6,390	7,835	7,329

3 Test Section Construction

Test section description

The full-scale test section, 80 ft long and 36 ft wide, was constructed under ERDC's Hangar 4 test facility to evaluate the structural performance of face bricks as a road surface in expeditionary environments. The test section was divided into six items, each 40 ft long by 12 ft wide.

Each item was constructed of the same subgrade and base materials and to the same thicknesses. The subgrade was constructed with approximately 2 ft of CH, and the base course was constructed with approximately 1 ft of GM. Item 1 was paved with the queen bricks, while Item 2 was paved with the reclaimed bricks. Items 3, 4, and 5 were paved with the standard modular bricks, utility bricks, and brick pavers, respectively. Item 6 was constructed of two layers of the standard modular bricks.

Figure 12 shows a plan view of the test section. The 4-in.-thick barrier shown around the edges of the test section and between the lanes in Figure 12 is the concrete border constructed to confine the bricks during installation and trafficking.

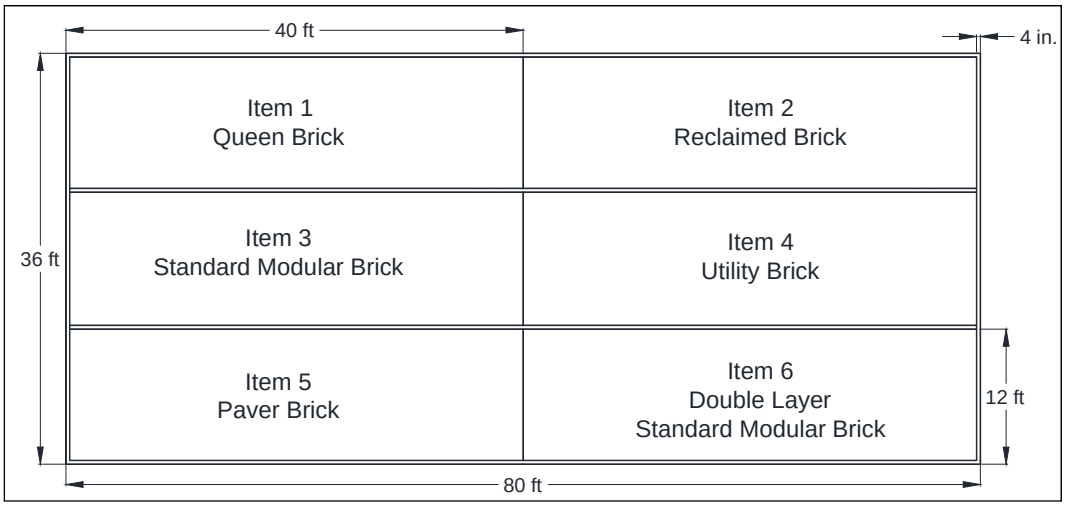

Figure 12. Test section plan view.

Table 8 presents the test variable matrix measured from the test section. The subgrade and base thicknesses are average thicknesses determined from center-line and cross-section profile readings during construction.

The subgrade thickness in Item 6 was approximately 3 in. less than the subgrade in the rest of the test section. This was done to account for the double-layered brick surface thickness used in Item 6 and because it was important for trafficking purposes that Items 5 and 6 be approximately the same finished elevation.

Table 8. Test section matrix.

Item	Brick Surface Thickness (in.)	Bedding Sand Thickness (in.)	Geotextile Thickness (in.)	Average Thickness (in.)	
				Base	Subgrade
1	2.75	1.25	0.04	12.90	22.11
2	2.38	1.25	0.04	11.80	22.67
3	2.25	1.25	0.04	12.50	22.66
4	3.50	1.25	0.04	12.87	22.90
5	2.50	1.25	0.04	12.20	22.00
6	4.50	1.25	0.04	12.27	20.01

Construction procedures

Construction began by excavating a 36-ft-wide by 80-ft-long by approximately 3.5-ft-deep test pit. The bottom of the pit was leveled and compacted. The test pit then was lined with an impermeable 6-mil polyethylene tarp to help retain the moisture in the constructed layers of the test section (Figure 13). The following sections describe the procedures used for constructing each layer of underlying material in the test section.

Subgrade

The subgrade material consisted of approximately 2 ft of high-plasticity CH. This material was used because it is locally available and has a relatively good affinity for retaining moisture. The material was processed outside the test pit so that the moisture content could be adjusted to the desired level (Figure 14). The processing included spreading the material to a uniform 12-in. depth at a nearby preparatory site, mixing the material with a rotary mixer, adjusting the moisture content of the material, mixing the CH again, and stockpiling the soil. Once the optimum moisture content was achieved (approximately 34 percent), the CH was placed in the test pit in four separate 6- to 8-in. lifts. A rubber tire roller was used to compact each lift to approximately 6 in. for a total thickness of about 2 ft. Figure 15 shows a motor grader leveling the subgrade.

Figure 13. Test pit lined with polyethylene tarp for retaining moisture.

Figure 14. Processing CH material for subgrade.

Figure 15. Motor grader being used to level subgrade.

Each compacted lift was subjected to nuclear density, nuclear moisture, oven moisture, and CBR testing; and the results are presented in Table 9. The subgrade then was finished using a vibratory steel wheel roller to achieve a smooth surface. The CH subgrade material reached the desired strength with an average in situ CBR of 6.

Table 9. In situ subgrade test results.

Subgrade Lift	Average CBR (%)	Average Oven Moisture Content (%)	Nuclear Density Gauge	
			Average Dry Density (pcf)	Average Moisture Content (%)
1	5.7	31.6	88.9	30.9
2	6.1	31.4	92.1	28.8
3	5.9	31.8	86.4	28.7
4	6.1	31.3	92.7	30.0
Average	6.0	31.5	90.0	29.6

The Troxler nuclear moisture-density gauge, calibrated with a certified Primary Calibration Standard Block, was used throughout the pavement structure to measure respective density and moisture content of each layer rapidly. The nuclear gauge nondestructively reports the dry density, wet density, and percent moisture of a soil.

Base

The base course, classified as a GM material, consisted of a blend of two sizes of gravel (30 percent each), silt (5 percent), and sand (35 percent). The blend was created by moving the appropriate amounts of each material into a stockpile and mixing them with a front-end loader. The blend then was spread to a uniform 12-in. depth at a nearby preparatory site where it was mixed with a rotary mixer and allowed to dry to the appropriate moisture content (Figure 16).

Figure 16. GM base course material drying to optimum moisture content.

Once the optimum moisture content was achieved, the GM was placed on top of the compacted subgrade in two uncompacted 8-in. lifts. Each lift was compacted to approximately 6 in. using steel wheel and rubber tire rollers. Figure 17 shows a rubber tire roller compacting the base course. Each compacted lift was subjected to nuclear density, nuclear moisture, oven moisture, and CBR testing, and the results are presented in Table 10. The elevation and uniform grade of the base material were verified by center-line and cross-section profile readings.

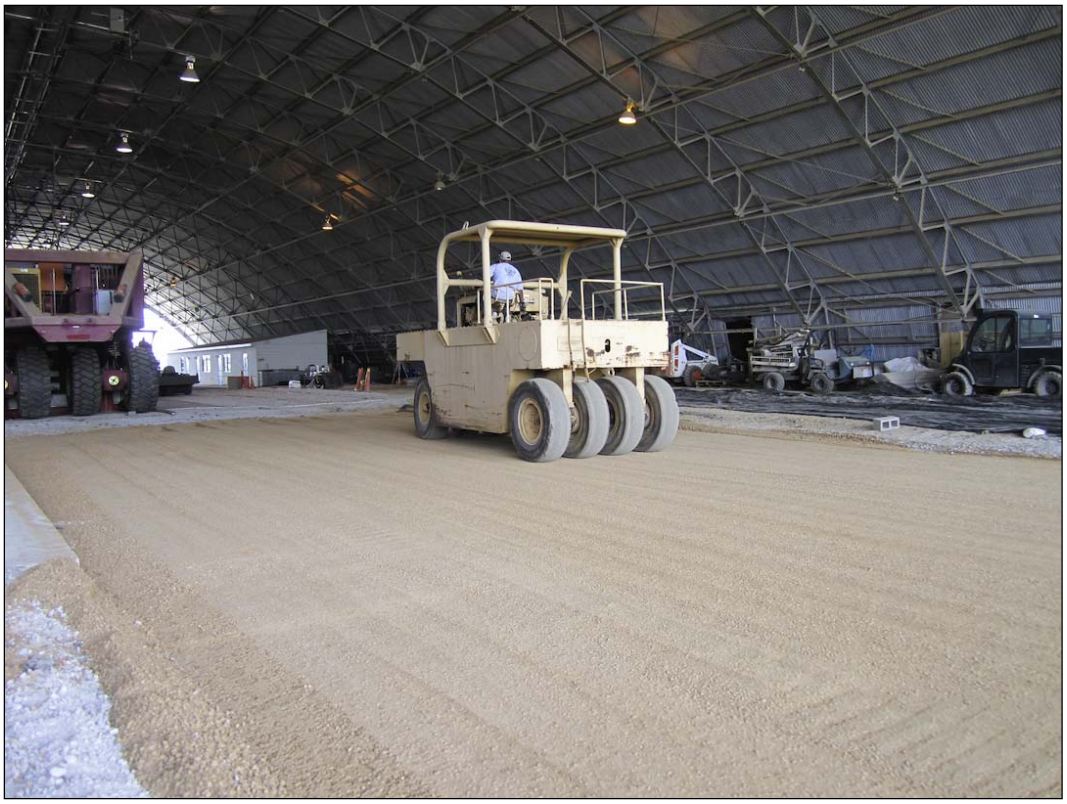

Figure 17. Rubber tire roller compacting GM base course material.

Table 10. In situ base test results.

Base Lift	Average CBR[a] (%)	Average Oven Moisture Content (%)	Nuclear Density Gauge	
			Average Dry Density (pcf)	Average Moisture Content (%)
1	25.7	3.1	132.7	3.5
2	25.8	2.6	129.7	3.0
Average	25.8	2.9	131.2	3.3

[a] CBRs difficult to measure because of loose gravel material, resulting in lower measured strength values.

The in situ base course CBRs were lower than those measured in the laboratory at approximately the same density and moisture content. The laboratory CBRs were measured on base course samples tightly compacted in a test cylinder, and the field CBR tests were conducted on in situ base course material that could not be as tightly compacted.

Therefore, it was difficult to measure the same strength in the field without the confinement of the brick surface layer. CBR testing is more reliable for cohesive soils than for gravelly soils. The base course material was believed to have greater actual strength than what the in situ CBR test results showed.

Dynamic Cone Penetrometer (DCP) tests were conducted on each test item as an alternative strength measurement to the in situ CBR tests conducted on the base layer. The DCP test measures the resistance of a material to penetration by repeatedly dropping a 17.6-lb sliding hammer down a 1-in.-diam metal rod. The measurements are recorded in terms of millimeters penetrated per hammer blow.

The DCP was used after the bricks were laid by drilling a 1-in.-diam hole through the brick to get to the surface of the base layer. The CBR of the base course in each item was determined based on a correlation procedure recommended in ASTM D 6951-03 (ASTM 2003). The DCP tests were conducted on each item immediately before trafficking began. Items 1 and 2 were trafficked at the same time. Approximately 3 weeks later, Items 3 and 4 were trafficked simultaneously. Items 5 and 6 were trafficked simultaneously approximately 2 weeks after trafficking of Items 3 and 4. DCP testing of Items 1, 2, and 3 measured CBRs ranging from 55 to 60, while the CBRs of Items 4, 5, and 6 ranged from 80 to 100. As expected, these correlated CBR results were much higher than the in situ CBR test results. Also, it was evident from the increasing CBR values determined from the DCP tests that the base material strengthened with time before traffic began.

Concrete edge restraint

A 4-in.-wide concrete edge restraint was added to the perimeter of the test section and between each lane to aid in keeping the bricks stable during construction and trafficking. The curbing was constructed with a machine that continuously poured concrete through a steel mold. The concrete had essentially zero slump because of the great number of fibers in the mixture. This was important to assure that the curb stayed in its desired form during placement. The concrete curb was constructed after the base course layer was completed. Figures 18 and 19 show the installation of the curb.

Geotextile and bedding sand

A geotextile was placed on top of the base course to serve as a barrier between the bedding sand and the base course layer. An approximately 1.25-in.-thick layer of bedding sand was placed on top of the geotextile as the bricks were installed. With a folding ruler, the bedding sand thickness was measured in random locations as it was spread and leveled.

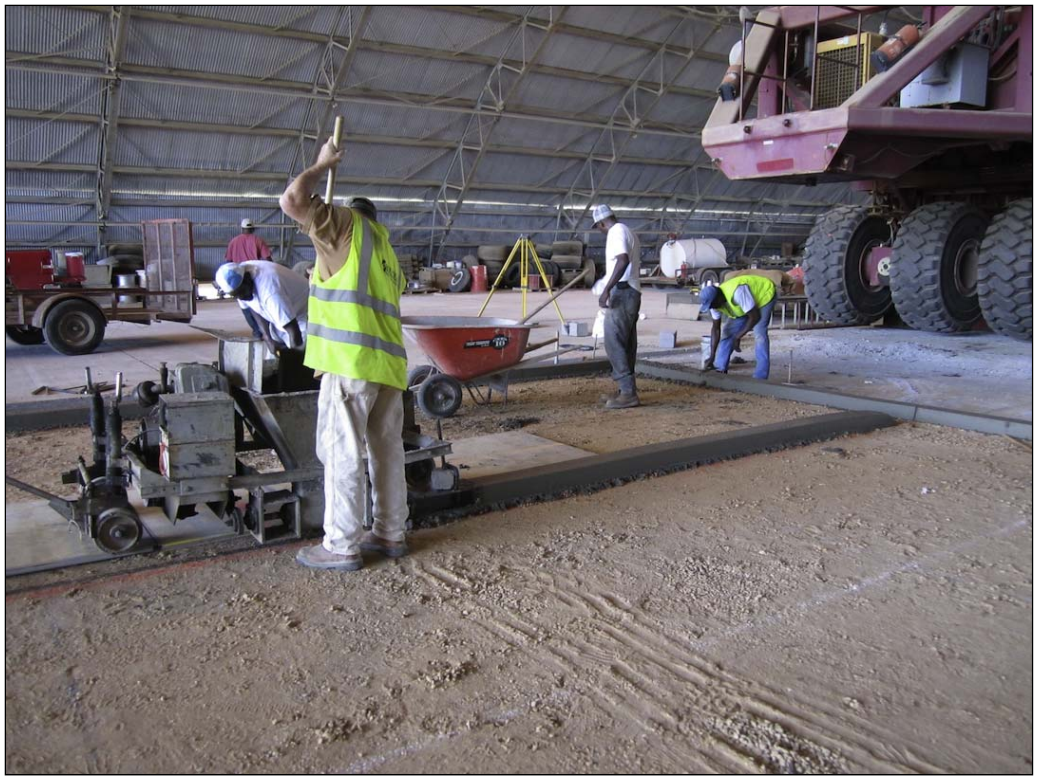

Figure 18. Installing concrete curbing between test section items.

Figure 19. Installing concrete curbing.

Brick surface

The bricks were laid by hand on top of the bedding sand in a herringbone pattern (45-deg angles to each other) between the concrete curbing. The bricks initially were tapped into place using a rubber mallet. After the bricks were in place, a vibrating plate compactor was used to compact the bricks into the bedding sand. Sand was then swept into the joints of the bricks for adhesion and stability. A vibrating plate compactor was used again to help compact the sand in the joints. The process was repeated until the joints were completely filled with compacted sand. Figures 20 through 25 summarize the brick installation process.

Instrumentation

Each item was instrumented with three 9-in.-diam Earth Pressure Cells (EPC) to measure the in situ pavement response to the truck loading. No instrumentation data was collected with the C-17 load cart traffic. EPCs were installed 2 in. into the base and 2 in. into the subgrade to measure throughout the pavement system the vertical stress distribution caused by

Figure 20. Installing queen bricks and measuring and spreading bedding sand.

Figure 21. Partial brick test section before jointing sand.

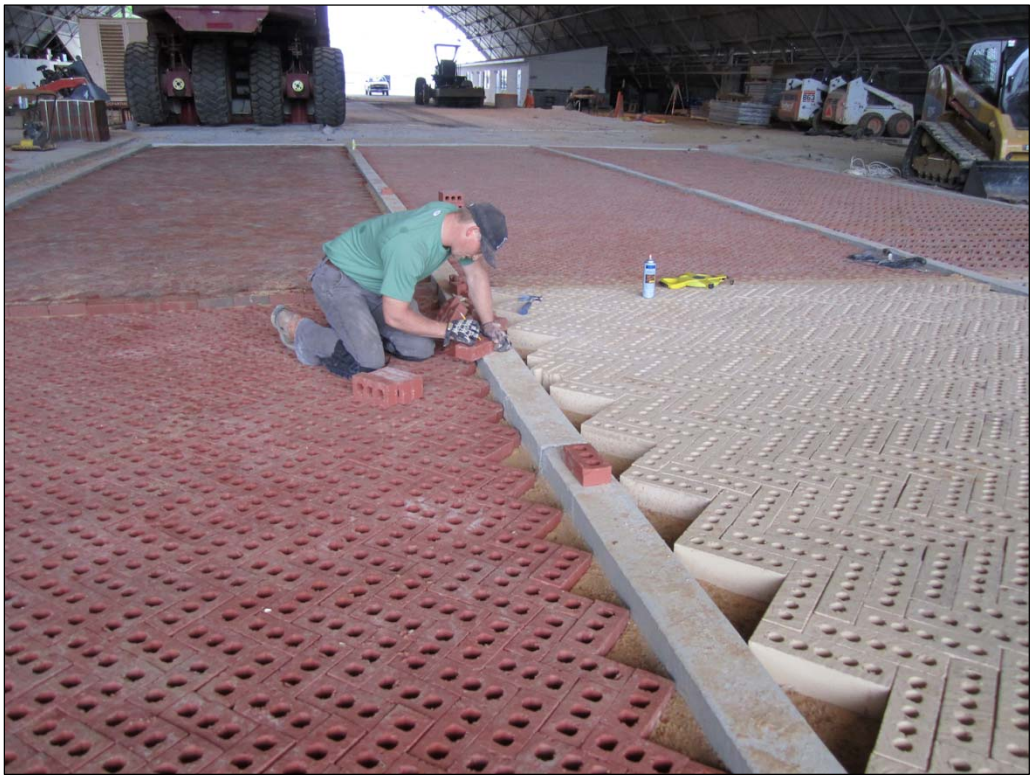

Figure 22. Measuring brick for installation at edges.

Figure 23. Sawing brick for installation at edges.

Figure 24. Using plate compactor to vibrate sand into joints.

Figure 25. Completed test section.

the wheel loads and tire pressures. Two EPCs were placed in the base to ensure that an accurate measurement was recorded because little to no information exists on the stress distribution under a brick surface. Two EPCs were installed in the center of the wheel path of the front and rear tires (one in the base and one in the subgrade), and one EPC was installed in the center of the path of the axle of the dual rear tires (in the base). Figures 26 and 27 present schematics of the instrumentation layout for the items.

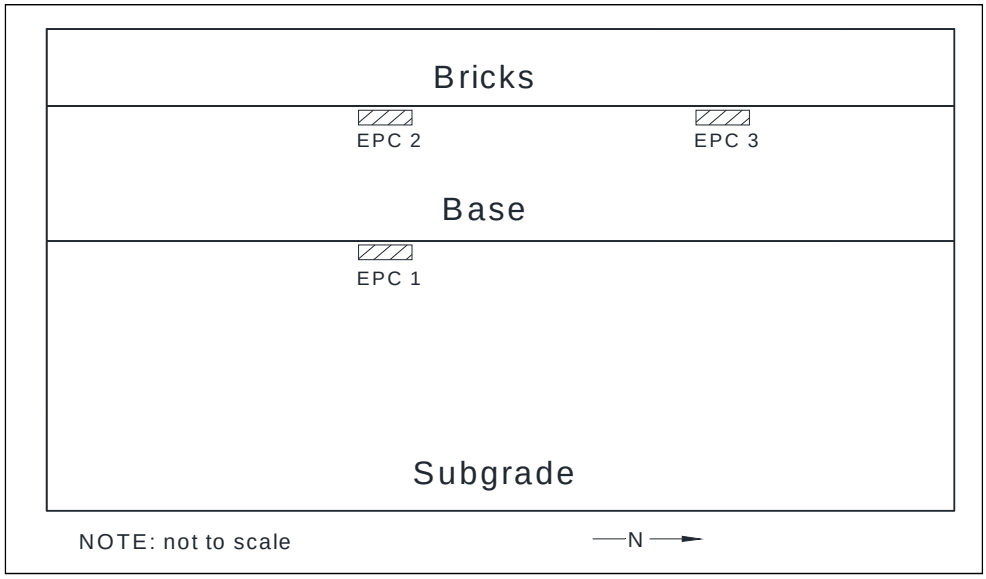

Figure 26. Example profile view showing instrumentation in each test item.

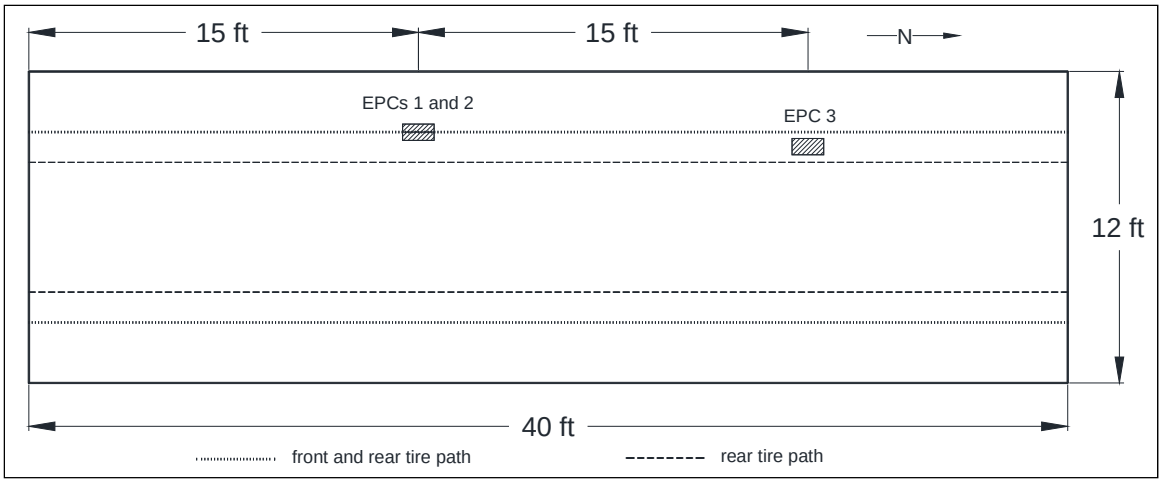

Figure 27. Plan view showing instrumentation locations of each test item.

4 Traffic and Evaluation Procedures

Traffic

Trafficking took place during the months of May, June, and July 2011 when the maximum daily air temperatures ranged from 65 to 99°F. The test section was free from environmental effects such as direct sunlight and rain because it was constructed under shelter at ERDC's Hangar 4 test facility.

The test section initially was trafficked in a channelized pattern using a dual-wheel, tandem-axle dump truck loaded to approximately 54,000 lb (Figure 28). Limestone was used to load the truck. The tire pressure of each wheel during trafficking was 109 psi. Trafficking was to conclude after 10,000 passes or when the test item failed. A flexible road pavement with truck traffic is considered failed when the brick surface layer has average surface rutting of 3 in.

Figure 28. Loaded commercial dump truck.

After completion of the dump truck traffic on each test item, the test section was trafficked with a single-wheel C-17 load cart to evaluate the brick surfaces for military aircraft parking. The C-17 load cart, with a load of

approximately 42,000 lb and a tire pressure of 142 psi, was trafficked down the center of each item in a channelized pattern. Trafficking was to conclude at 1,000 passes or shortly after the test item failed. The failure criterion for military aircraft traffic on flexible pavements typically is based upon 1 in. of surface rutting. Figures 29 and 30 show the single-wheel C-17 load cart on the test section.

Data collection

At selected pass intervals, the traffic was stopped, and the brick pavements were inspected for breakage, raveling, and rutting. Data collection during the scheduled truck traffic breaks included (1) rod and level measurements of left wheel path profiles and cross sections at each quarter point, (2) permanent deformation (rut depth) measurements, and (3) pressure cell measurements under dynamic loading. Data collection for the C-17 traffic included (1) rod and level measurements of the wheel path and cross sections at each quarter point and (2) permanent deformation measurements. With the exception of the instrumentation measurements, all data were collected at the same three quarter points (Stations 10, 20, and 30)

Figure 29. Single-wheel C-17 load cart.

Figure 30. Single-wheel C-17 load cart on test section.

each time. The instrumentation data were collected at Stations 15 and 30. The station numbers correspond to the distance from the beginning of the test item (north end; Station 0) in linear feet. The following paragraphs further explain the data collection procedures.

Rut depth

Rut depth measurements for each item were recorded in the far left and far right wheel paths of the channelized truck traffic. For the aircraft traffic, rut depth measurements were recorded in the center, west of the center, and east of the center wheel path.

For all traffic, the maximum total rut was recorded. The maximum total rut is defined as the elevation between the peak of the upheaval and the bottom of the ruts. Figure 31 shows a rut being measured in Item 1 after an interval of truck traffic.

Center-line and cross-section profiles

Rod and level measurements were conducted to aid in the calculation of the surface elevation change with increasing traffic. Longitudinal profiles were measured in the center of the far left wheel path for the truck traffic

Figure 31. Rut depth measurements on Item 1.

and in the center of the wheel path for the C-17 traffic. Cross-section profiles were measured at each quarter point (Stations 10, 20, and 30). All measurements were recorded in 6-in. increments. The results were used to illustrate the permanent surface deformation in the wheel paths and across each item with an increase in pass level. Figure 32 shows longitudinal profiles being measured in the left wheel path of Item 1 after an interval of truck traffic.

Instrumentation response

The instrumentation data, consisting of pressure cell measurements, was collected using dynamic readings over each device or stack of devices. At the start of the traffic intervals, the instrumentation data were recorded for approximately ten passes to show the response as the wheel moved toward and away from each device (Figure 33). Instrumentation data were not collected during C-17 trafficking.

Figure 32. Longitudinal rod and level profile readings on Item 1.

Figure 33. Collecting instrumentation measurements during truck traffic.

Forensic investigation

After all trafficking of the test section was completed, a 3-ft-wide trench was excavated across the center (Station 20) of each test item for forensic investigation. Each layer of the pavement structure at the center of the C-17 wheel path rut and in areas outside of the rut was removed and assessed. DCP tests, CBR tests, and oven moisture tests were completed at each location on each foundation layer (Figure 34). Furthermore, rod and level cross-section profile measurements (6-in. increments) were performed on the surface of each layer to aid in determining where failure occurred.

Figure 34. Subgrade CBR testing in trenched test item.

5 Brick Pavement Performance Results

Performance analysis

Failure of flexible road pavements subjected to truck traffic typically is defined as 3 in. of permanent deformation. Failure of flexible airfield pavements subjected to aircraft traffic is typically defined as 1 in. of permanent deformation. The definitions of failure for both types of traffic are based on pavement serviceability. Both vehicle and aircraft traffic need a smooth-riding surface for safety. Also, rut depths typically increase exponentially once a pavement receives permanent deformations at approximately its failure depth.

It is important to consider during the performance analysis that the test section was constructed and trafficked in a sheltered environment without the harsh effects of rain, direct sunlight, etc. Deterioration rates of the pavements likely will increase with precipitation or continued exposure to sunlight. The following sections give the evaluation results of each item for the vehicle and aircraft traffic.

Truck evaluation

Item 1

Item 1 was trafficked to 10,010 passes without failure. The queen bricks showed loss or settlement of sand between the bricks in the wheel paths after 10 passes. Figure 35 shows voids with missing sand between the bricks inside the wheel path at around 200 passes and compacted sand between the bricks outside of the wheel path. The bricks remained relatively flat throughout trafficking. There was little movement and little to no breaking of the queen bricks with the truck traffic.

The satisfactory performance of the queen bricks was surprising. The queen bricks had an average laboratory compressive strength of approximately 4,800 psi and an approximately 55 percent loss of material when they underwent the LAA test. Figure 36 shows Item 1 at the completion of 10,010 passes of truck traffic.

Figure 35. Item 1 truck traffic at approximately 200 passes.

Figure 36. Item 1 at completion of 10,010 passes of truck traffic.

Rut depths

Item 1 was capped at 10,010 passes with an average rut depth of 0.73 in. in the far left wheel path and 0.59 in. in the far right wheel path. Figure 37 shows the measured rut depths at the quarter points in the far left wheel path with increasing pass level. The measured ruts at Station 30 increased at a more rapid rate, around 800 passes, likely because of inconsistent compaction efforts during construction. The occasional minor decreases in rut depth were due to the position of the bricks when traffic was halted; some bricks might have been tilted slightly.

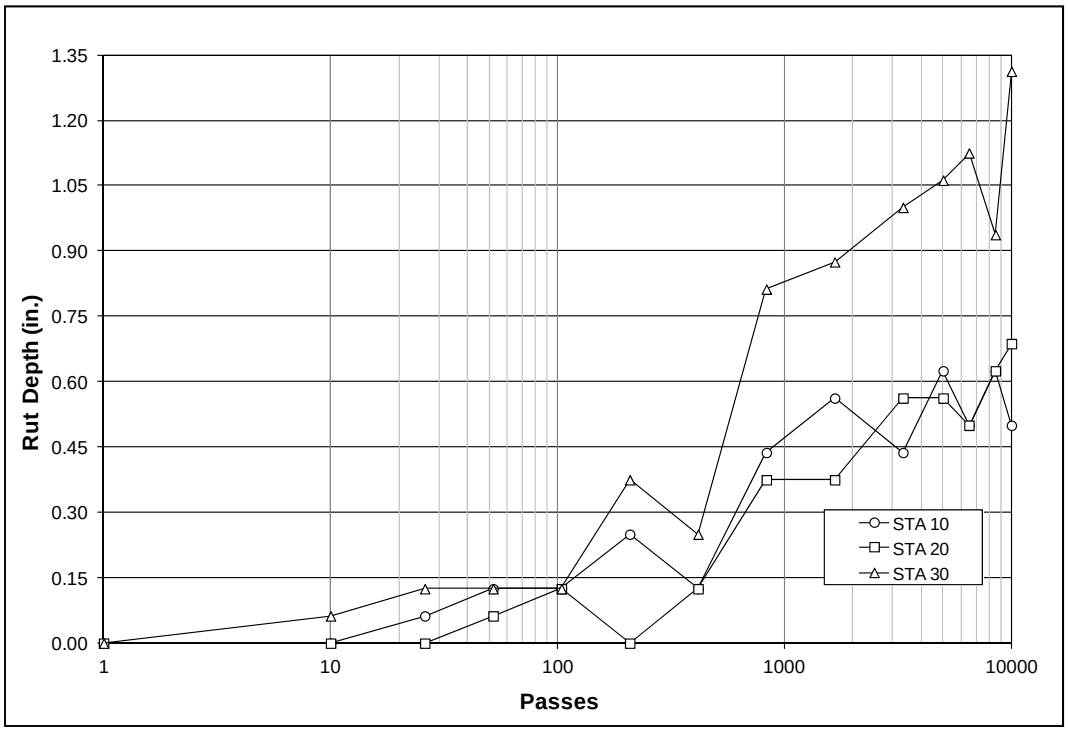

Figure 37. Item 1 rut depth measurements in left wheel path of truck traffic (west).

Profiles

Figure 38 shows the longitudinal profiles plotted against increasing passes. The profiles reveal that Item 1 was slightly weaker around Station 30. The longitudinal profiles were measured in the far left wheel path, which is the same area as the rut depth measurements shown in Figure 37. Immediate settlement of about 0.10 in. was shown after the first 10 passes. This likely was due to the bricks settling into the bedding sand with their first received load. There was a small, gradual decrease in elevation with each increasing pass interval. The greatest rut shown with the longitudinal profiles is approximately 0.84 in.

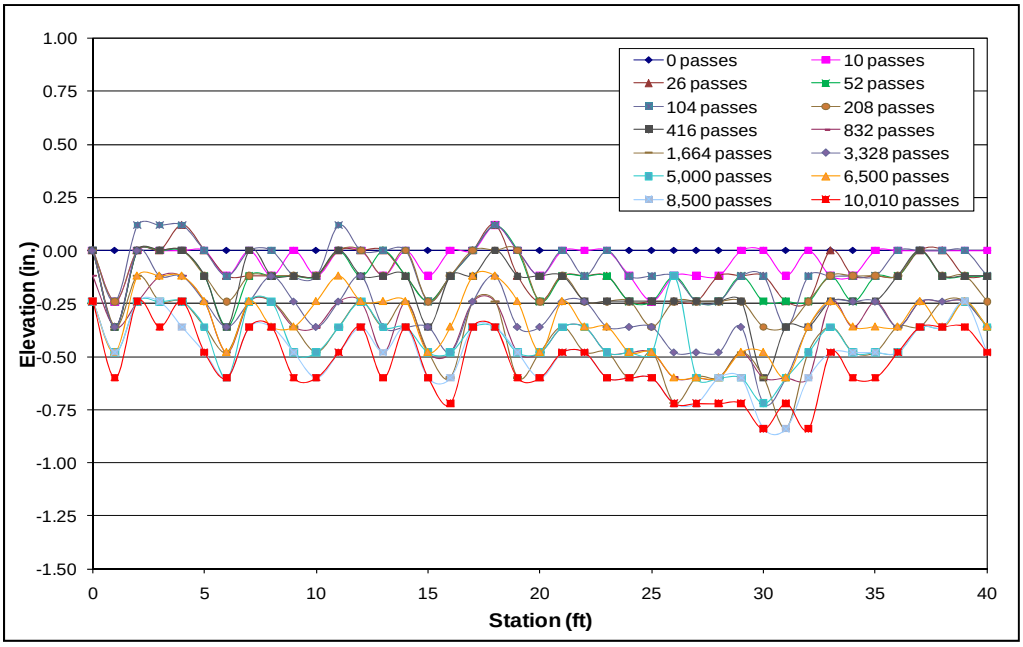

Figure 38. Item 1 longitudinal profiles in left wheel path of truck traffic.

Figure 39 shows the cross-section profiles measured at Station 30. Note that this was the weakest area of Item 1. The cross-section profiles show some upheaval of bricks during specific traffic intervals. There was movement of the bricks with traffic. The greatest upheaval was a spike of 0.48 in., and the greatest rut was 0.96 in.

Instrumented pavement response

Dynamic pressure measurements from the in situ instrumentation were collected at selected traffic intervals. Figure 40 shows a plot of average maximum pressure measurements recorded throughout the pavement structure for Item 1. The EPC measurements in the subgrade showed there was minimal change in pressure with increasing pass level. The EPCs installed in the base showed similar trends of decreasing pressure with increasing passes. The measurements of the EPC installed under the wheel path in the base were comparable with the measurements of the EPC installed between the two tires in the base.

Item 2

Item 2 consisted of recycled bricks. Figure 41 shows the bricks before trafficking. The recycled bricks performed adequately to 10,010 passes without failure. Note that the laboratory tests revealed an average compressive strength of only 3,500 psi and a 44 percent loss in material measured with the LAA tests.

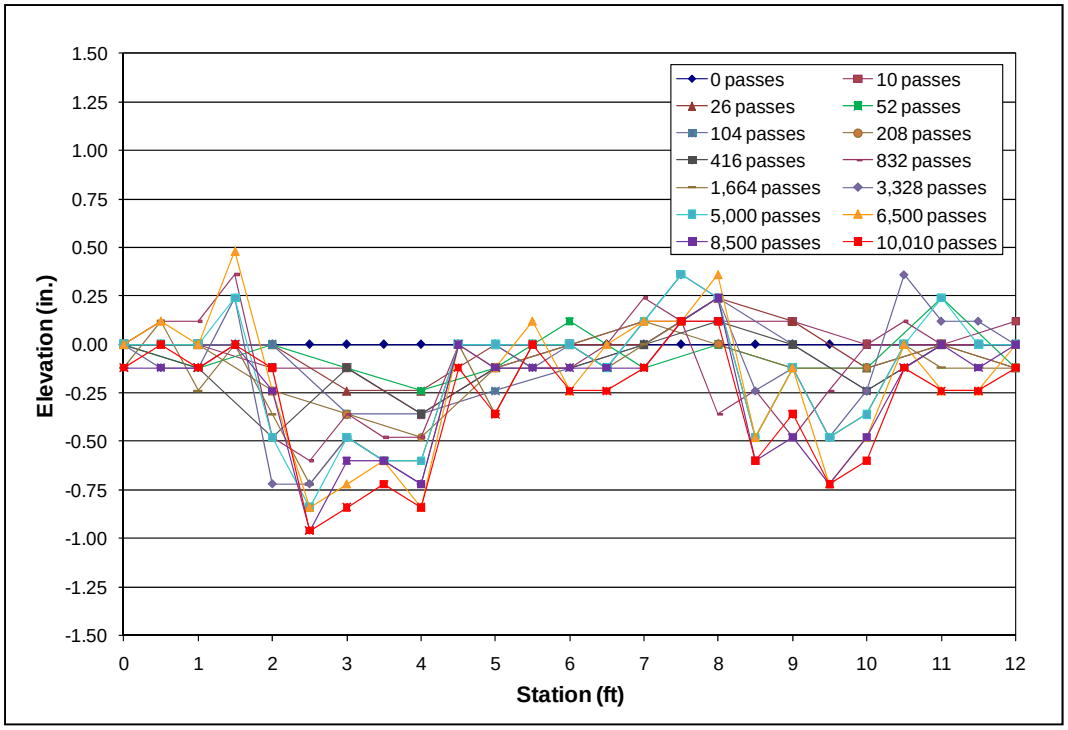

Figure 39. Item 1 cross-section profiles at Station 30 with truck traffic.

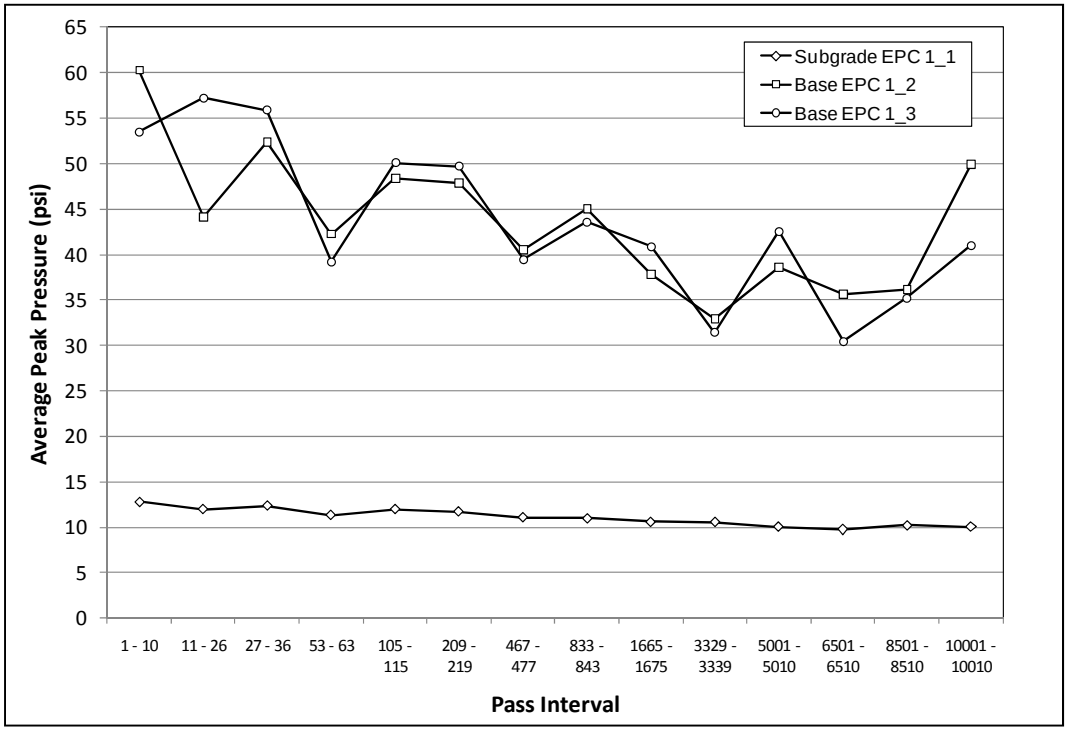

Figure 40. Item 1 average peak pressure measurements at various traffic intervals.

Figure 41. Reclaimed bricks before truck traffic.

As was the case for Item 1, there was movement or settlement of the bricks after 10 passes. The bricks began shoving upward around 400 passes, and very few broken bricks were observed beginning around 800 passes. After 5,000 passes, there were more broken bricks and a larger amount of shoved, tilted bricks (Figure 42). Figure 43 shows Item 2 after the completion of truck traffic at 10,010 passes.

Rut depths

After 10,010 passes, the average rut depths in the left and right wheel paths for Item 2 were 0.80 and 1.10 in., respectively. Figure 44 shows the rut depths increasing with pass level in the right wheel path. The rut depths at the three quarter points (Stations 10, 20, and 30) had similar measurements. Figure 44 also shows the rut depth beginning to increase at a greater rate around 200 passes.

Profiles

Figures 45 and 46 show the longitudinal and cross-section profiles (Station 30), respectively, of Item 2. The profiles show almost immediate brick settlement and shifting at 10 passes. The cross-section profiles show a sufficient amount of upheaval with shifted bricks outside the wheel paths, particularly the right wheel path (Stations 7.5 to 11.5).

Figure 42. Reclaimed bricks at 5,000 passes of truck traffic.

Figure 43. Item 2 at completion of 10,010 passes of truck traffic.

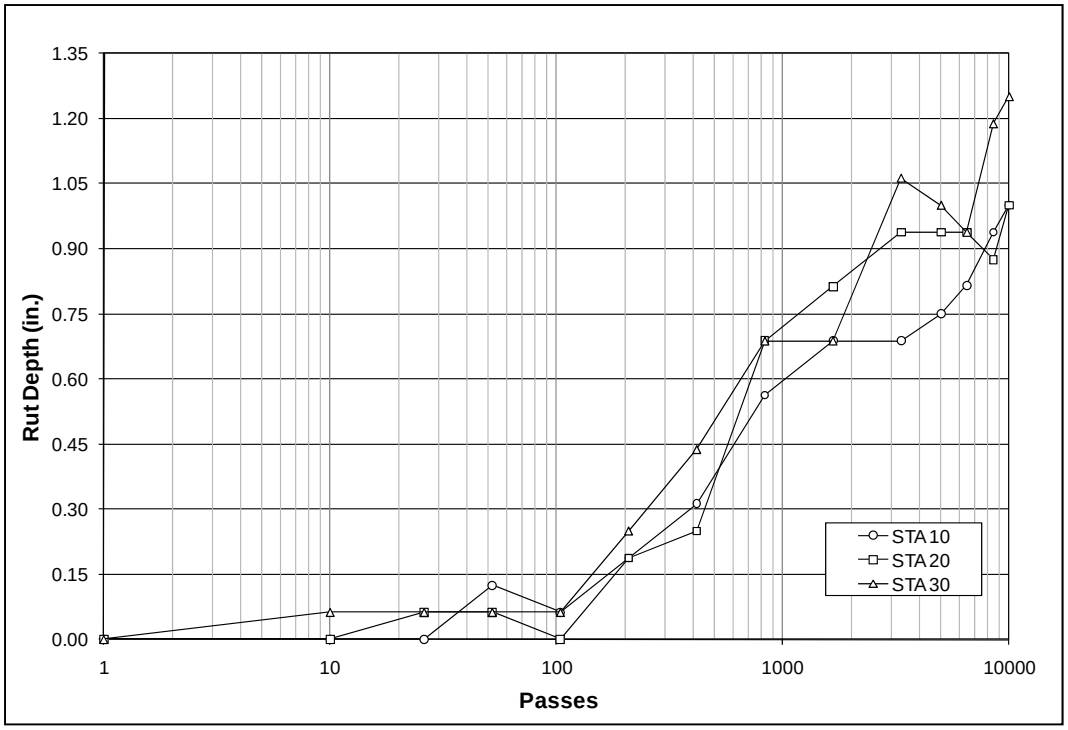

Figure 44. Item 2 rut depth measurements in right wheel path of truck traffic.

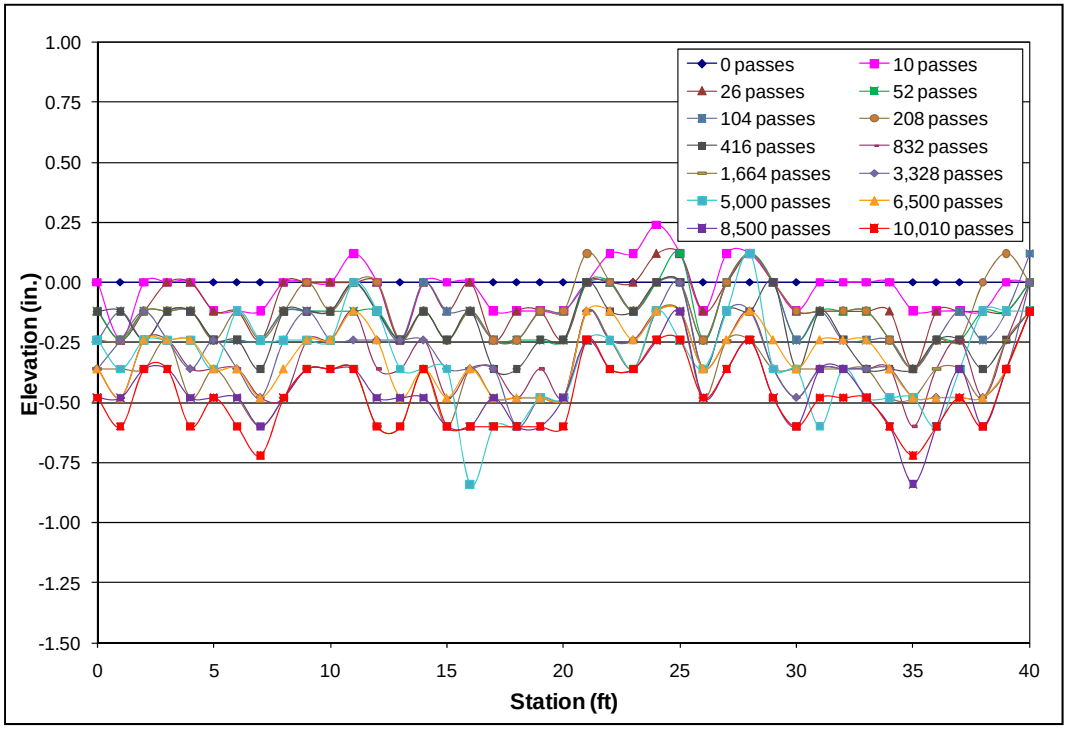

Figure 45. Item 2 longitudinal profiles in left wheel path of truck traffic.

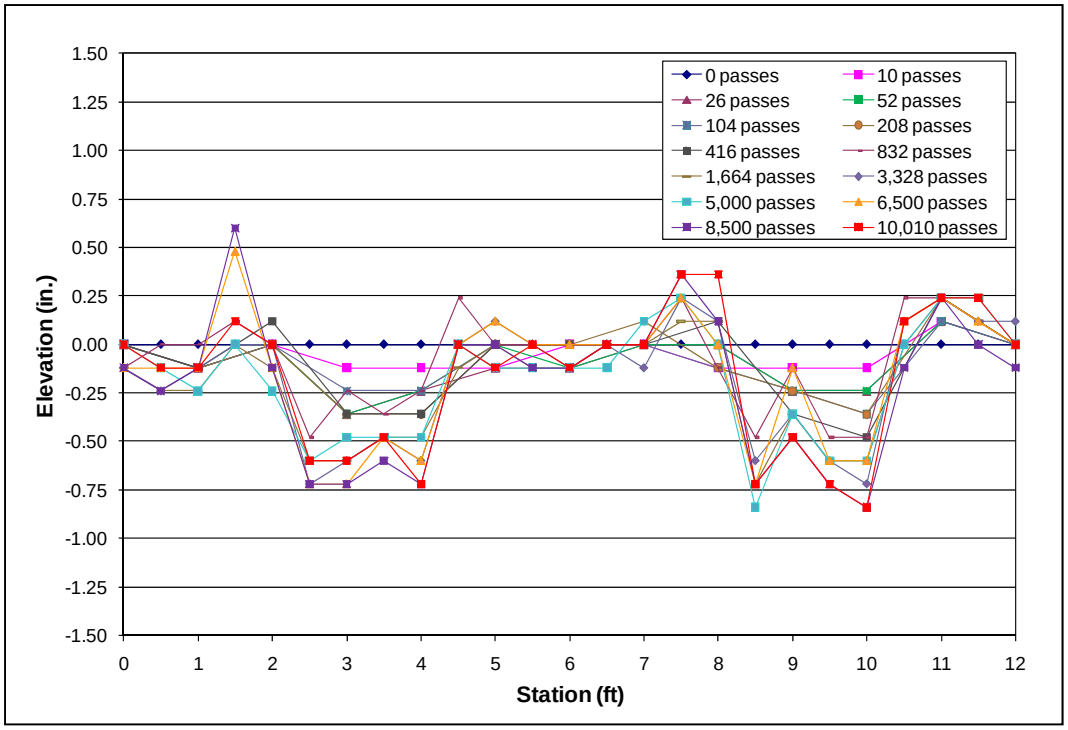

Figure 46. Item 2 cross-section profiles at Station 30 with truck traffic.

Instrumented pavement response

Figure 47 shows the average peak pressure measurements in the base and subgrade with dynamic loading during the traffic intervals. The subgrade EPC measured a somewhat steady pressure of 15 psi, although there was a slight decreasing trend with increasing traffic. The two EPCs installed on top of the base did not give similar measurements in the first 500 passes, as was the case for Item 1. EPC 2_2 was installed directly under the tire, while EPC 2_3 was installed between the two tires; it was not surprising for EPC 2_2 to have higher pressures than EPC 2_3. Also, given that there was movement of the bricks during trafficking, there likely was slight movement of the EPCs.

Item 3

The standard modular bricks of Item 3 were trafficked until 10,010 passes were reached without being close to the failure point of 3 in. of surface rutting. The performance of the standard modular bricks was not surprising. The laboratory tests revealed a compressive strength of approximately 19,500 psi and about 26 percent loss with the LAA tests.

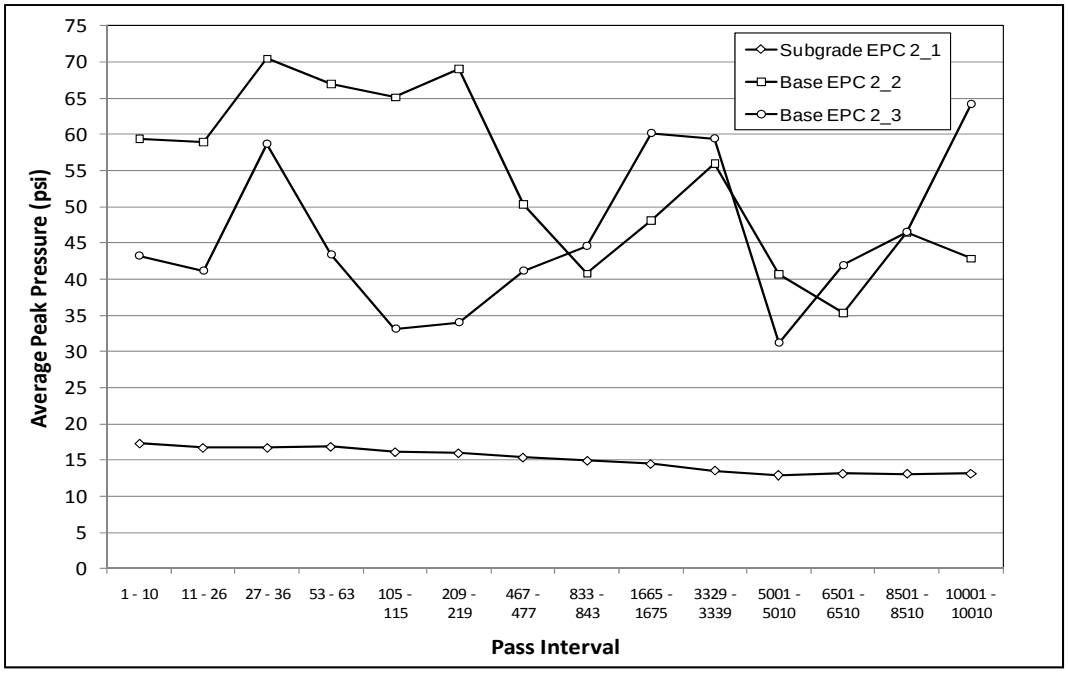

Figure 47. Item 2 average peak pressure measurements at various traffic intervals.

Figure 48 shows the bricks in the wheel path before the truck trafficking began. After the 10,010 pass cap, there was only slight upheaval outside of the wheel paths (approximately 0.25 in.). Figure 49 shows the area where the most upheaval was observed following traffic completion. There also were a few broken bricks within the test item beginning with about pass 1,200; most were broken in half.

Rut depths

The rut depths measured from the left wheel path are plotted against pass level in Figure 50. Judging by the large increase in rut depth rate at approximately 800 passes, Station 20 appeared to be a slightly weaker area than the rest of the test item. The average rut depth measured from Item 3 (calculated from the left and right wheel paths) was 0.65 in.

Profiles

Figures 51 and 52 show the longitudinal profiles in the left wheel path and the cross-section profiles at Station 10, respectively. The longitudinal profiles show there was essentially no upward shifting of the bricks inside the wheel path; however, there was some upheaval outside of the wheel paths beginning with 50 passes, as shown in Figure 52. The profile plots show there was steady settlement of the standard modular bricks with traffic.

Figure 48. Item 3 wheel path before truck traffic.

Figure 49. Item 3 wheel path at 10,010 passes of truck traffic.

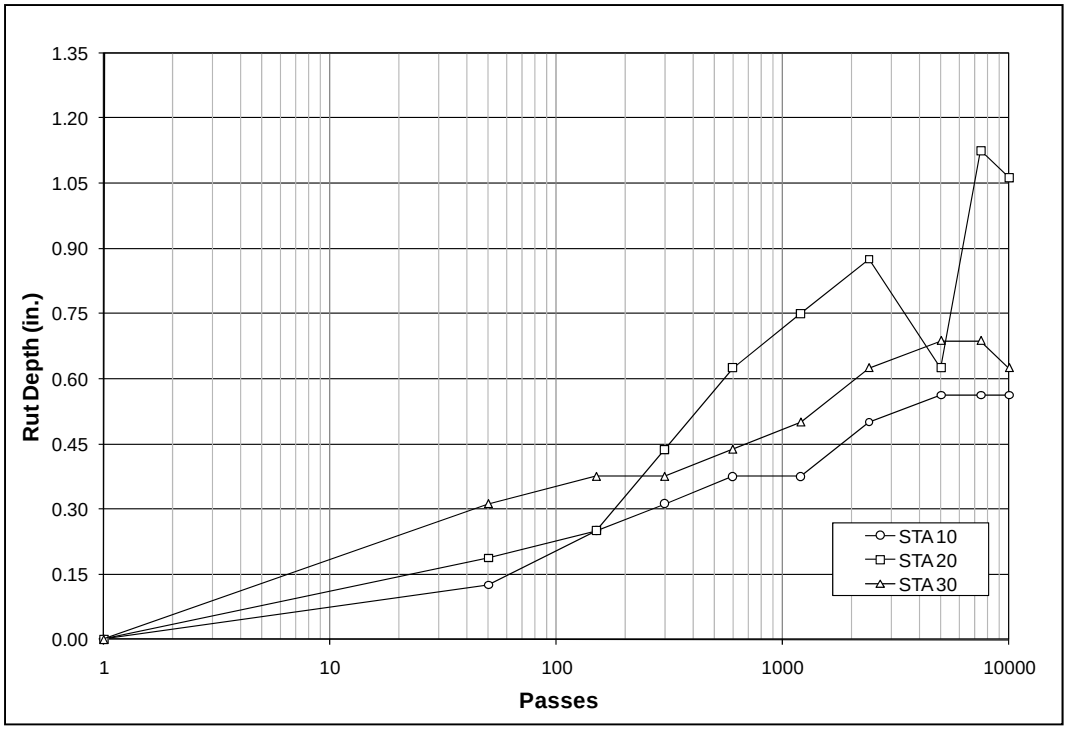

Figure 50. Item 3 rut depth measurements in left wheel path of truck traffic.

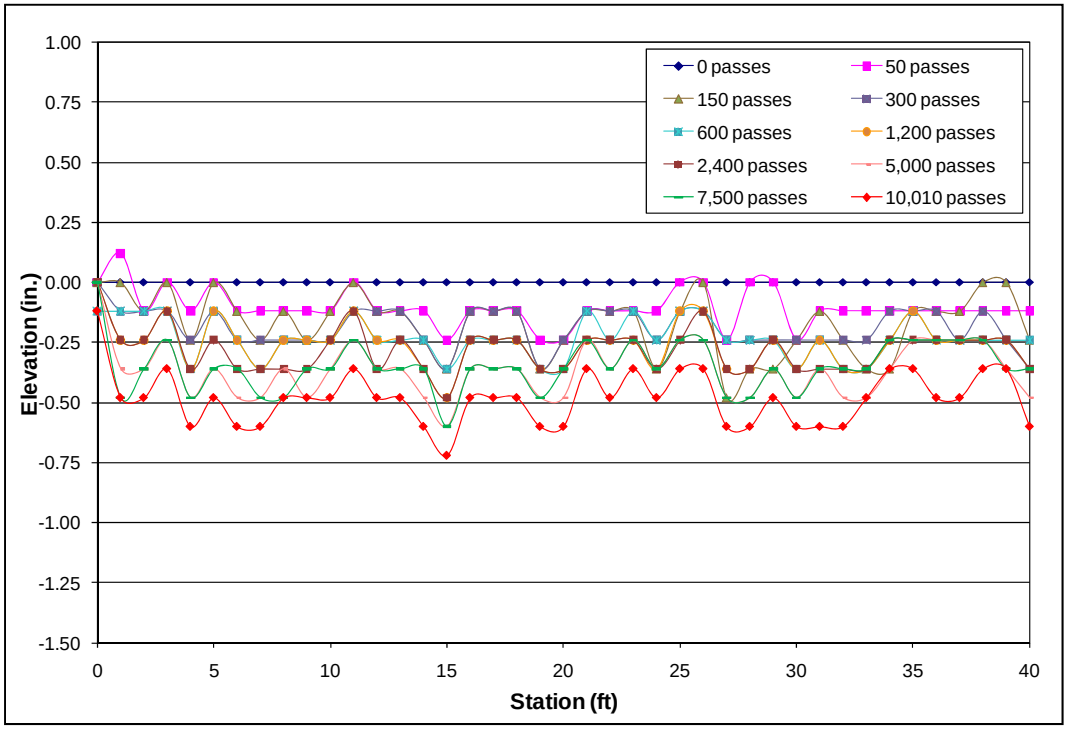

Figure 51. Item 3 longitudinal profiles in left wheel path of truck traffic.

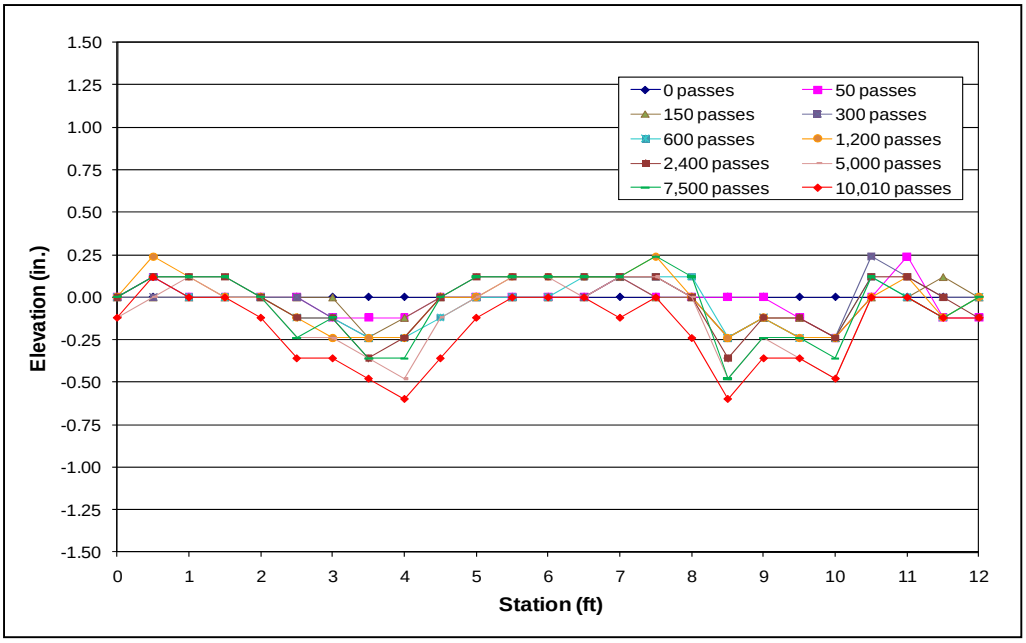

Figure 52. Item 3 cross-section profiles at Station 10 with truck traffic.

Instrumented pavement response

Figure 53 shows the average peak pressure measurements recorded with the EPCs during truck trafficking. The EPC installed in the subgrade measured essentially 15 psi throughout trafficking. With the exception of a couple of traffic intervals, the two EPCs installed in the base measured similar average peak pressures. With dynamic truck loads on standard modular bricks, the average maximum pressures in the base were approximately 40 psi (EPCs installed approximately 5.5 in. deep).

Item 4

Item 4 consisted of the thicker, wider, and longer utility bricks. Figure 54 shows the utility bricks in the wheel path before the truck traffic began. The average compressive strength determined in the laboratory for the bricks was approximately 10,600 psi. Laboratory LAA tests measured approximately 42 percent loss of material.

Overall, the utility bricks performed well with little rutting and movement. Traffic was capped at 10,010 passes with an average rut depth of 0.46 in. Figure 55 shows an overall view of Item 4 at 1,200 passes. Chipped and broken corners were observed on some of the utility bricks starting around 1,200 passes. The chipped and broken corners can be seen in Figure 56. Figure 57 shows the bricks after the completion of 10,010 passes of truck traffic.

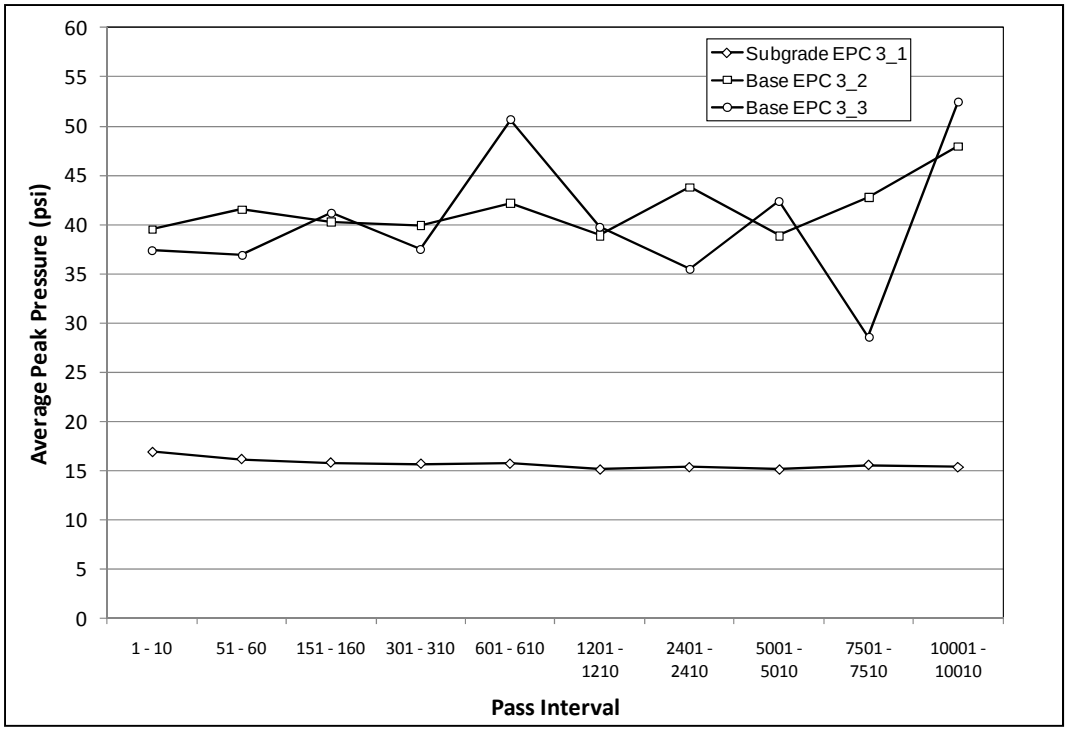

Figure 53. Item 3 average peak pressure measurements at various traffic intervals.

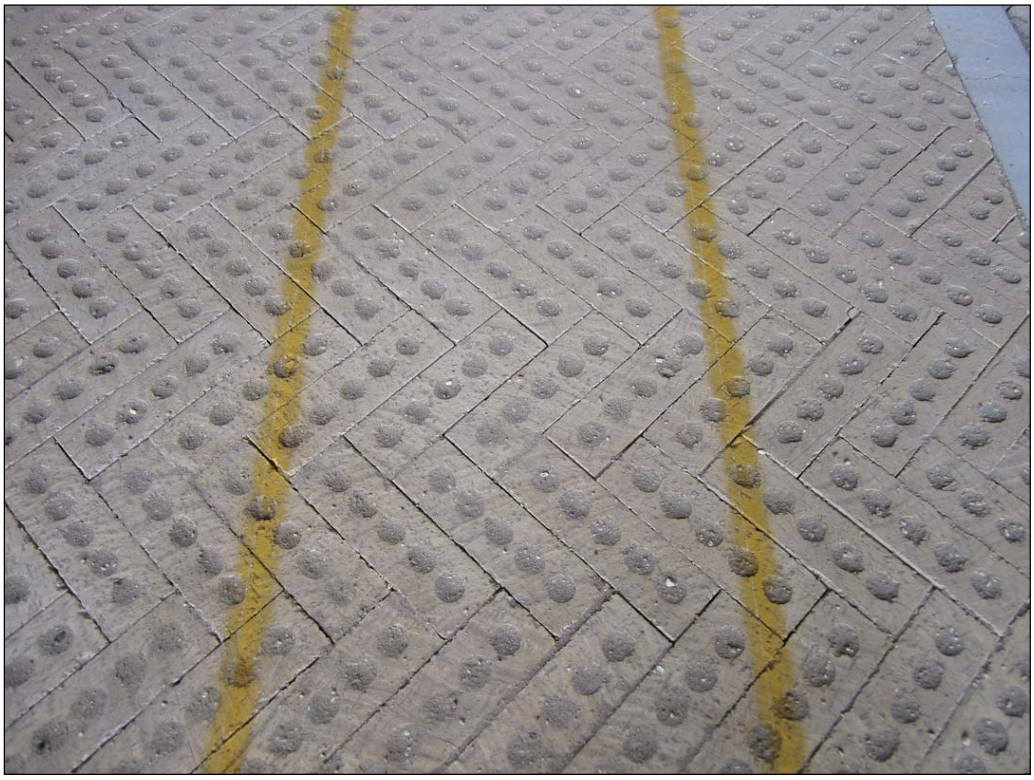

Figure 54. Item 4 utility bricks before truck traffic.

Figure 55. Item 4 overall view at 1,200 passes of truck traffic.

Figure 56. Chipped and broken edges of utility bricks in Item 4 at 1,200 passes of truck traffic.

Figure 57. Item 4 at 10,010 passes of truck traffic.

Rut depths

The rut depths were measured at various traffic intervals in the left and right wheel paths. The average rut depths at 10,010 passes in the left and right wheel paths were 0.43 and 0.48 in., respectively. Figure 58 shows the rut depth measurements with increasing passes in the right wheel path. The occasional minor decreases in rut depth, particularly toward the end of trafficking, were due to the position of the bricks when traffic was halted; there was more brick movement as the traffic level increased.

Profiles

The longitudinal profiles in the left wheel path are shown in Figure 59. The longitudinal profiles show the north end of the test item (Stations 20 to 40) is slightly weaker than the south end. This was observed after the first 50 passes of truck traffic. The greatest rut, one of approximately 0.75 in., was observed on the north end of the test item at 10,010 passes.

Figure 60 shows the cross-section profiles with increasing traffic at Station 20. The positions of the four rear wheels are easily visible in the cross-section profile plot. From Figure 60, the two left wheels are between Stations 2 and 4.5, and the two right wheels are between Stations 8 and 10.5. There is approximately 6 in. of space between each outside and

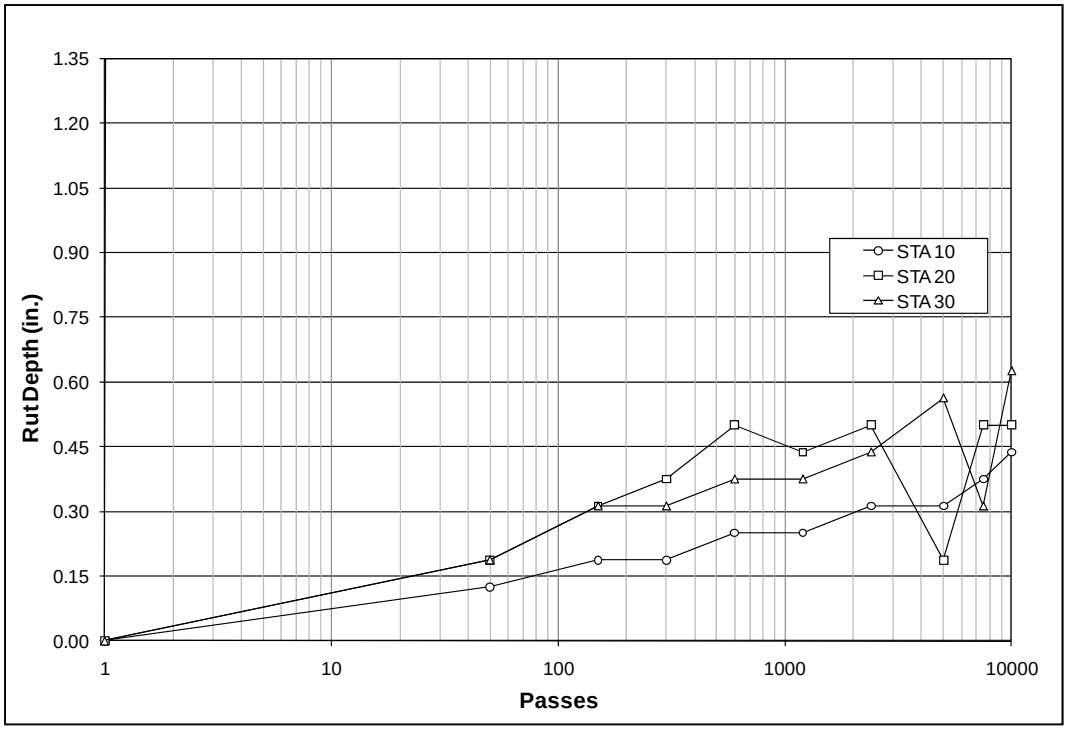

Figure 58. Item 4 rut depth measurements in right wheel path of truck traffic.

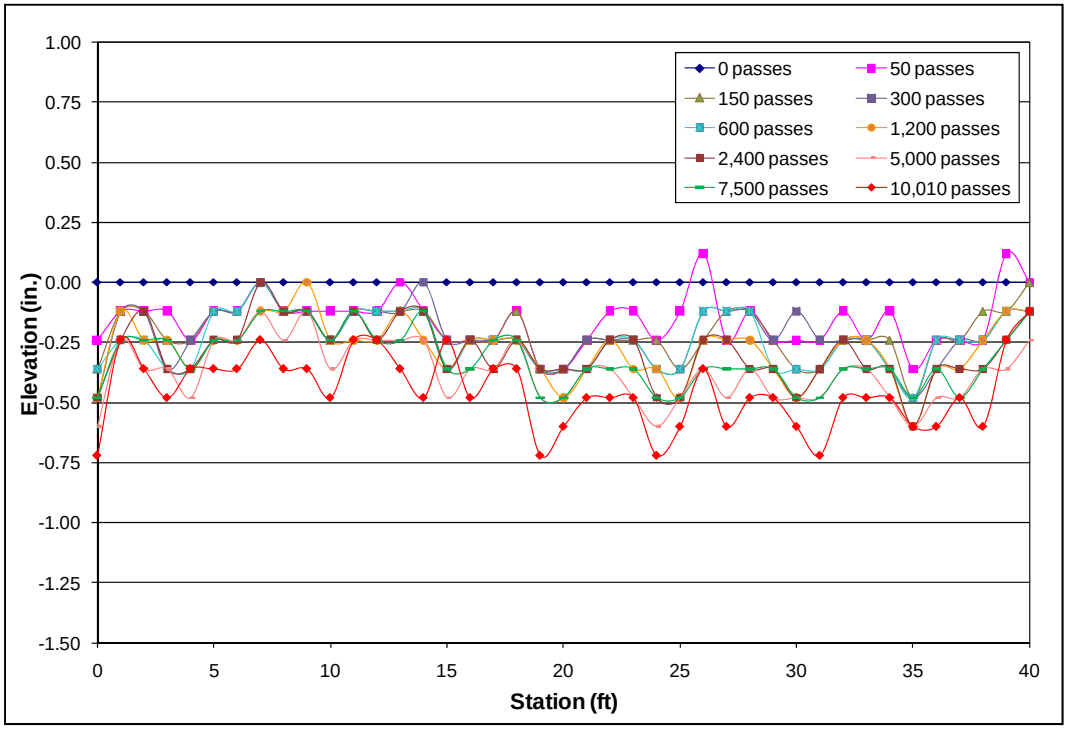

Figure 59. Item 4 longitudinal profiles in left wheel path of truck traffic.

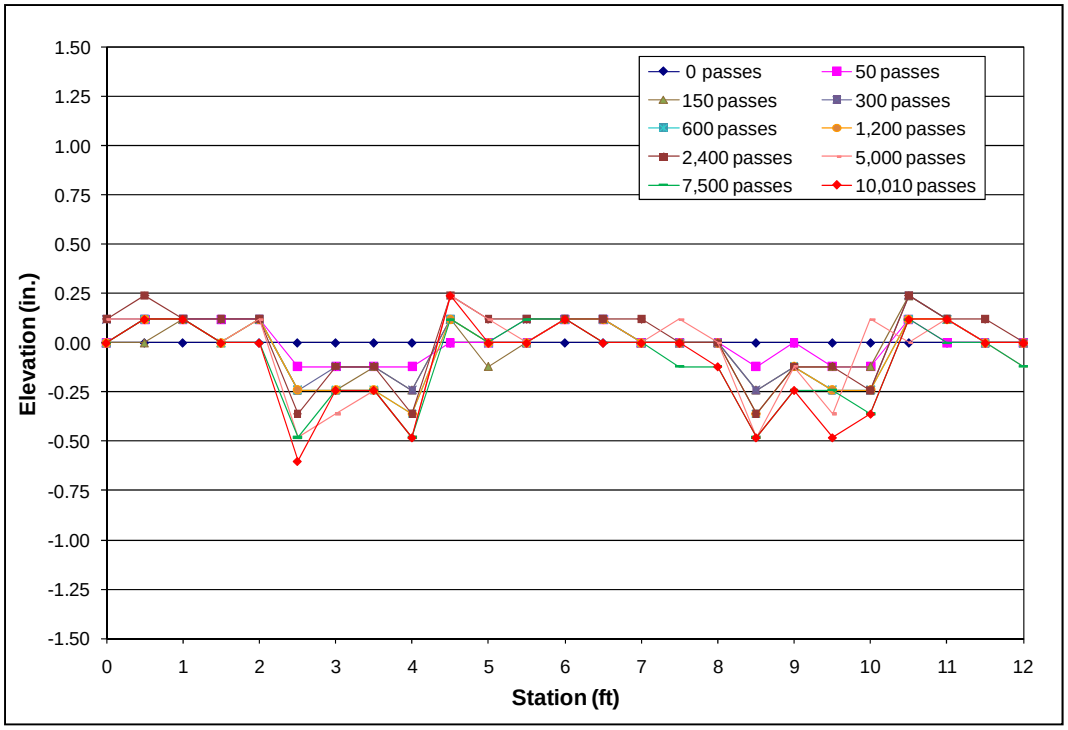

Figure 60. Item 4 cross-section profiles at Station 20 with truck traffic.

inside tire. The cross-section profile at Station 20 shows there is minimal upheaval of the utility bricks (maximum of 0.25 in.), and the greatest rut does not exceed 0.60 in.

Instrumented pavement response

Figure 61 shows the average peak EPC measurements in the subgrade and base at various truck traffic intervals. EPC 4_1, installed in the subgrade, showed a somewhat steady pressure of approximately 10 psi. Not surprisingly, the EPC installed under the wheel path in the base, EPC 4_2, recorded pressures slightly higher than the EPC installed between the two tires in the base, EPC 4_3. More direct pressure was applied to EPC 4_2.

Item 5

Item 5 consisted of the brick pavers, which were used as the control for the evaluation. Figure 62 shows the brick pavers before trafficking. Note the tight fit of the bricks in the test item. This is due to the brick pavers' uniform shape.

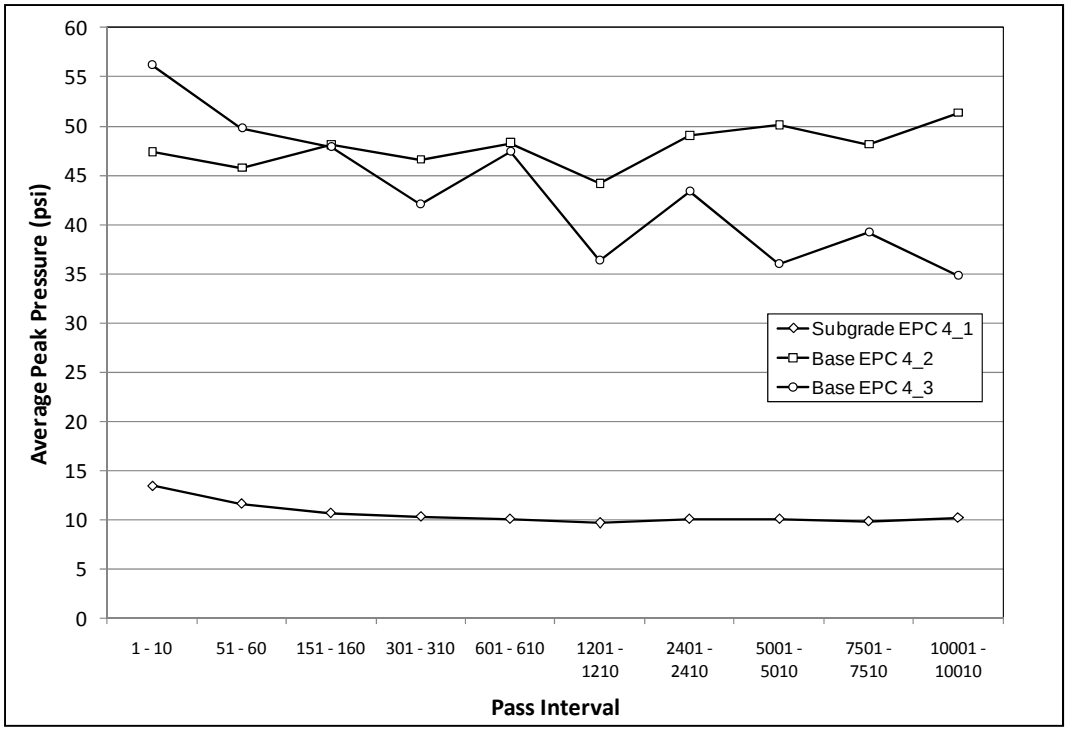

Figure 61. Item 4 average peak pressure measurements at various traffic intervals.

Figure 62. Item 5 brick pavers before truck traffic.

A comparison of all bricks tested showed the brick pavers did not have the highest compressive strength, but they did have the lowest percentage of material lost, as determined from the LAA tests. The average compressive strength determined in the laboratory was approximately 17,300 psi, and the LAA measured an average material loss of 23 percent.

Item 5 was trafficked to 10,010 passes without being close to the 3-in.-deep rut failure point. The brick pavers were observed to begin shifting upward at the corners outside of the wheel paths around 2,400 passes. Almost no brick pavers were broken during the truck trafficking. Figure 63 shows the brick pavers at 10,010 passes.

Figure 63. Item 5 overall view at 10,010 passes of truck traffic.

Rut depths

Figure 64 shows the rut depths measured in the right wheel path of Item 5. The average rut depth in the right wheel path was 0.52 in., and the average rut depth in the left wheel path was 0.49 in. These averages are well below the failure point of 3 in. of surface rutting. The rut depths at the quarter points were similar throughout trafficking.

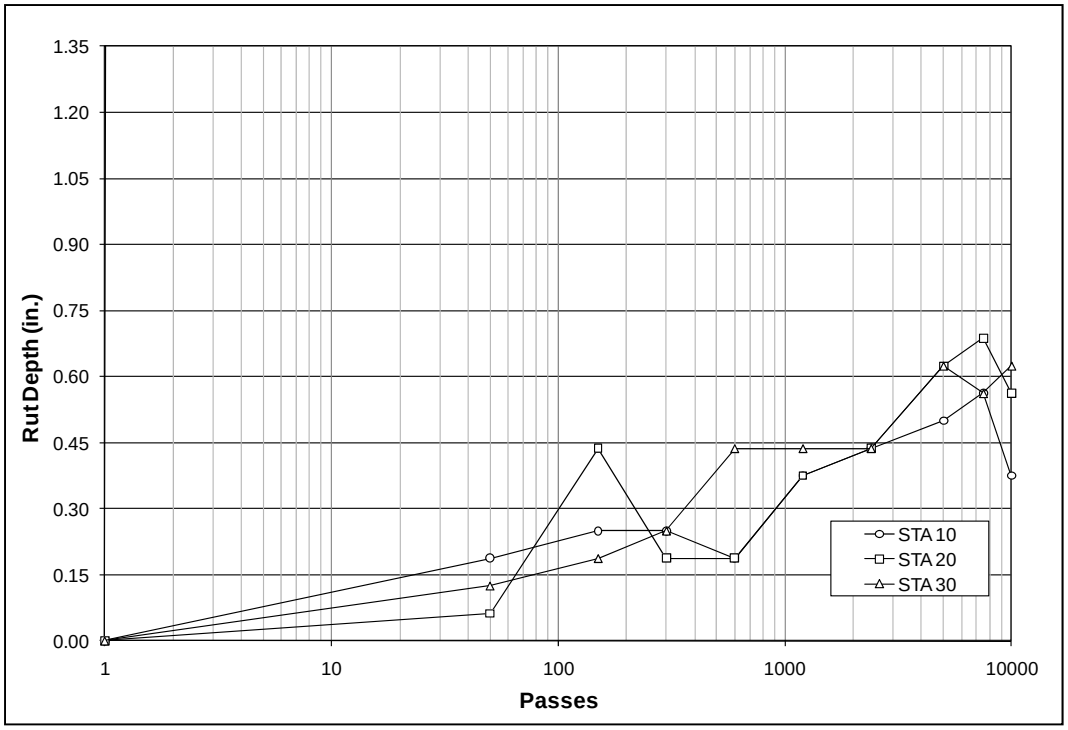

Figure 64. Item 5 rut depth measurements in right wheel path of truck traffic.

Profiles

Rod and level measurements were plotted to visualize the longitudinal and cross-section profiles shown in Figures 65 and 66, respectively. The longitudinal profiles measured in the left wheel path show a small but steady decrease in elevation with an increase in traffic. The cross-section profiles at Station 20 show a small amount of upheaval outside the wheel paths. Both figures show maximum rut depths of approximately 0.50 in. at 7,500 and 10,010 passes.

Instrumented pavement response

The average peak pressures measured with the EPCs are shown in Figure 67. A large decrease in peak pressure is observed with EPC 5_3 beginning at 1,200 passes. At approximately 1,200 to 2,400 passes, some of the bricks were observed to be moving a small amount. This might have caused more movement in the base course, affecting the measurements of EPC 5_3. The EPC installed in the top of the subgrade showed peak measurements similar to those of the previous test items.

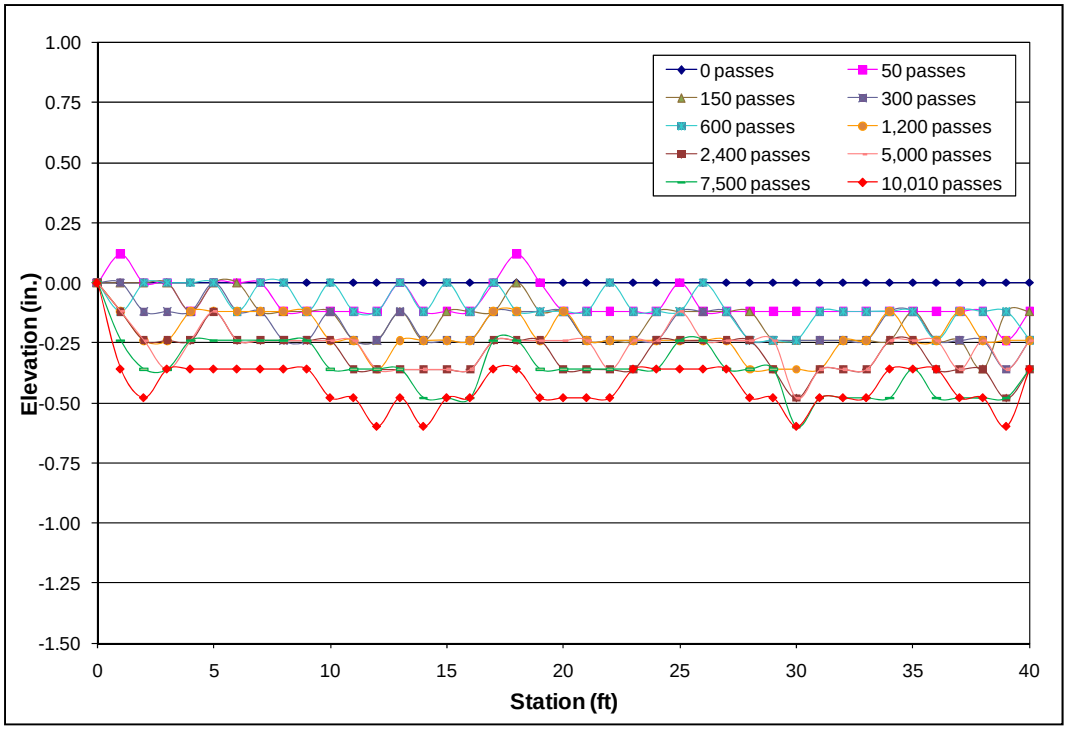

Figure 65. Item 5 longitudinal profiles in left wheel path of truck traffic.

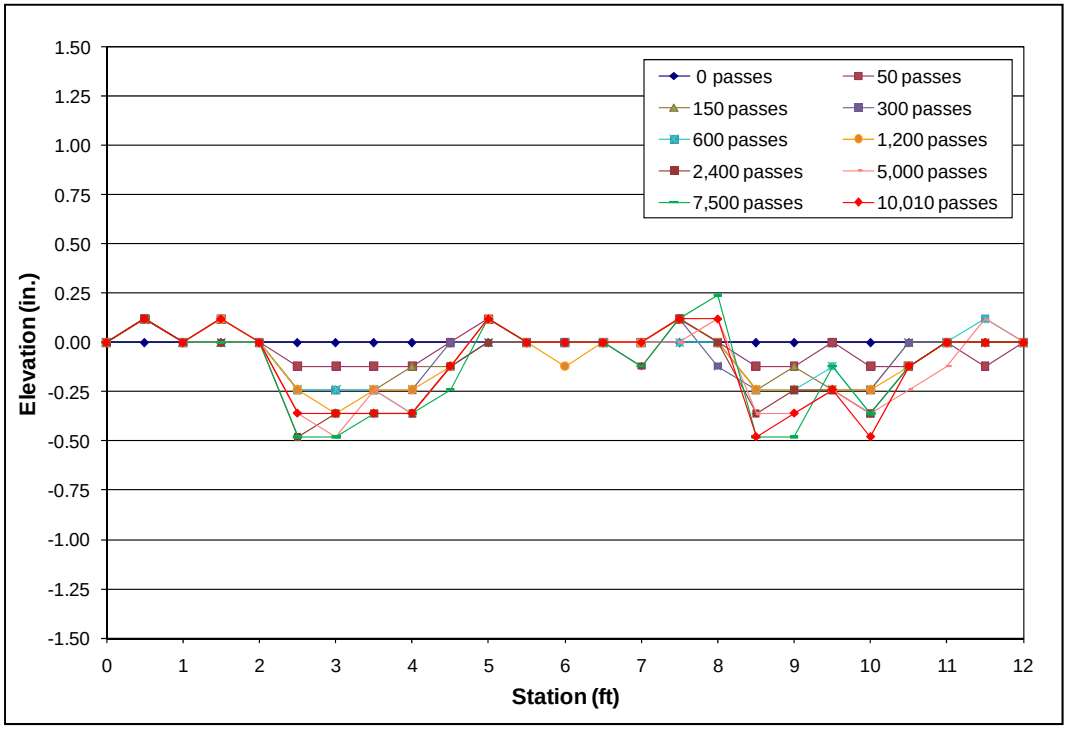

Figure 66. Item 5 cross-section profiles at Station 20 with truck traffic.

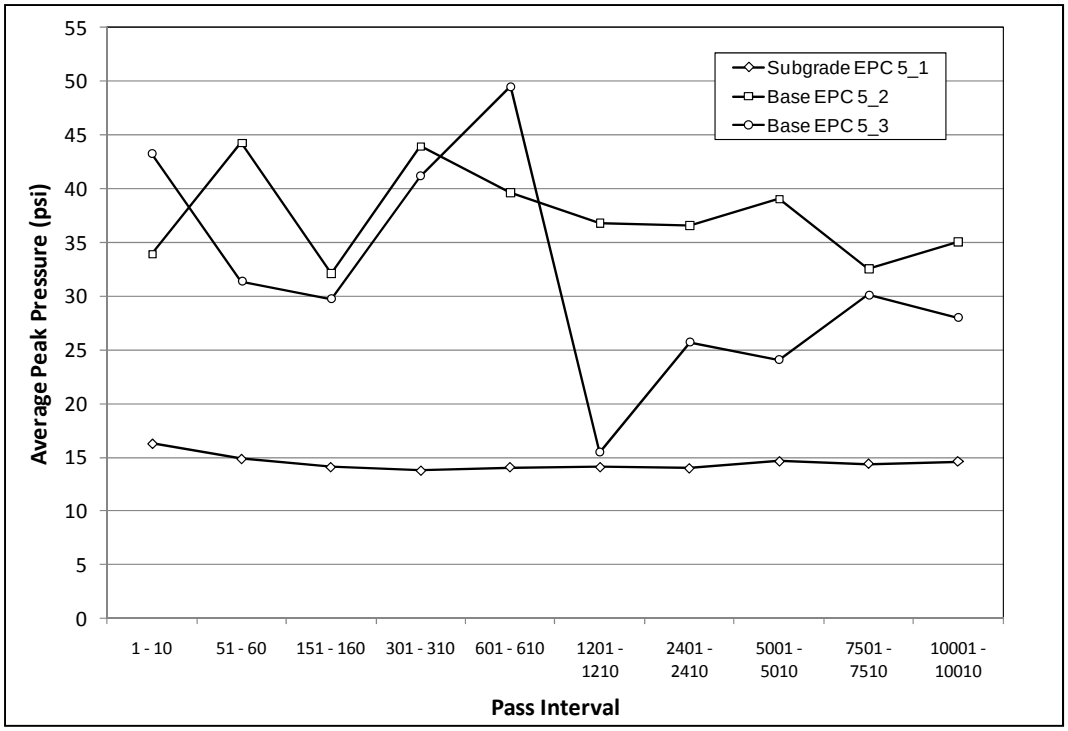

Figure 67. Item 5 average peak pressure measurements at various traffic intervals.

Item 6

Item 6's double layer of standard modular bricks was trafficked to 10,010 passes without failure (Figure 68). The top and bottom layers of bricks were laid in opposite directions. Some of the bricks were observed to begin breaking in half between 1,200 and 2,400 passes. Also, sand was observed to be missing from the majority of the holes in the bricks located in the wheel paths beginning at 2,400 passes. Figures 69 and 70 show overall views of the test item at approximately 5,000 passes, and Figure 71 shows the bricks in the wheel path at 10,010 passes.

Rut depths

Figure 72 shows the rut depths measured in the right wheel path of Item 6. The average rut depth in the test item was 0.28 in. The average rut depth of the double layer of standard modular bricks was almost 2.5 times lower than the average rut depth of the single layer of standard modular bricks (Item 3).

Figure 68. Item 6 before truck traffic.

Figure 69. Overall view of Item 6 at approximately 5,000 passes of truck traffic.

Figure 70. Item 6 at approximately 5,000 passes of truck traffic.

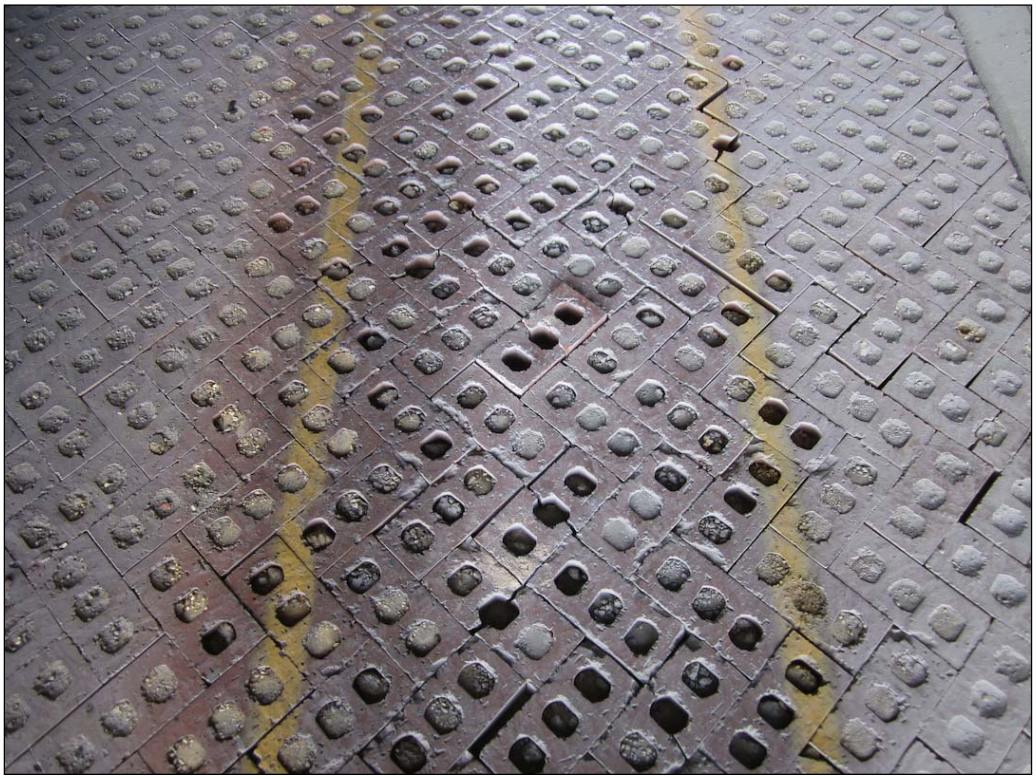

Figure 71. Item 6 wheel path at 10,010 passes of truck traffic.

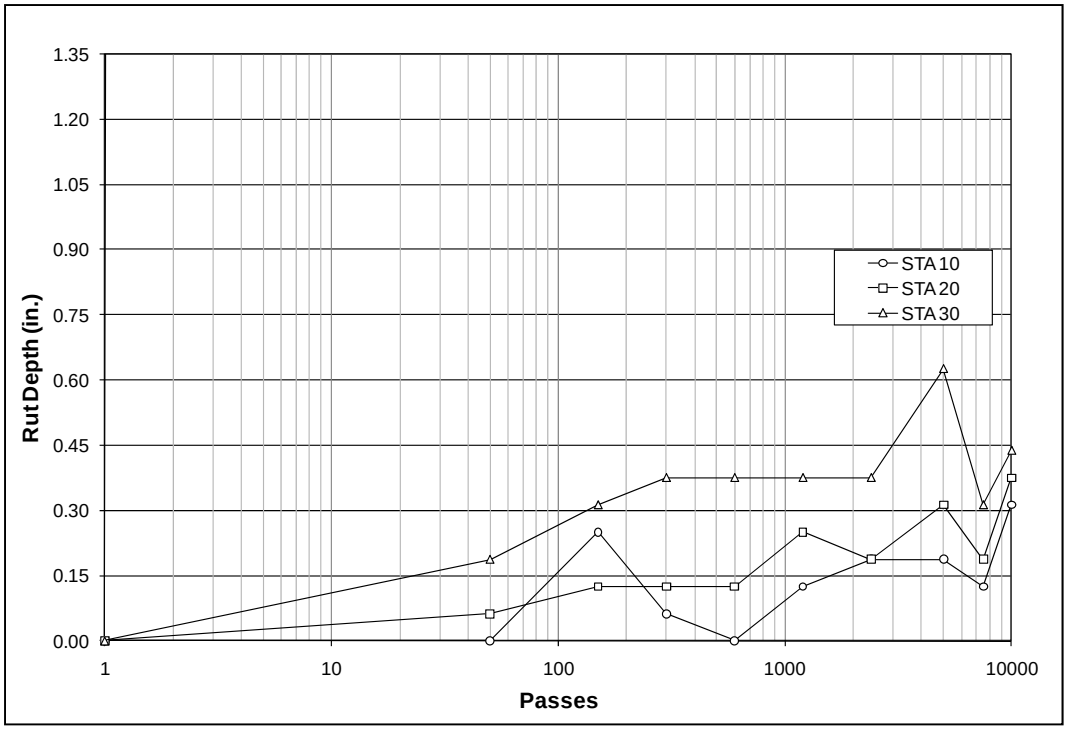

Figure 72. Item 6 rut depth measurements in right wheel path of truck traffic.

Profiles

Figure 73 shows the longitudinal profiles measured in the left wheel path. The profiles show a slow and somewhat inconsistent decrease in elevation. The cross-section profiles at Station 30, shown in Figure 74, indicate minimal upheaval of the standard modular bricks outside the wheel paths. This likely is due to having another layer of bricks, rather than a level of base course materials, immediately underneath the top layer of bricks.

Instrumented pavement response

Figure 75 shows the average peak pressures measured from the EPCs installed in the test item. The pressures measured in the subgrade were slightly lower than the majority of the pressures measured in the subgrades of the other test items. This is due to the thicker surface layer of bricks. The two EPCs installed at the top of the base measured similar peak pressures of approximately 50 psi throughout trafficking.

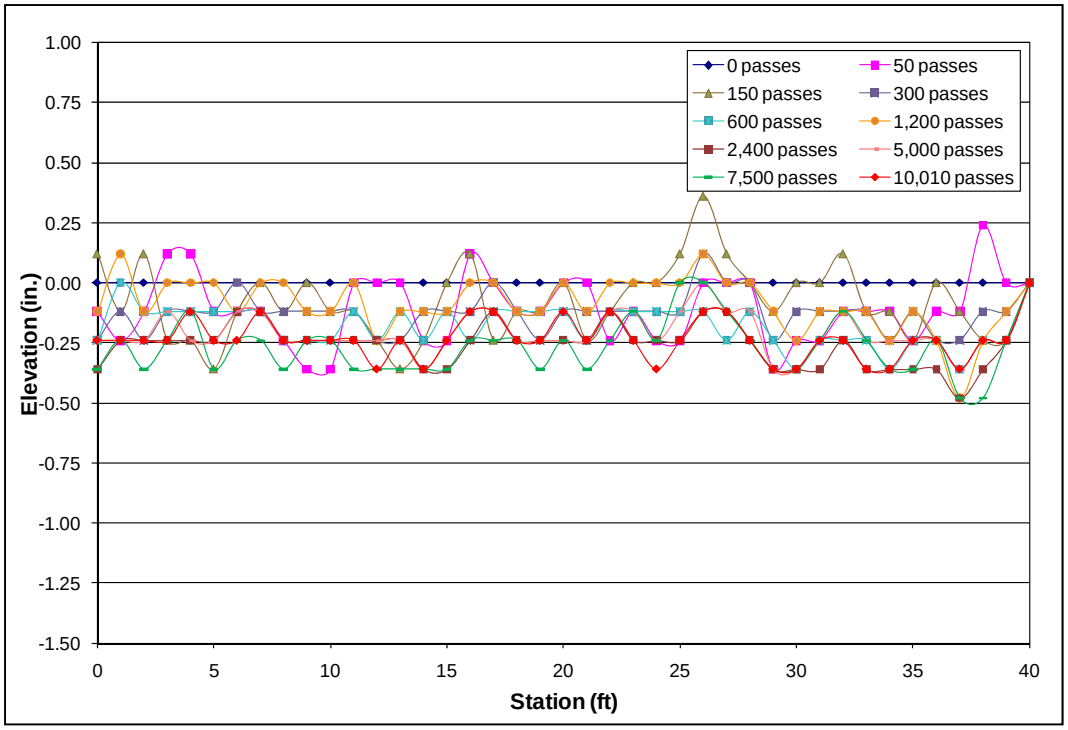

Figure 73. Item 6 longitudinal profiles in left wheel path of truck traffic.

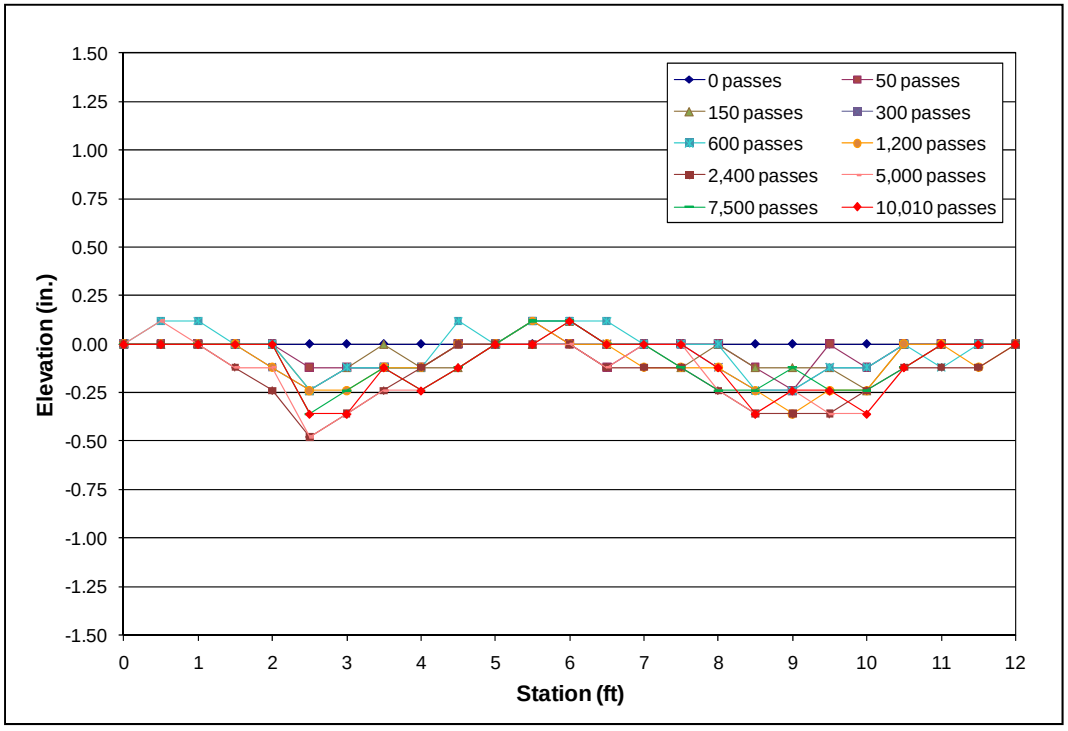

Figure 74. Item 6 cross-section profiles at Station 30 with truck traffic.

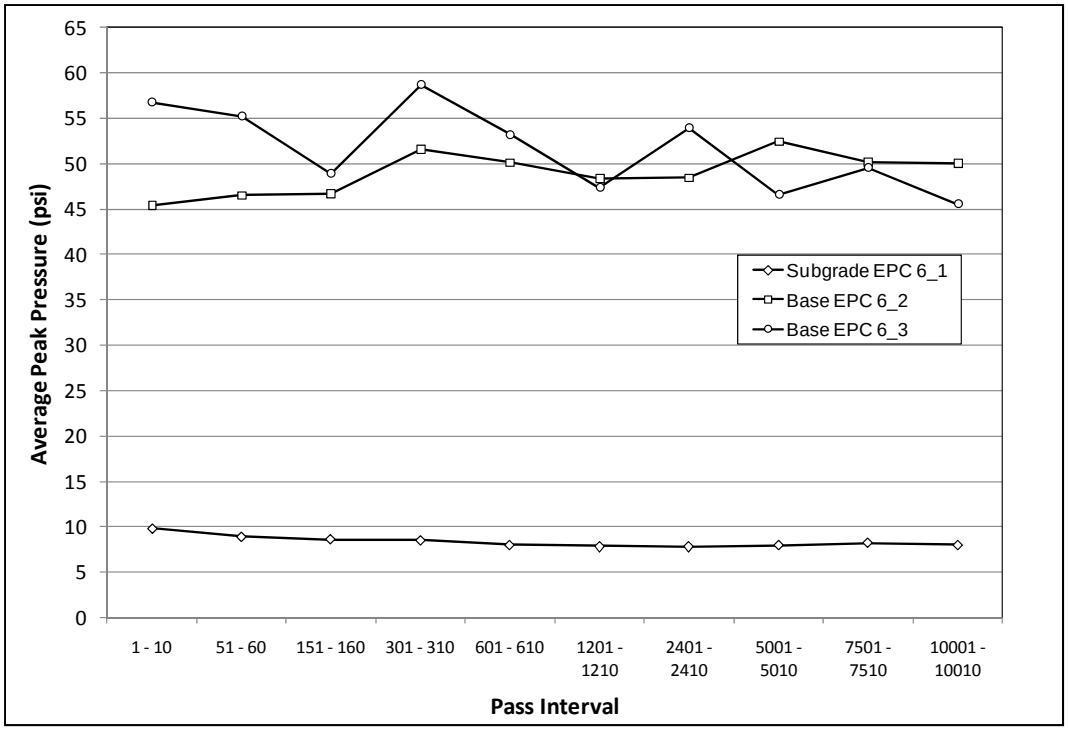

Figure 75. Item 6 average peak pressure measurements at various traffic intervals.

C-17 evaluation

Item 1

The queen bricks in Item 1 were not able to sustain the full load of the single-wheel C-17 traffic. Traffic was halted at 88 passes with more than 3 in. of surface rutting. The threshold of failure for flexible airfield pavements subjected to aircraft traffic is 1 in. of surface rutting. The majority of the queen bricks were crushed under the C-17 load. The crushed bricks have the potential to damage aircraft. Figure 76 shows the single-wheel C-17 load cart trafficking during its first pass on Item 1. Figure 77 shows the C-17 wheel path at 88 passes. Note the crushed and broken bricks inside the wheel path.

Rut depths

Rutting of Item 1 began almost instantly when the C-17 traffic was applied to the bricks. Figure 78 shows the rut depths measured with increasing traffic. The rut depths were recorded in the center of the wheel path. At 88 passes, the average rut depth was 3.29 in. Failure likely occurred around 25 passes of the single-wheel C-17 load cart traffic.

Figure 76. Item 1 during first pass of single-wheel C-17 traffic.

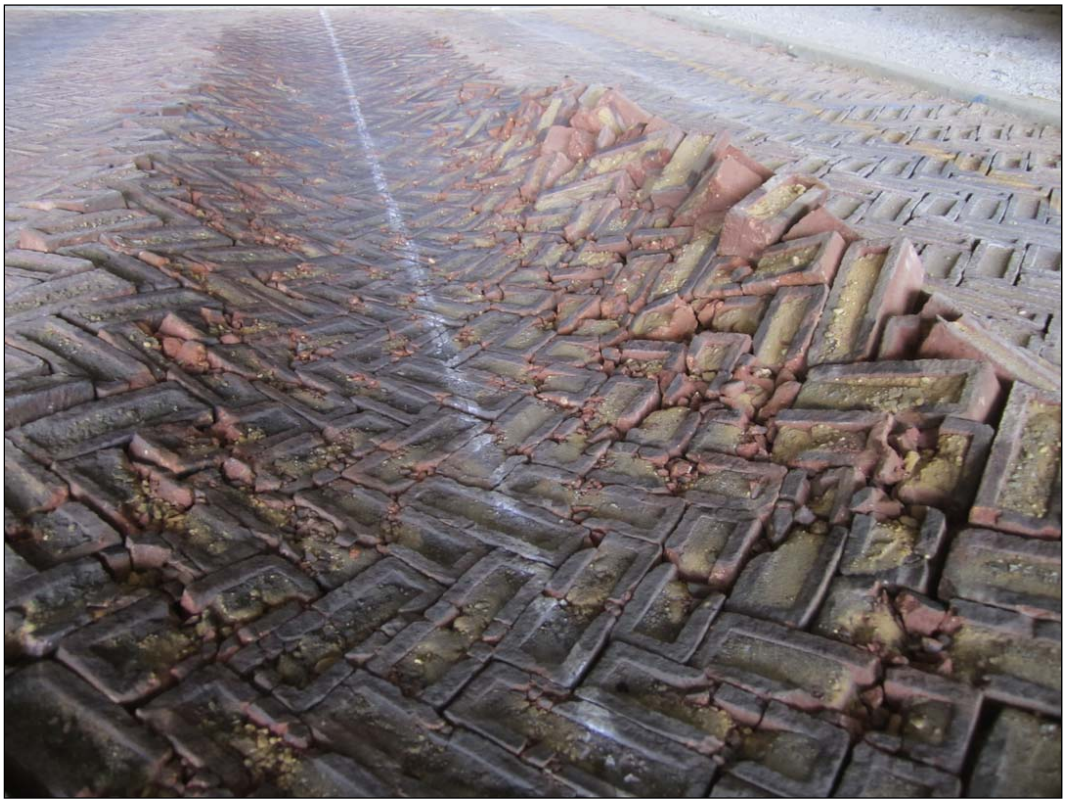

Figure 77. Item 1 wheel path at 88 passes of C-17 traffic.

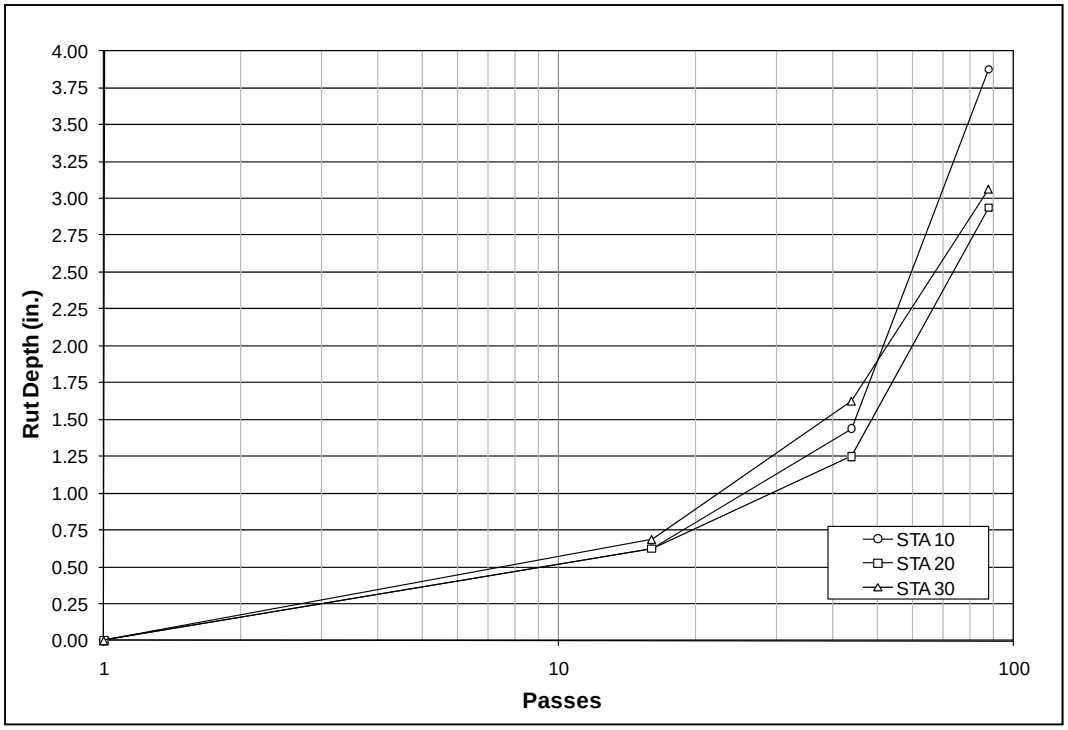

Figure 78. Item 1 rut depth measurements with C-17 traffic.

Profiles

Figure 79 shows the center-line profile measurements of the single-wheel C-17 wheel path. The rutting was somewhat consistent throughout trafficking until after approximately 44 passes. Figure 80 shows the cross-section profiles at Station 10. At 16 passes, there was at most 0.50 in. of rutting but little upheaval. This likely indicates consolidation of an underlying layer. The rutting and upheaval had increased drastically by 88 passes.

Item 2

Item 2 consisted of the reclaimed bricks. Measureable rutting was observed with the first pass of the C-17 load cart. Traffic was completed at 44 passes with average surface rutting beyond the failure point of 1 in. The reclaimed bricks were not able to handle the C-17 aircraft load. Figure 81 shows the rutting in the test item at 16 passes. Many of the bricks were broken or had crushed corners during trafficking. Figure 82 shows the bricks in the center of the wheel path at 44 passes.

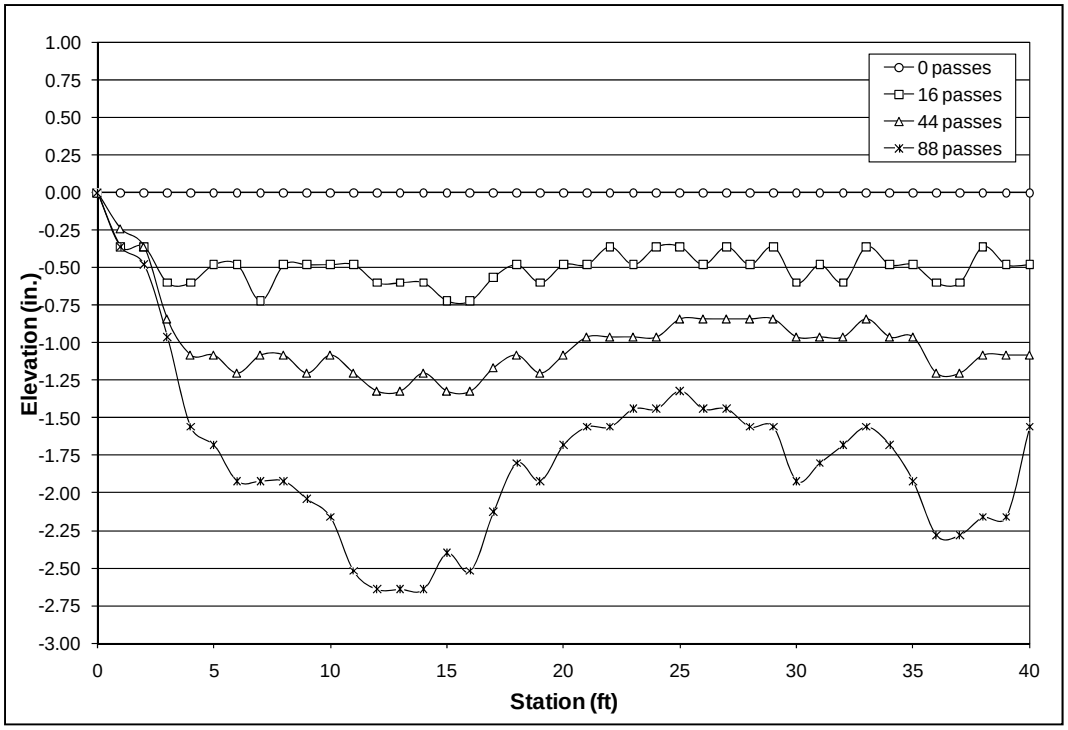

Figure 79. Item 1 center-line profile measurements with C-17 traffic.

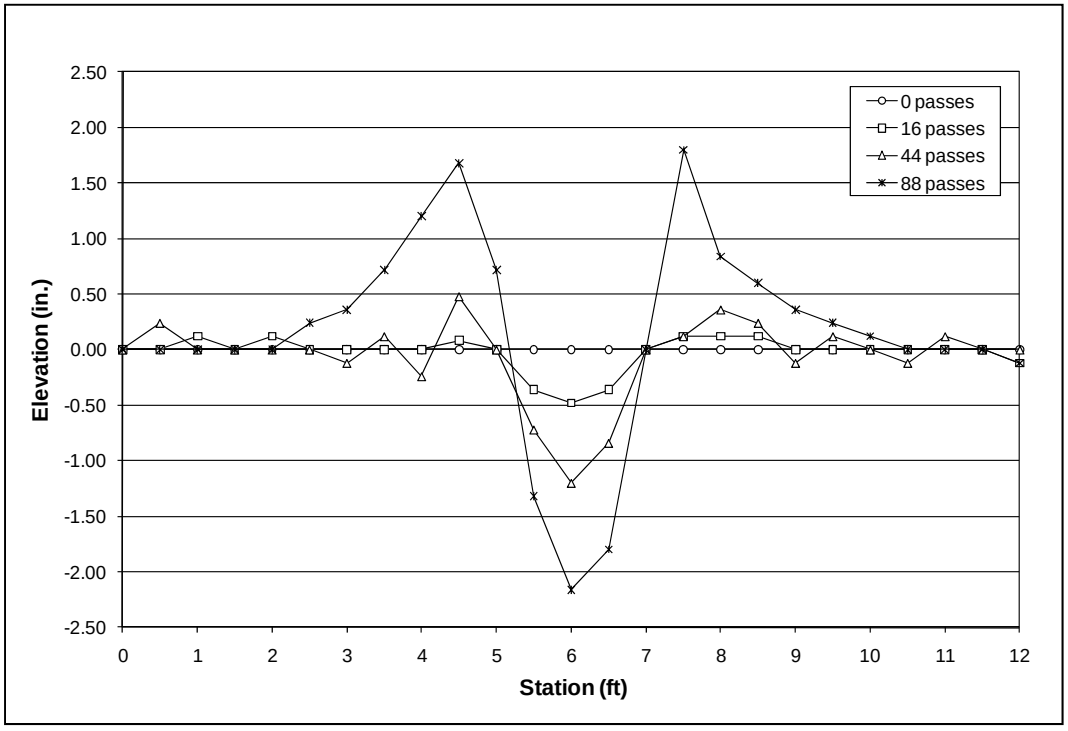

Figure 80. Item 1 cross-section profiles at Station 10 with C-17 traffic.

Figure 81. Item 2 at 16 passes of single-wheel C-17 traffic.

Figure 82. Center of wheel path of Item 2 at 44 passes of C-17 traffic.

Rut depths

Item 2 was trafficked until an average surface rutting of 4.13 in. occurred at 44 passes. Figure 83 shows the rut depth measurements with increasing traffic. Failure with 1 in. of surface rutting likely occurred between 12 and 16 passes.

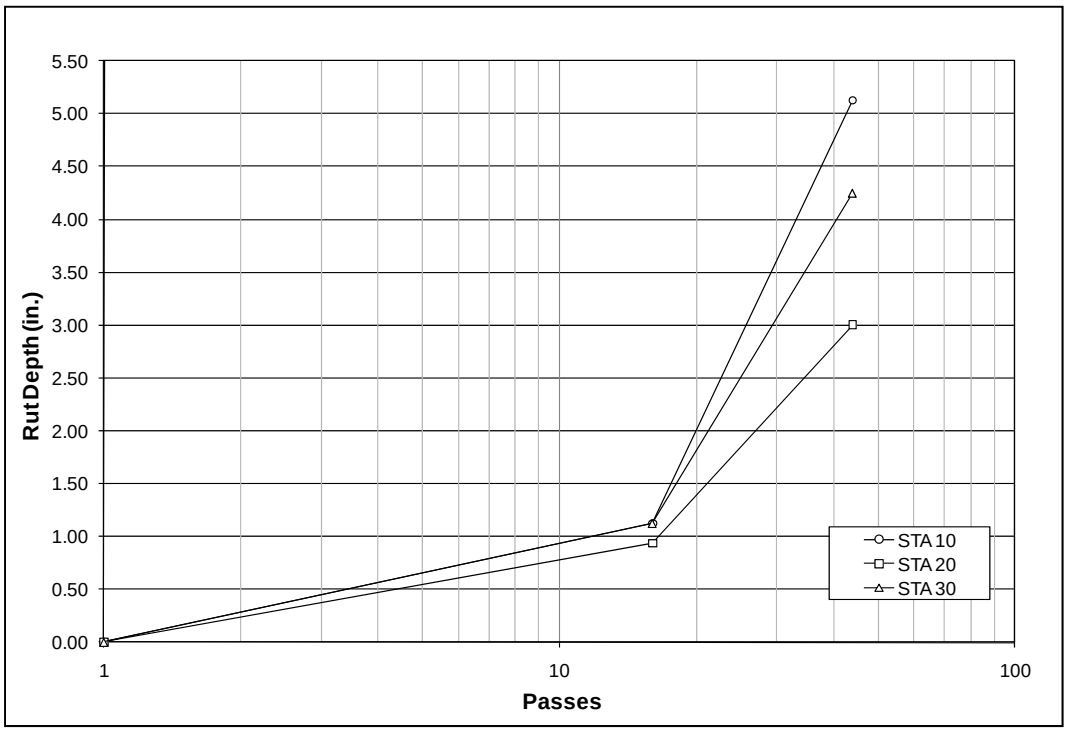

Figure 83. Item 2 rut depth measurements with C-17 traffic.

Profiles

Figures 84 and 85 show the center-line and cross-section (Station 10) profiles of Item 2, respectively. The uneven elevation at 44 passes is due to apparent weak areas on each end of the test item. The large amount of upheaval at 44 passes shown in Figure 85 indicates movement or consolidation in the surface and underlying layers.

Item 3

The standard modular bricks in Item 3 were trafficked to 74 passes. These bricks were not able to sustain many passes of the C-17 load before failure. Between 20 and 40 passes, the majority of the bricks in the wheel path began to break or shatter. Figures 86 and 87 show the standard modular bricks at 74 passes.

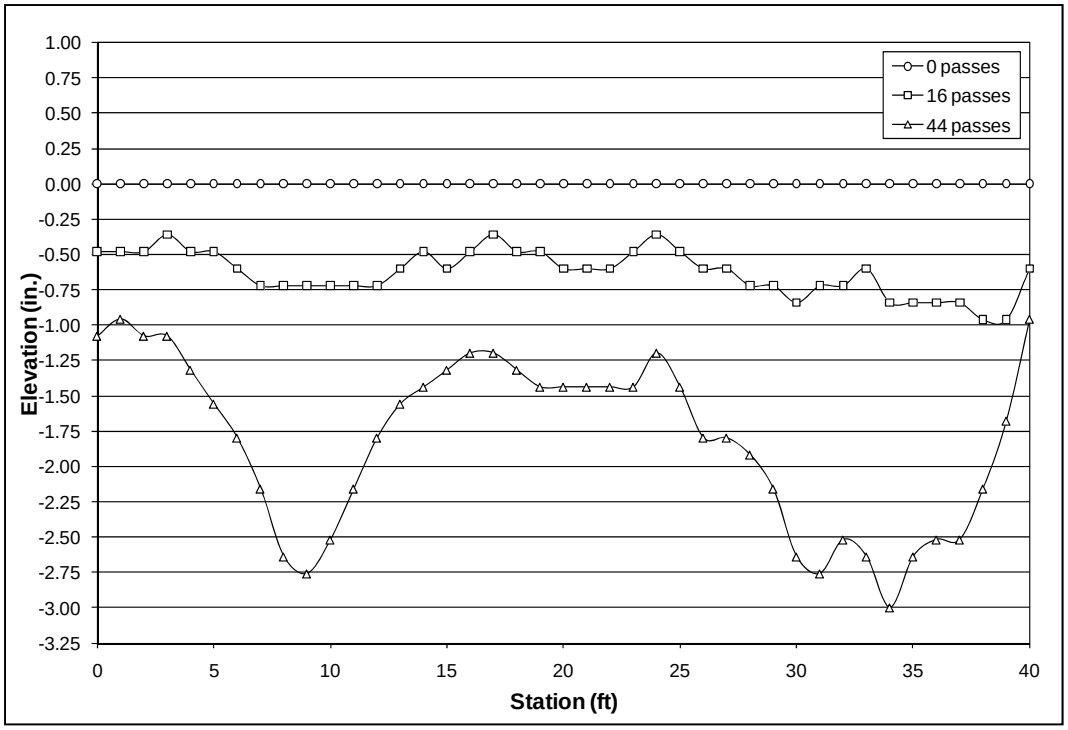

Figure 84. Item 2 center-line profiles measurements with C-17 traffic.

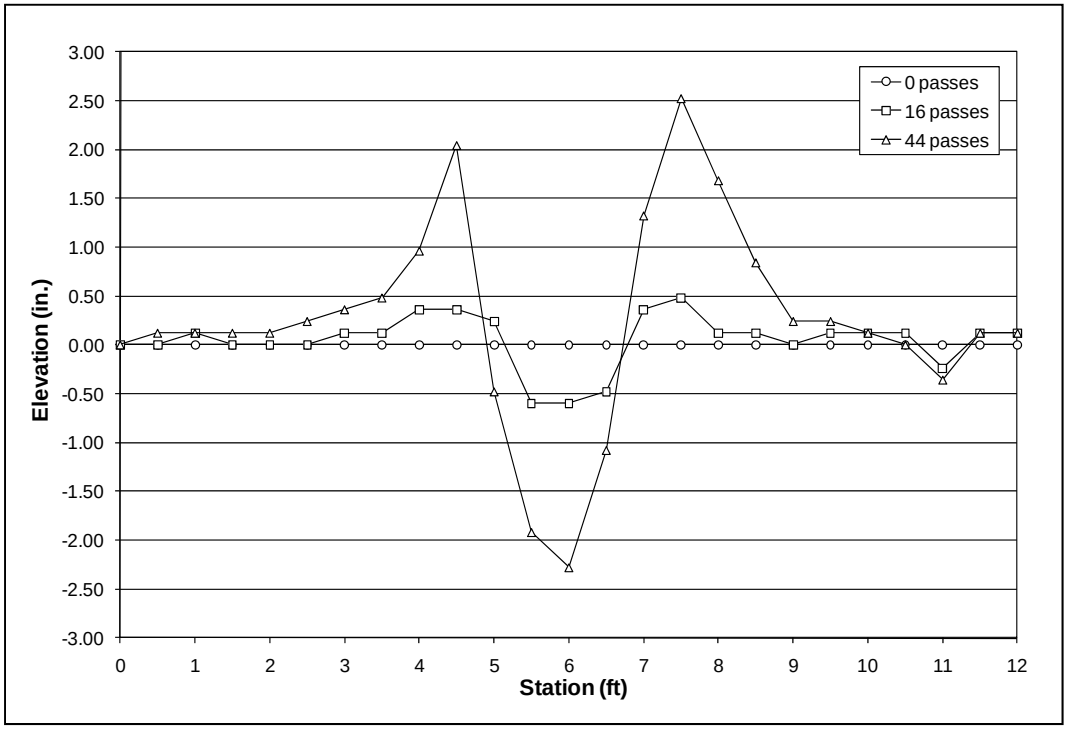

Figure 85. Item 2 cross-section profiles measurements at Station 10 with C-17 traffic.

Figure 86. Overall view of Item 3 at 74 passes of C-17 traffic.

Figure 87. Item 3 rut depth measurement at Station 30 at 74 passes of C-17 traffic.

Rut depths

Figure 88 shows the rut depths measured at the quarter points of Item 3. Rutting at Stations 10, 20, and 30 was consistent until approximately 45 passes. After 40 passes, the rutting at Station 30 accelerated at a more rapid rate. This possibly is due to inconsistent compaction efforts of the pavement structure during construction. The average surface rutting at 74 passes was 3.87 in. According to the rut depth measurements, Item 3 likely failed around 25 passes.

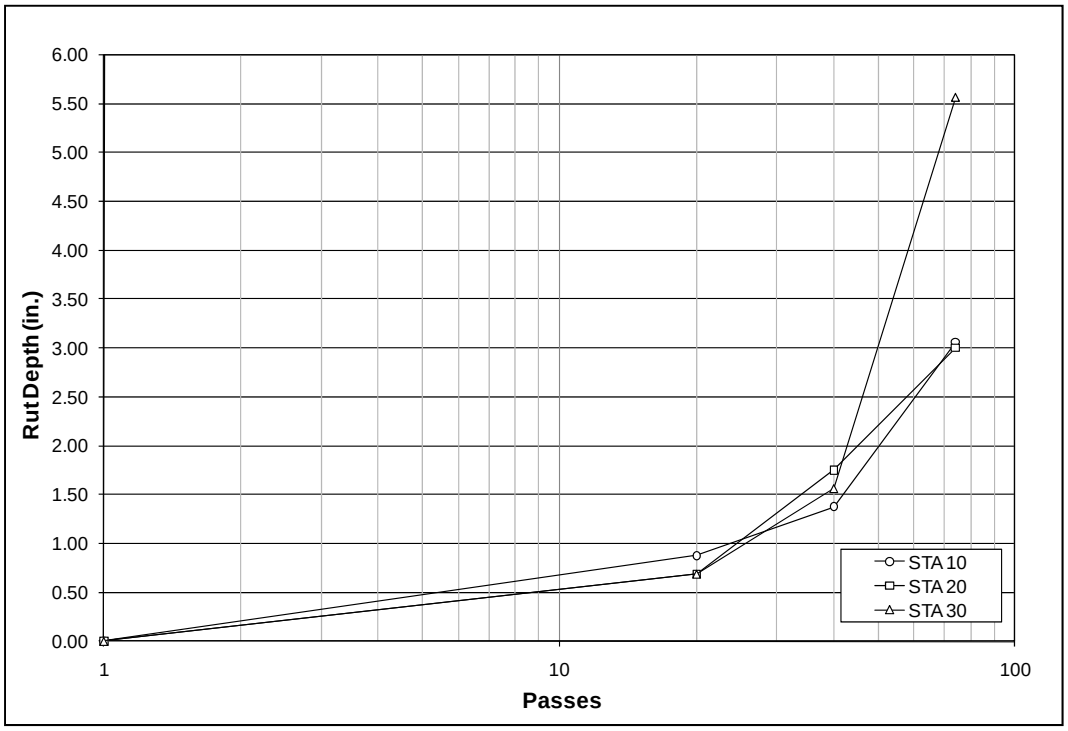

Figure 88. Item 3 rut depth measurements with C-17 traffic.

Profiles

The center-line wheel path profiles are shown in Figure 89. After 20 passes, the rut depth along the wheel path was approximately 0.50 in. After 40 passes, the rut depth doubled to approximately 1.00 in. Figure 90 shows the cross-section profiles at Station 30. This was the weakest area in the test item. The rutting rates of the cross-section and center-line profiles were similar. The elevation decreased significantly at 74 passes.

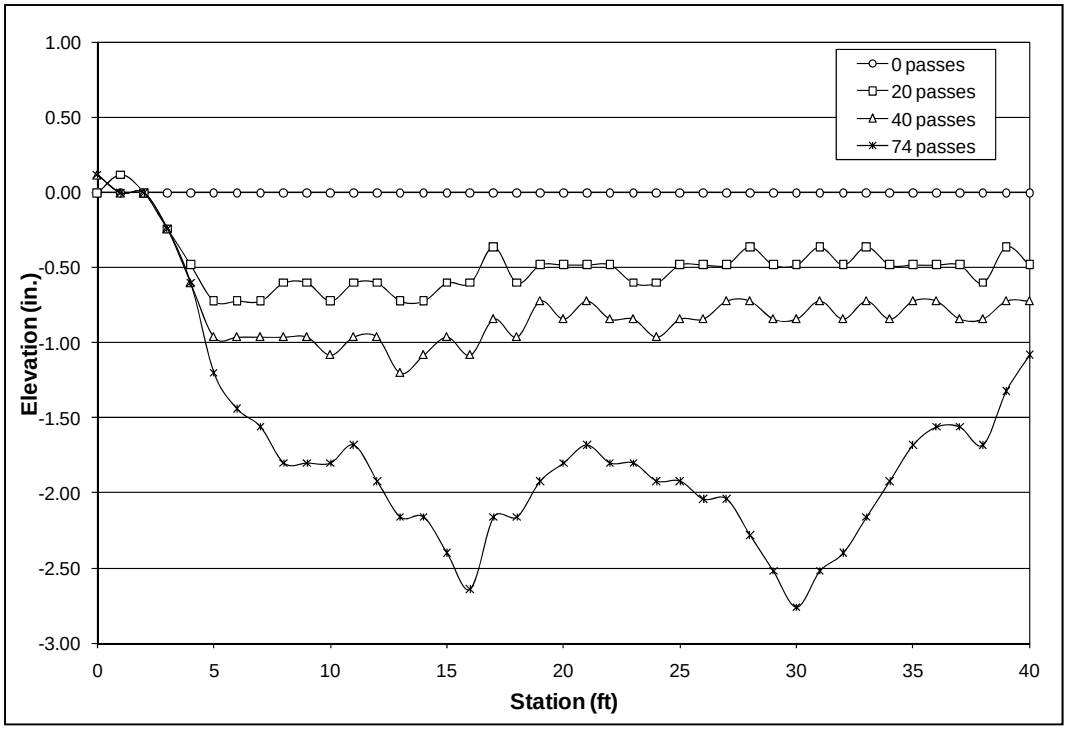

Figure 89. Item 3 center-line profile measurements with C-17 traffic.

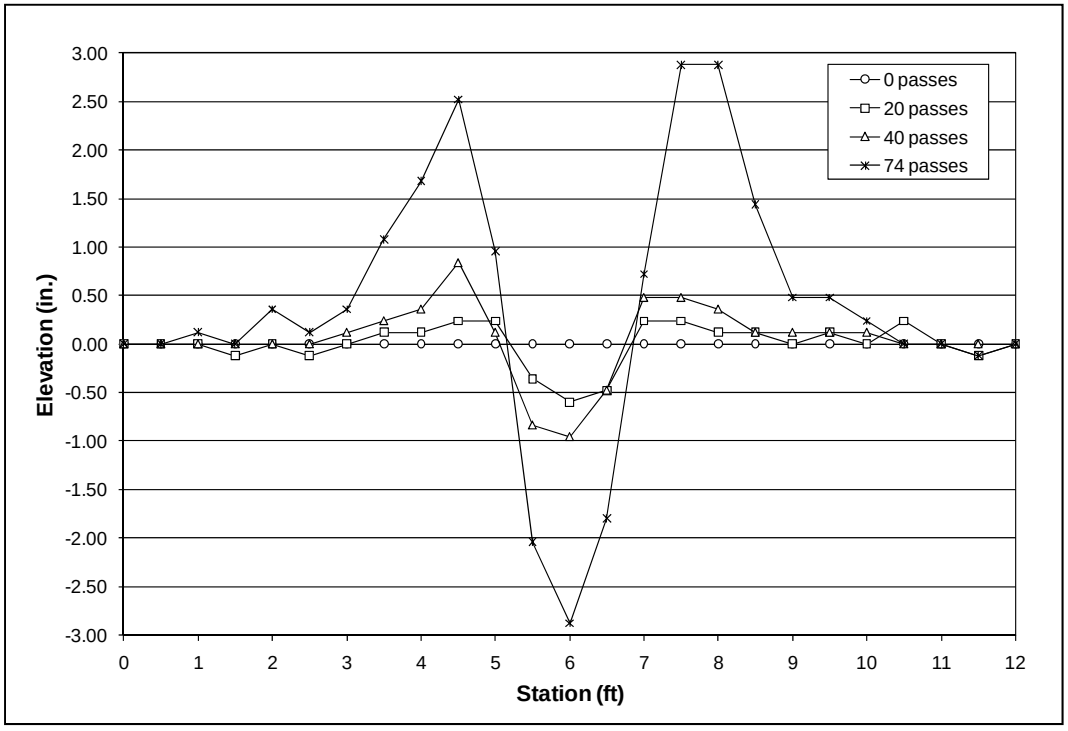

Figure 90. Item 3 cross-section profile measurements at Station 30 with C-17 traffic.

Item 4

Item 4 was trafficked with the C-17 load cart until 138 passes. The utility bricks were not able to handle the aircraft load without failure. Figure 91 shows the load cart trafficking on Item 4 at approximately 75 passes. There were very few broken bricks during trafficking.

Figure 91. C-17 load cart trafficking near Station 30 at approximately 75 passes on Item 4.

Rut depths

The increasing rut depths with passes of Item 4 are shown in Figure 92. The area around Station 20 apparently was slightly weaker than the areas around Stations 10 and 30. The average rut depth of Item 4 at 138 passes was 4.46 in. Failure with an average surface rut of 1 in. likely occurred around 30 passes.

Profiles

Figures 93 and 94 show the center-line and cross-section profiles of Item 4, respectively. The center-line profiles illustrate that the area around Station 20 was weaker, as was shown with the rut depth measurements in Figure 92. The cross-section profiles shown in Figure 94 were of the weaker area of Station 20; this was the worst case for the test item.

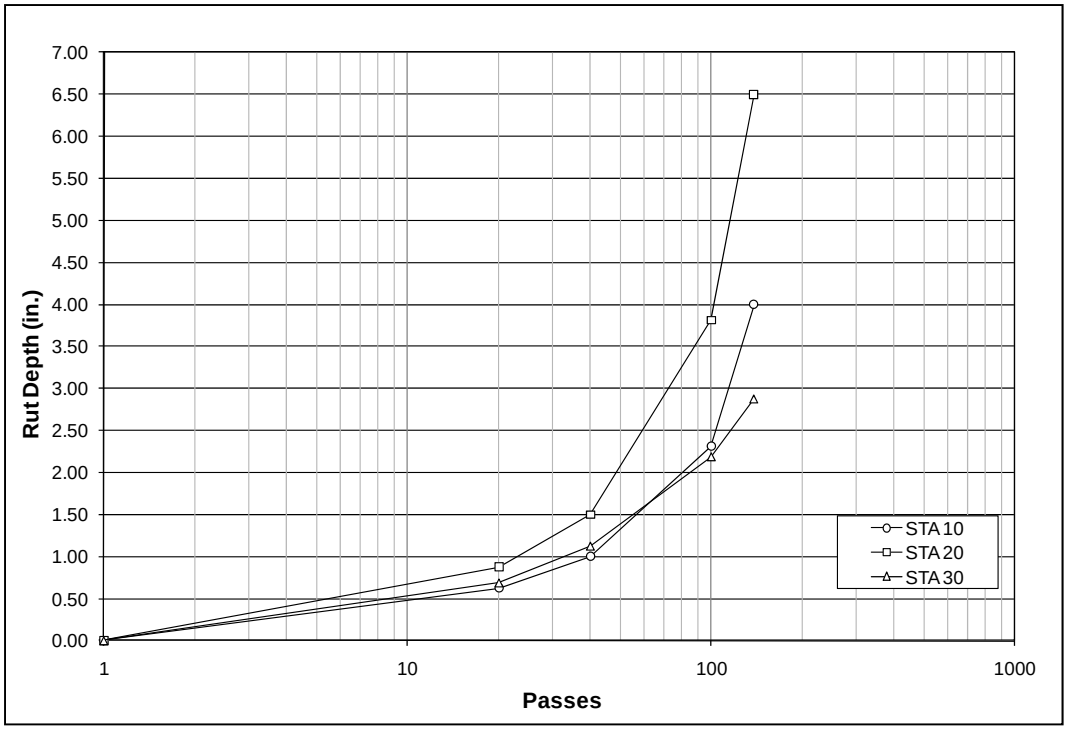

Figure 92. Item 4 rut depth measurements with C-17 traffic.

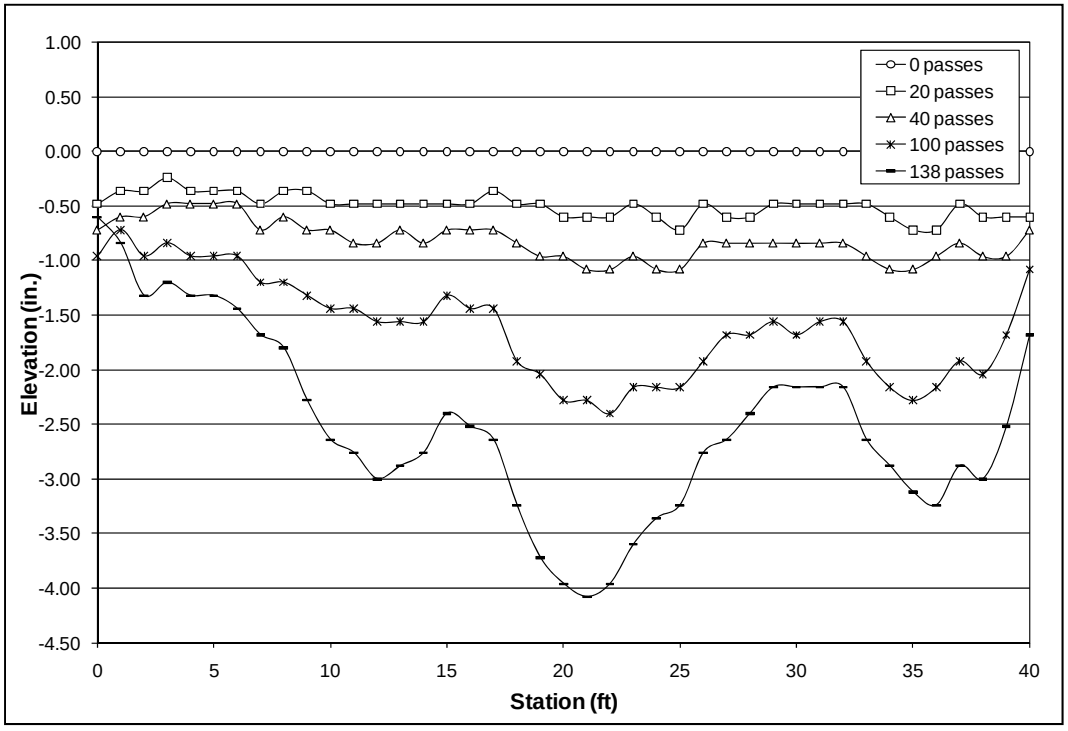

Figure 93. Item 4 center-line profile measurements with C-17 traffic.

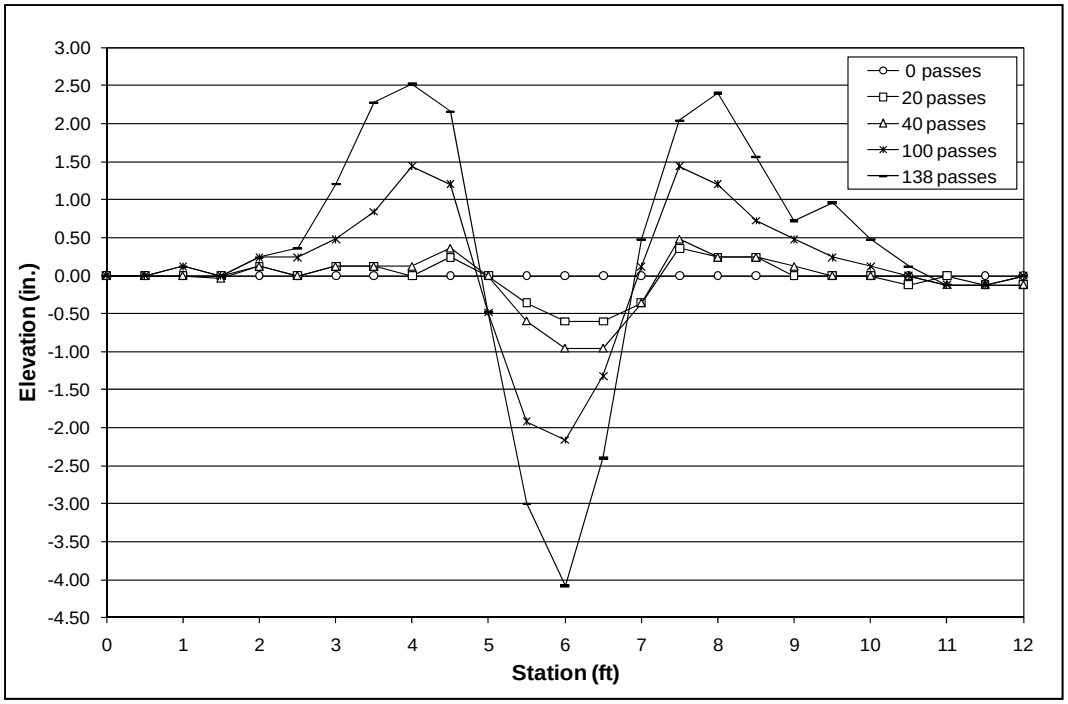

Figure 94. Item 4 cross-section profile measurements at Station 20 with C-17 traffic.

Item 5

The brick pavers were unable to withstand many passes of the fully loaded single-wheel C-17 load cart. Traffic was stopped at 150 passes with close to an average of 4 in. of surface rutting. Minor breakage, mainly spalling along the edges and at the corners of some of the bricks, was observed during trafficking. Figure 95 shows the wheel path of the brick pavers at the completion of aircraft traffic.

Rut depths

The average rut depth of Item 5 at 150 passes was 3.77 in. Figure 96 shows the measured rut depths as the pass level increased. Station 20 had a greater rate of failure after 104 passes. The brick pavers likely failed around 35 passes.

Profiles

The center-line and cross-section profiles, shown in Figures 97 and 98, respectively, were plotted to illustrate the changing elevation of the test item with increasing passes. The cross-section profiles shown in Figure 98 were from Station 20. The area around Station 20 deteriorated more rapidly after 104 passes, as illustrated in Figures 97 and 98.

Figure 95. Item 5 wheel path at 150 passes of C-17 traffic.

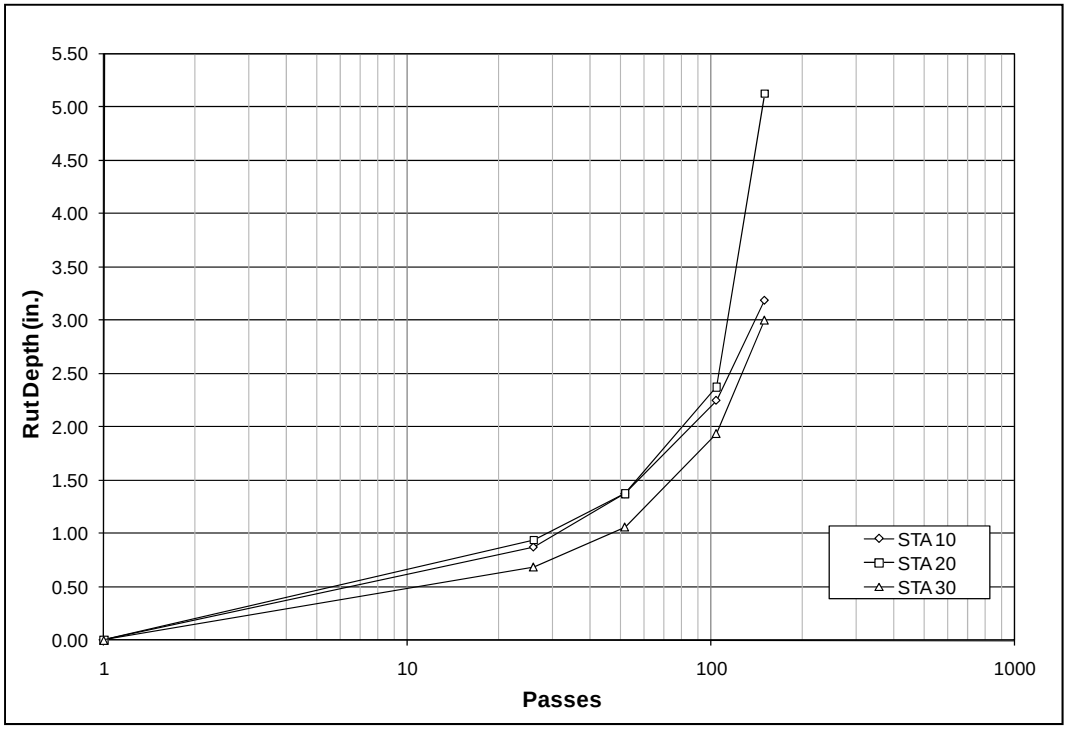

Figure 96. Item 5 rut depth measurements with C-17 traffic.

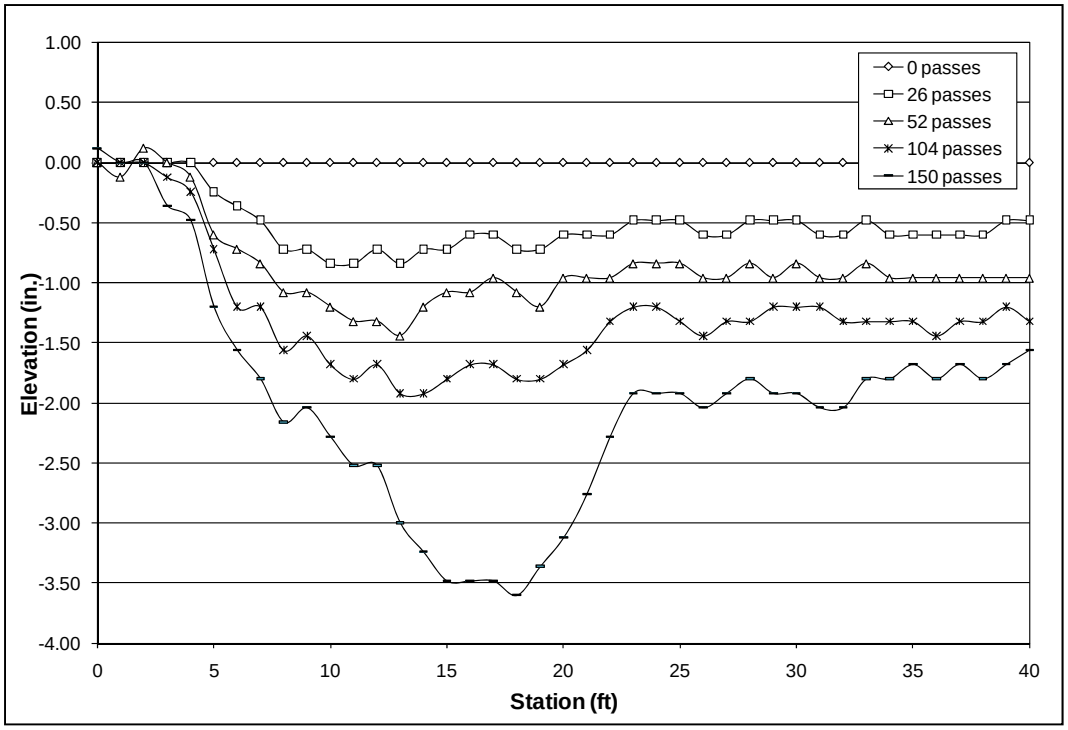

Figure 97. Item 5 center-line profile measurements with C-17 traffic.

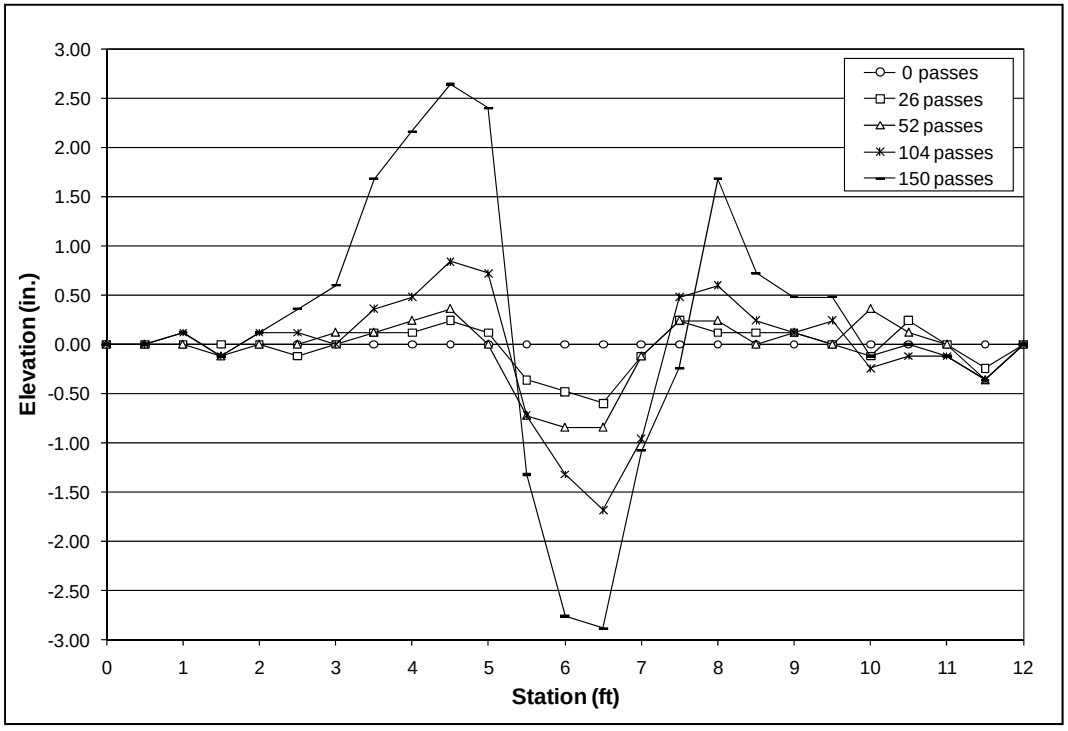

Figure 98. Item 5 cross-section profile measurements at Station 20 with C-17 traffic.

Item 6

The double-layered standard modular bricks of Item 6 were trafficked until 300 passes. After 104 passes, the area from Stations 30 to 40 consolidated to the point that the rut was too deep for the load cart to traffic. According to the rut depth measurements, Station 30 also was slightly weaker with the truck traffic (Figure 72).

Figure 99 shows an overall view of Item 6 at 104 passes. Notice the condition of the brick surface in the area near the top of the picture (from Station 30 to the end of the item). Cross-section profiles and rut depth measurements were not collected at Station 30 after 104 passes. Because the rest of the test item was performing sufficiently, the C-17 load cart traffic continued from Station 0 to approximately Station 29 until 300 passes.

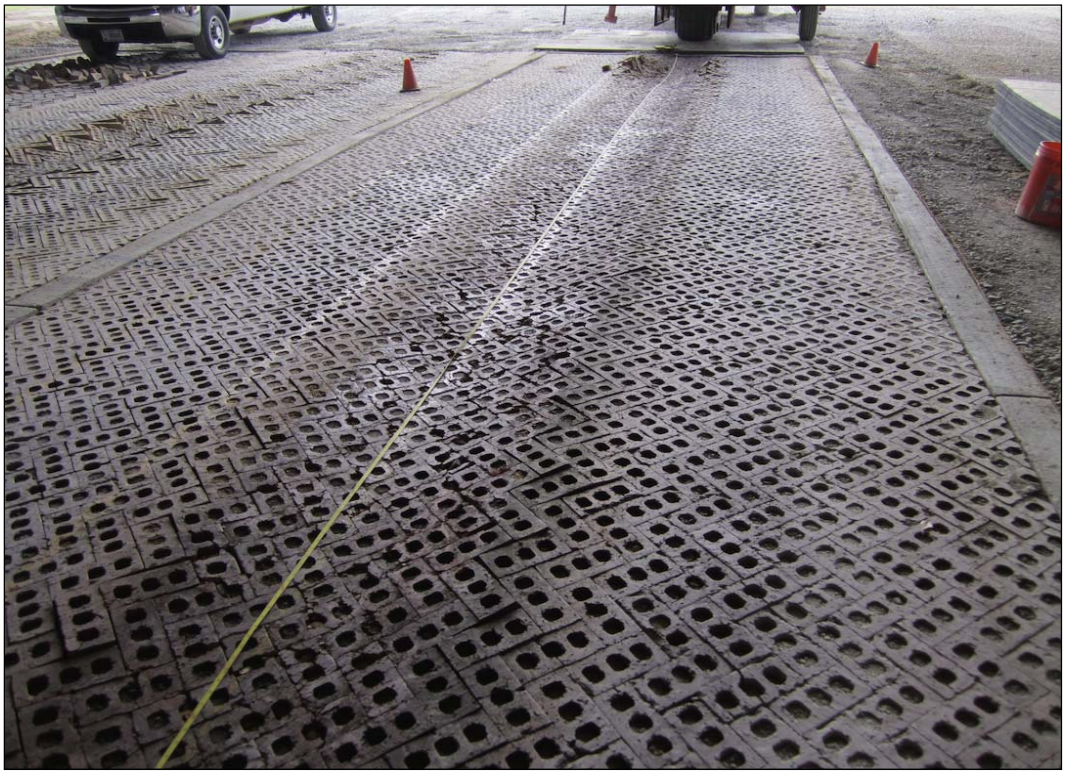

Figure 99. Item 6 overall view at 104 passes of C-17 traffic.

Figure 100 shows an overall view of the wheel path at 300 passes. Note the crushed and broken bricks inside the wheel path. Removal of the top layer of bricks after traffic completion revealed the same amount of crushed and broken bricks on the underlying layer of standard modular bricks. The crushed bricks could cause damage to aircraft.

Figure 100. Item 6 overall view at 300 passes of single-wheel C-17 traffic.

Rut depths

The measured rut depths from the quarter points of the test item are plotted against pass level in Figure 101. The average rut depth from Stations 10, 20, and 30 at 104 passes was 1.63 in. The average rut depth from Stations 10 and 20 at 300 passes was 4.22 in. Failure of Item 6 (measured from Stations 10 and 20) likely occurred at close to 60 passes.

Profiles

Traffic was stopped from Station 30 to Station 40 after 104 passes; however, the center-line profile measurements were collected and are plotted in Figure 102. With the exception of Station 30 and beyond, the elevation decreased somewhat steadily as the pass level increased.

The cross-section profiles at Station 20 are plotted in Figure 103. Although there was a greater rate of upheaval beginning with 250 passes, the elevation decreased at a steady rate, just as the center-line profiles showed.

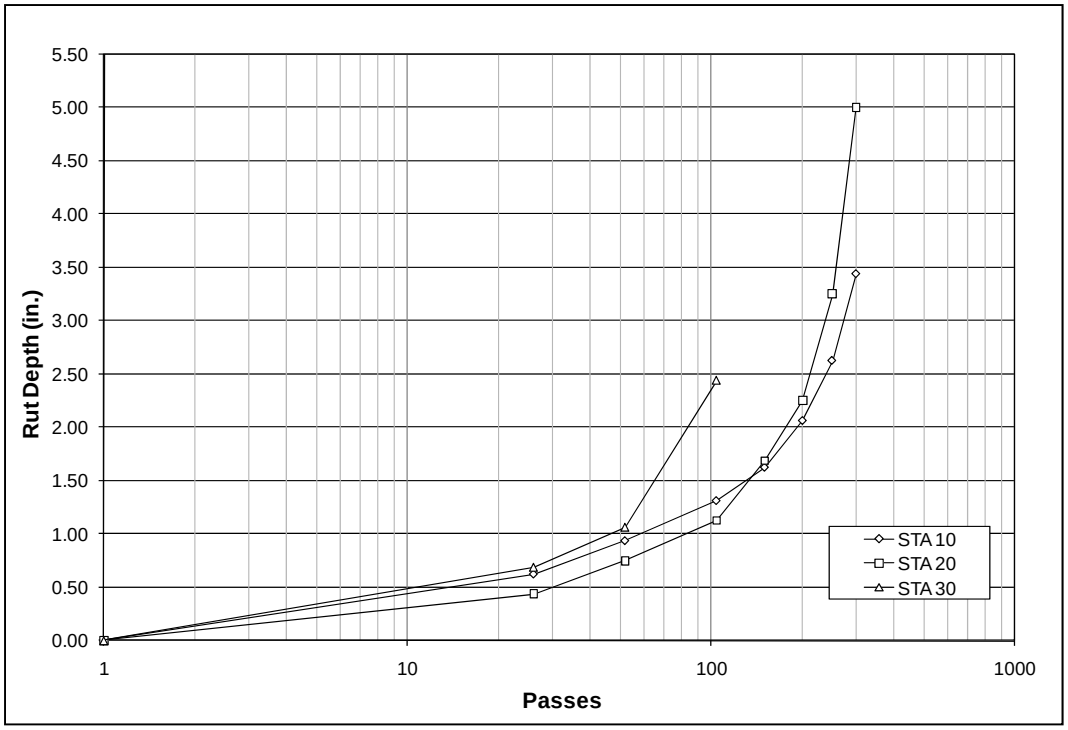

Figure 101. Item 6 rut depth measurements with C-17 traffic.

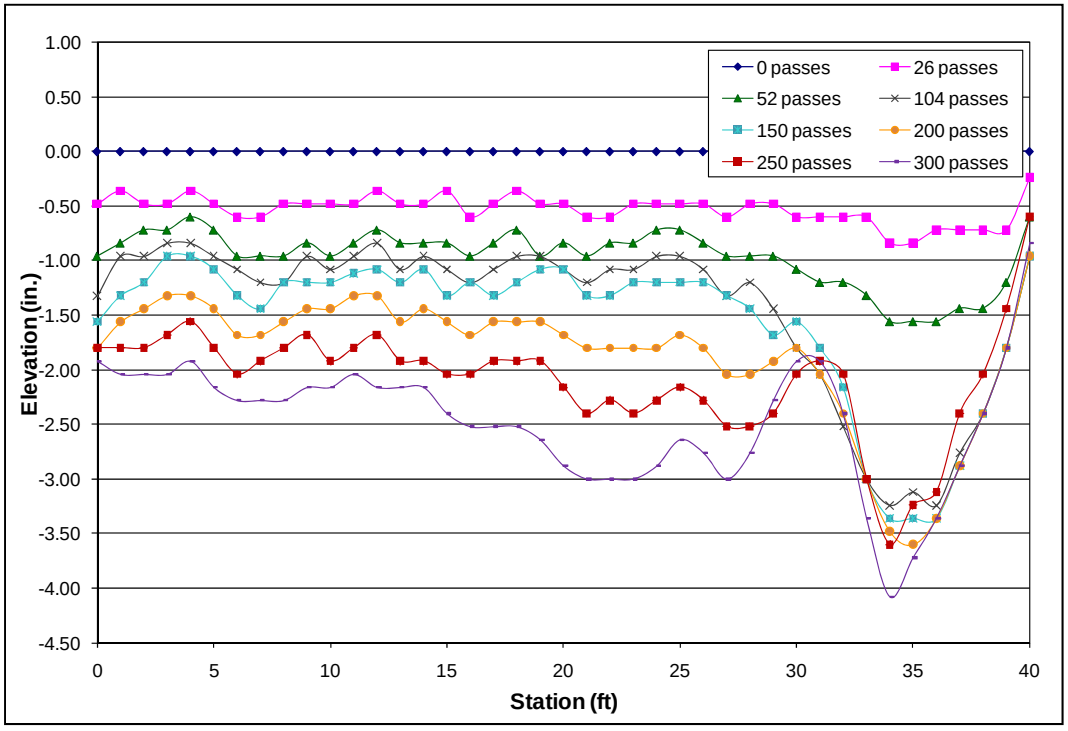

Figure 102. Item 6 center-line profile measurements with C-17 traffic.

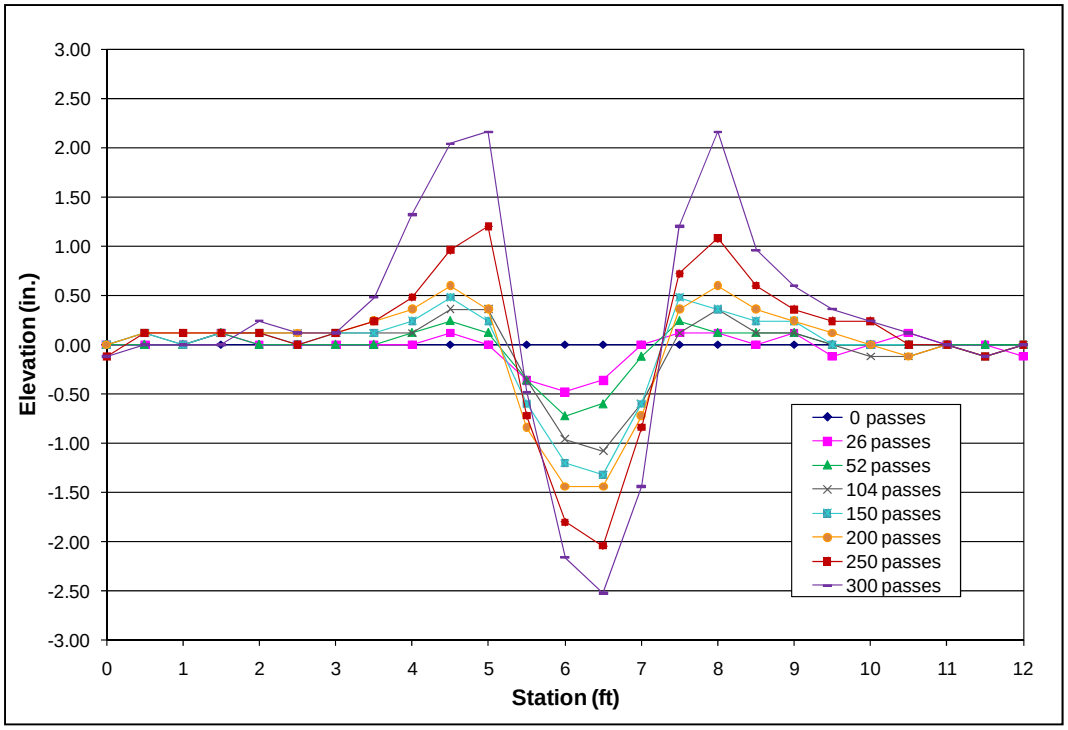

Figure 103. Item 6 cross-section profile measurements at Station 20 with C-17 traffic.

Forensic assessment

Overall, there was little permanent surface deformation after the completion of the truck traffic. Figure 104 shows the test section at the conclusion of all truck traffic. The forensic investigation was conducted to evaluate the pavement structure after the completion of the aircraft traffic, when the most damage occurred. Figure 105 shows an overall view of the test section at the conclusion of the C-17 traffic.

A 3-ft-wide trench was dug across the center (Station 20) of each test item for the forensic investigation. The trenches were dug after the completion of the single-wheel C-17 traffic. Each layer of the pavement structure was removed individually for evaluation. Oven moisture contents and CBRs were measured inside and outside of the wheel path of the C-17 load cart on each pavement layer. Figure 106 shows a CBR test on the base layer of Item 2. DCP tests also were conducted inside the wheel path of the C-17 load cart as an alternative strength measurement for the base course. CBR tests were difficult to run accurately on the base course material during pre-testing. The DCP tests were conducted by drilling through the brick surfaces and getting a strength measurement of the compacted base course.

Figure 104. Test section after truck traffic.

Figure 105. Test section after single-wheel C-17 traffic.

Figure 106. CBR post-testing on Item 2 base course after trafficking.

Table 11 presents the post-test CBRs and oven moisture contents for the base material. For Items 1 through 4, the base strength inside the wheel path of the single-wheel C-17 decreased significantly compared to outside the wheel path. The DCP results on the base material inside the rut compared well with the CBR results inside the rut. Overall, the post-test DCP results in the base material, which were much lower than the pre-test DCP results (80 to 100 CBR post-test truck/pre-test C-17 measurements), likely were due to base course movement caused by the C-17 traffic. The post-test moisture contents of each item were approximately 1 to 1.5 percent lower than the pre-test measurements. The decrease in moisture content was not surprising, as GM material tends to lose moisture over time.

Table 12 presents the post-test CBR and oven moisture content test results on the subgrade material. The slight increase of the CBRs most likely was due to the moisture content of the subgrade decreasing.

Cross-section profiles were measured from the surface of each underlying layer to determine the location(s) of failure. Figures 107 through 112 show the cross-section profiles of the pavement structure for each item. The plots indicate consolidation and shear movement in the C-17 wheel path of every layer of the pavement structure. However, the subsurface consolidation and shear movement occurred mainly in the base layer of each item.

Table 11. C-17 traffic post-test base measurements.

Item	Base CBR (%)		Base Moisture (%)		DCP-estimated CBR in rut (%)
	Outside Rut	Inside Rut	Outside Rut	Inside Rut	
1	78.7	42.3	1.2	1.5	50
2	81.7	46.0	2.4	1.9	30
3	52.7	34.0	1.5	1.0	38
4	72.7	40.3	1.7	1.8	30
5	31.4	41.1	2.1	1.6	35
6	45.4	48.8	1.8	1.8	48

Table 12. C-17 traffic post-test subgrade measurements.

Item	Subgrade CBR (%)		Subgrade Moisture (%)	
	Outside Rut	Inside Rut	Outside Rut	Inside Rut
1	8.1	7.7	30.1	30.3
2	8.5	8.3	32.0	28.9
3	7.7	8.4	31.3	30.0
4	7.4	6.4	29.6	25.8
5	8.4	7.2	21.7	35.4
6	6.9	6.3	23.9	40.2

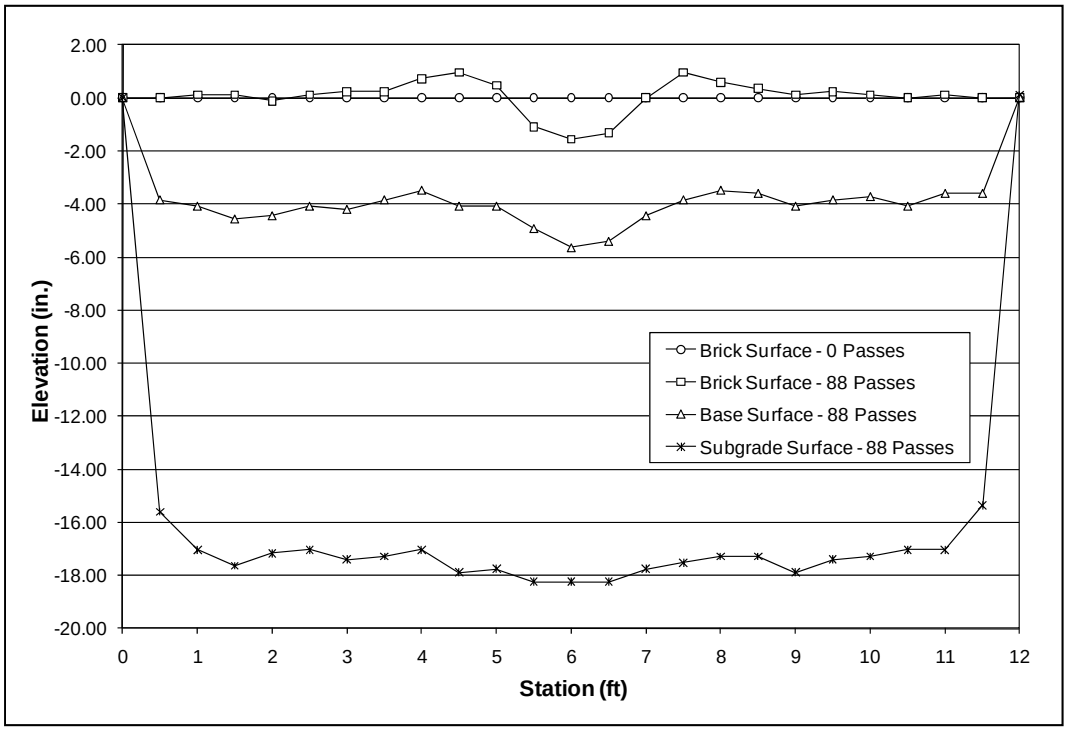

Figure 107. Item 1 cross-section profile measurements after C-17 traffic.

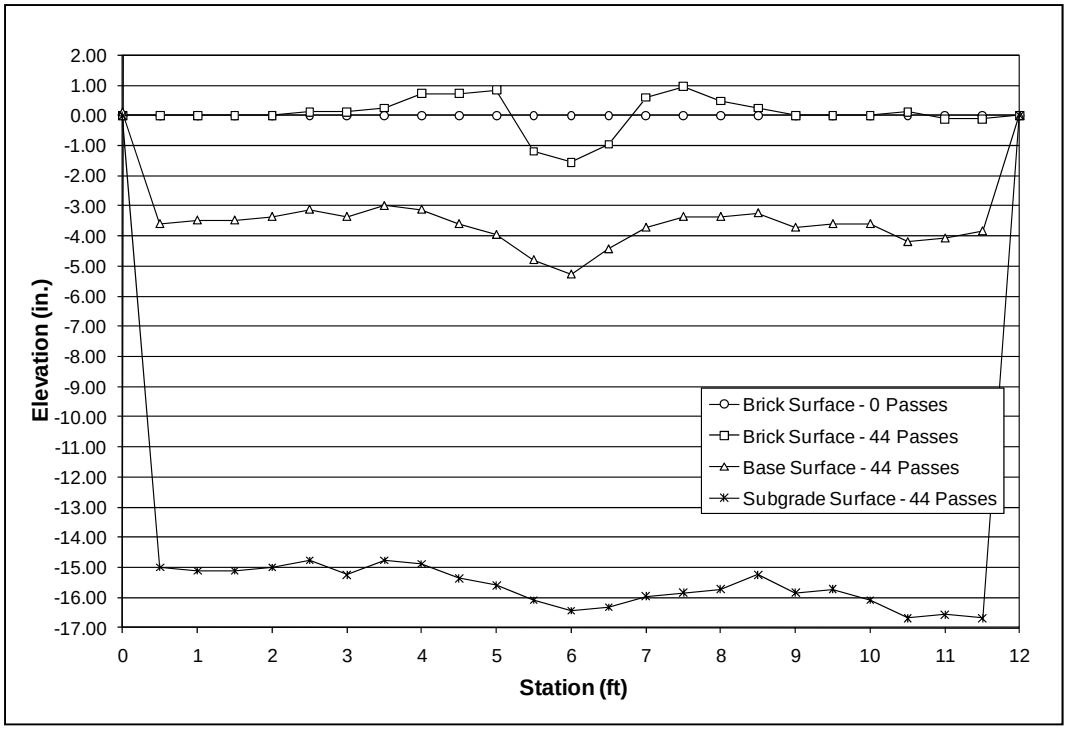

Figure 108. Item 2 cross-section profile measurements after C-17 traffic.

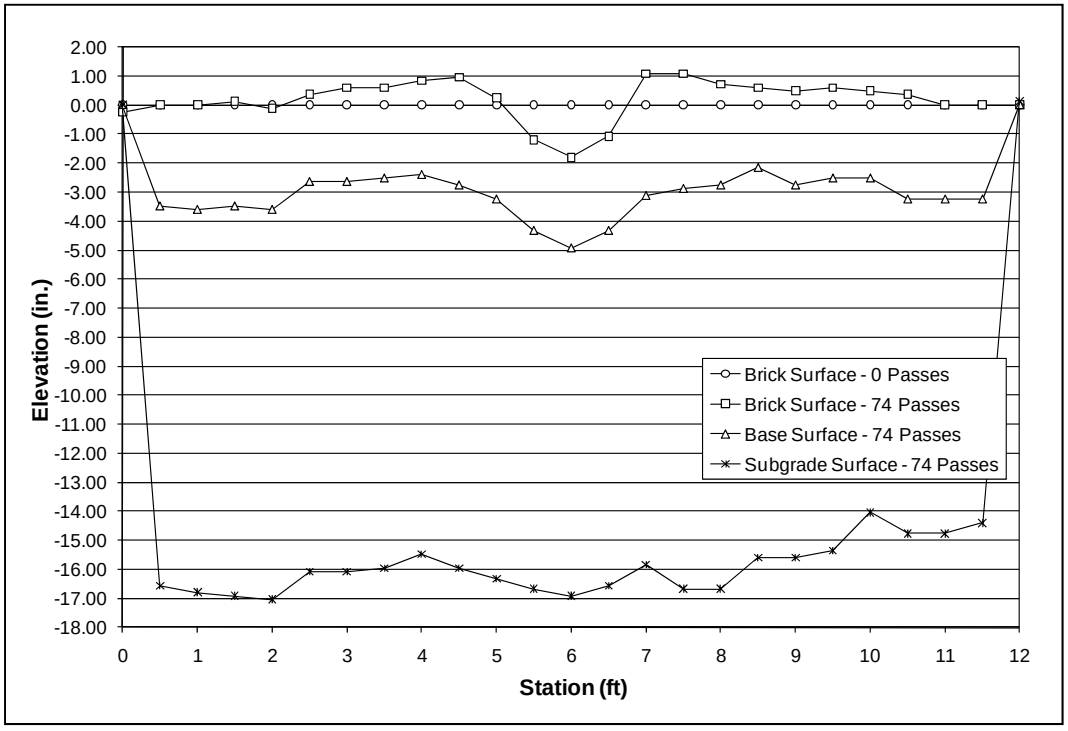

Figure 109. Item 3 cross-section profile measurements after C-17 traffic.

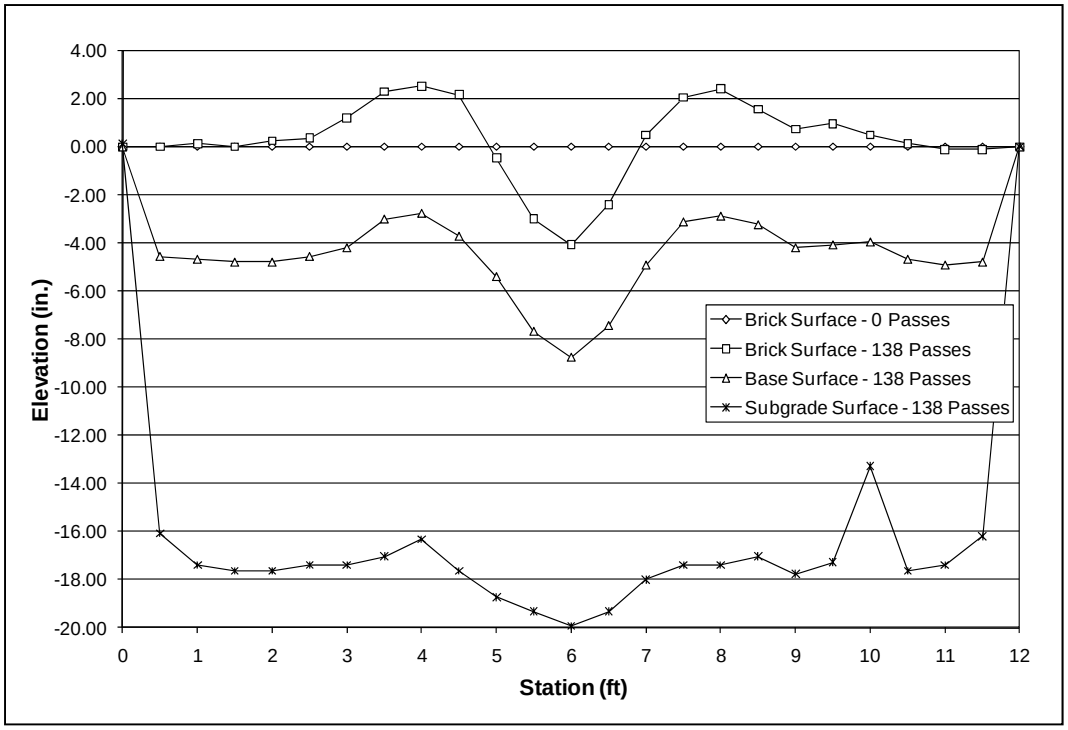

Figure 110. Item 4 cross-section profile measurements after C-17 traffic.

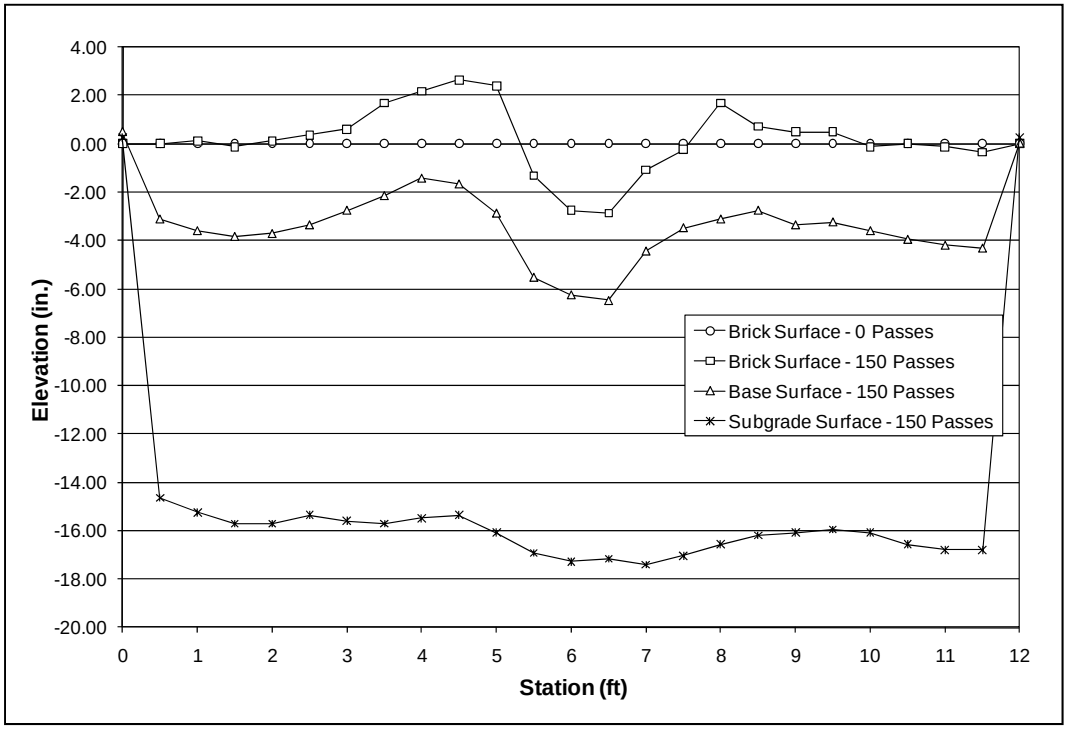

Figure 111. Item 5 cross-section profile measurements after C-17 traffic.

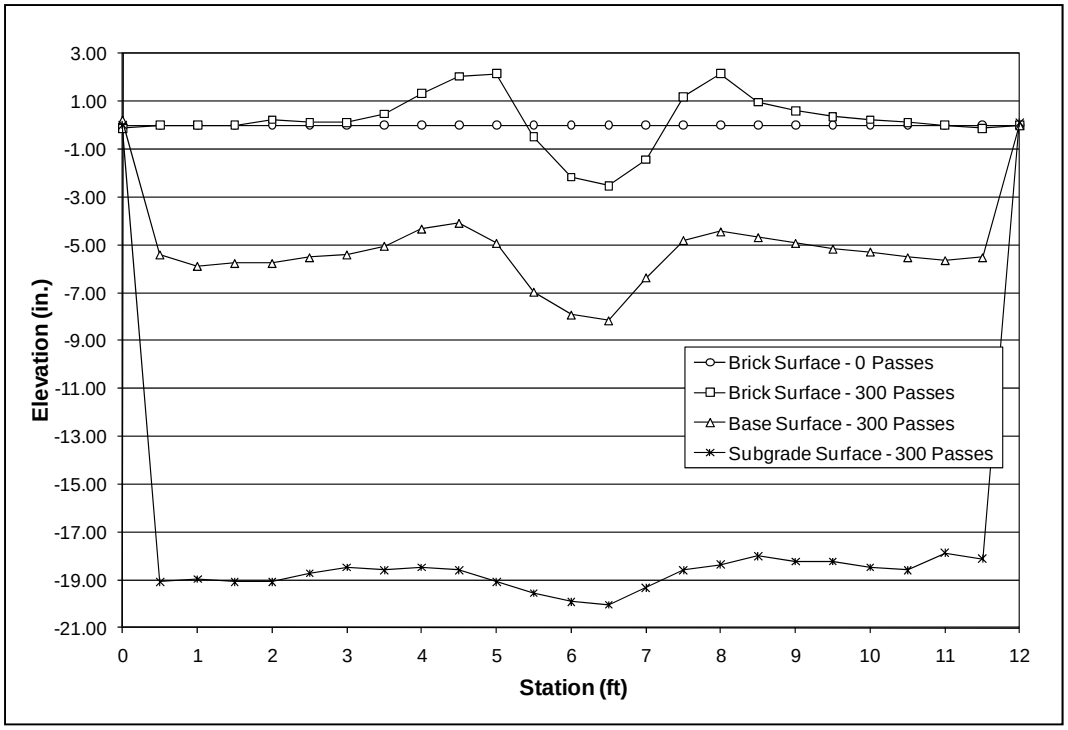

Figure 112. Item 6 cross-section profile measurements after C-17 traffic.

Summary

Table 13 summarizes the performance of the bricks from the laboratory and field testing. The brick types were ranked after each test, with 1 being the best, to determine which brick type was the most durable, reliable, least susceptible to frost, etc. Table 13 shows that the best laboratory performers were not necessarily the best field performers.

The overall performances of the bricks for road surfaces, based on the overall laboratory test results and the measured rut depths in the field, are as follows:

- Queen bricks had undesirable performance in the laboratory but performed well in the field. They performed as well as the standard modular, utility, and paver bricks in the field.
- Reclaimed bricks had the least desirable performance in the laboratory and in the field.
- Standard modular and paver bricks had the most desirable performances in the laboratory, and they performed well in the field. They performed as well as the utility and queen bricks in the field.

- Utility bricks had average performance in the laboratory and performed well in the field. The field performance was similar to the queen, standard modular, and paver bricks.
- The double layer of standard modular bricks had the most desirable performance in the field.

These overall performance evaluations are relative comparisons. Based on the limited field testing conducted during this study, brick surfaces are not capable of handling aircraft loads.

Table 13. Laboratory and field performance summary of bricks.

Brick Type	Laboratory Performance										Field Performance			
											Truck Traffic		C-17 Traffic	
	Compressive Strength (psi)	Rank	LAA: % Loss	Rank	5-hr Boil Absorption (%)	Rank	24-hr Cold Absorption (%)	Rank	Specific Gravity	Rank	Avg. Rut (in.)[a]	Rank	Failure Pass[b]	Rank
Queen (Item 1)	4,781	4	55.84	5	16.9	4	11.1	4	2.02	4	0.66	5	25	5
Reclaimed (Item 2)	3,574	5	44.03	4	17.2	5	23.4	5	2.02	5	0.95	6	15	6
Standard Modular (Item 3)	19,571	1	26.46	2	8.1	2	4.9	2	2.24	2	0.65	4	25	4
Utility (Item 4)	10,597	3	41.65	3	8.6	3	5.3	3	2.22	3	0.46	2	30	3
Paver (Item 5)	17,272	2	22.79	1	7.1	1	4.8	1	2.32	1	0.51	3	35	2
Double Layer Standard Modular (Item 6)	n/a	n/a	n/a	n/a	n/a	n/a	n/a	n/a	n/a	n/a	0.28	1	60	1

[a] Average surface rut measured at 10,010 passes of commercial dump truck traffic. Failure of flexible road pavements with truck traffic is 3 in. of surface rutting.

[b] Approximate failure pass; failure of flexible aircraft pavements is 1 in. of surface rutting.

6 Conclusions and Recommendations

ERDC was tasked by the Air Force Civil Engineer Support Agency to evaluate the use of face bricks for road paving and aircraft parking in expeditionary environments. The face bricks most likely would be recycled material from existing infrastructure. This report presents the procedures, results, and analysis of the full-scale field testing and evaluation of face bricks for use on roads and aircraft parking ramps in expeditionary environments.

Conclusions

The following conclusions were drawn from the full-scale field testing and evaluation of the bricks:

- The bricks tested under controlled environmental conditions are capable of withstanding low-volume truck loads of approximately 54,000 lb. Each brick type was trafficked to 10,010 passes and measured less than 1 in. of surface rutting. Failure of flexible road pavements subjected to truck traffic is defined as 3 in. or more of surface rutting.
- The bricks tested under controlled environmental conditions are not capable of withstanding fully-loaded C-17 traffic. The brick types tested all failed with approximately 1 in. of surface rutting between 15 and 60 passes of the load cart. The brick pavers failed at around 35 passes. Failure of flexible airfield pavements subjected to aircraft traffic is 1 in. of surface rutting.
- Although the laboratory results showed large differences in strength, the queen bricks and the standard modular bricks had similar field performance when subjected to both the truck and single-wheel C-17 traffic.
- The double-layered standard modular bricks performed significantly better than the other evaluated brick types for both types of traffic. In terms of rut depth, the double-layered standard modular bricks performed approximately 2.5 times better than the single layer of standard modular bricks subjected to both the truck traffic and the aircraft traffic.
- The reclaimed bricks performed considerably worse than the other brick types for both truck and aircraft traffic.

- The queen and standard modular brick types crushed under the aircraft traffic. The crushed bricks could potentially damage aircraft.
- Literature stated that concrete block pavers with compressive strengths of 8,000 psi have proven to be adequate for military road applications. The compressive strengths of all brick types tested, with the exception of the queen and reclaimed brick, exceeded 8,000 psi. The reclaimed bricks were the worst performing bricks for both types of traffic. However, the queen bricks performed relatively well in the field.
- The forensic investigation revealed consolidation and shear movement of all pavement structure layers, particularly the base layer, after trafficking with the single-wheel C-17 load cart.

Recommendations

The following recommendations are made based upon the results of the field testing:

- The bricks were evaluated in controlled environmental conditions, sheltered from precipitation or direct sunlight. Some of the previous laboratory tests conducted on the bricks revealed potential durability issues during freezing and thawing periods. Also, rain is a critical environmental variable that influences road performance. The laboratory tests conducted previously on the bricks revealed that the water absorptions of the bricks were higher than the recommended maximum of 1 percent for aggregate used in construction applications. Thus, the bricks would take longer to dry out during periods of rain. This also could increase the chance for durability problems related to cyclical freezing and thawing. A full-scale brick-paved road test section should be constructed and evaluated for truck traffic with various periods of known precipitation.
- There are numerous tracked vehicles (e.g., tanks, bulldozers, etc.) in theater environments. The bricked road pavements should be evaluated for the grouser effects of tracked vehicles.
- Crushed recycled bricks for use as a base course material for roads should be evaluated. Crushed brick is a material that could be readily available in areas where resources are scarce.
- It might also be beneficial to evaluate crushed bricks as aggregate for use in asphalt or concrete mixtures.

References

American Society for Testing and Materials. 2003. *Standard test method for use of the dynamic cone penetrometer in shallow pavement applications*. Designation D 6951-03. West Conshohocken, PA: American Society for Testing and Materials.

_____. 2006. *Standard practice for classification of soils for engineering purposes (Unified Soil Classification System)*. Designation: D 2487-06. West Conshohocken, PA: American Society for Testing and Materials.

_____. 2007a. *Standard test method for CBR (California Bearing Ratio) of laboratory-compacted soils*. Designation D 1883-07. West Conshohocken, PA: American Society for Testing and Materials.

_____. 2007b. *Standard test methods for laboratory compaction characteristics of soil using standard effort*. Designation D 698-07 Method C. West Conshohocken, PA: American Society for Testing and Materials.

Anderton, G. L. 1991. *Concrete block pavements for airfields*. Technical Report GL-91-12. Vicksburg, MS: U.S. Army Waterways Experiment Station.

Bell, H. 2011. *Brick paving systems in expeditionary environments: Laboratory testing*. ERDC/GSL TR-11-8. Vicksburg, MS: U.S. Army Engineer Research and Development Center.

Brick Industry Association. 2009. *Technical notes on brick construction. Dimensioning and estimating brick masonry*. Reston, VA: Brick Industry Association.

REPORT DOCUMENTATION PAGE

Form Approved
OMB No. 0704-0188

1. REPORT DATE *(DD-MM-YYYY)*	2. REPORT TYPE	3. DATES COVERED *(From - To)*
July 2012	Final	

4. TITLE AND SUBTITLE
Brick Paving Systems in Expeditionary Environments: Field Testing

5a. CONTRACT NUMBER

5b. GRANT NUMBER

5c. PROGRAM ELEMENT NUMBER

6. AUTHOR(S)
Haley P. Bell and Quint Mason

5d. PROJECT NUMBER

5e. TASK NUMBER

5f. WORK UNIT NUMBER

7. PERFORMING ORGANIZATION NAME(S) AND ADDRESS(ES)

U.S. Army Engineer Research and Development Center
Geotechnical and Structures Laboratory
3909 Halls Ferry Road
Vicksburg, MS 39180-6199

8. PERFORMING ORGANIZATION REPORT NUMBER
ERDC/GSL TR-12-24

9. SPONSORING / MONITORING AGENCY NAME(S) AND ADDRESS(ES)
Headquarters, Air Force Civil Engineer Support Agency
139 Barnes Avenue, Suite 1
Tyndall AFB, FL 32403-5319

10. SPONSOR/MONITOR'S ACRONYM(S)

11. SPONSOR/MONITOR'S REPORT NUMBER(S)

12. DISTRIBUTION / AVAILABILITY STATEMENT
Approved for public release; distribution is unlimited.

13. SUPPLEMENTARY NOTES

14. ABSTRACT
Personnel of the U.S. Army Engineer Research and Development Center were tasked by Headquarters, Air Force Civil Engineer Support Agency, to determine the feasibility of using face bricks as an alternative to concrete or asphalt paving for low-volume roads and military aircraft parking aprons in expeditionary environments. Because paving materials and equipment can be scarce in these areas, the use of recycled bricks from existing infrastructure might provide a local resource for constructing pavements suitable for meeting the military's mission requirements. The field testing documented in this report follows a laboratory study in which a series of tests, including compressive strength, absorption, Los Angeles abrasion, and specific gravity, were conducted on selected face bricks. The success of the laboratory testing led to the full-scale field testing and evaluation of the face bricks under a commercial dump truck load of approximately 54,000 lb and then under a 45,000-lb single-wheel C-17 aircraft load cart. The field testing indicated that brick-paved roads constructed with a moderately high strength base are capable of sustaining more than 10,000 passes of truck traffic without failure. The same brick-paved roads were not capable of withstanding C-17 aircraft traffic. Further results from the evaluation are presented, including material characterization test data, rut depth measurements, wheel path and cross-section profile measurements, instrumentation response data, and forensic assessments. Recommendations for continuing the study through the use of additional full-scale field test sections also are provided.

15. SUBJECT TERMS
Brick paver
Brick paving
C-17
Face brick
Rut depth
Aircraft traffic
Truck traffic

16. SECURITY CLASSIFICATION OF:			17. LIMITATION OF ABSTRACT	18. NUMBER OF PAGES	19a. NAME OF RESPONSIBLE PERSON
a. REPORT	b. ABSTRACT	c. THIS PAGE		100	19b. TELEPHONE NUMBER *(include area code)*
UNCLASSIFIED	UNCLASSIFIED	UNCLASSIFIED			